Preliminary Corrosion Studies of Candidate Materials for Supercritical Water Oxidation Reactor Systems

by

John Clarke Orzalli

M.S. in Systems Management
Golden Gate University, 1990
B.S. in Marine Engineering
United States Naval Academy, 1978

Submitted to the Department of Ocean Engineering and the Department of Materials Science and Engineering in Partial Fulfillment of the Requirements for the Degrees of

Naval Engineer

and

Master of Science in Materials Science and Engineering

at the
Massachusetts Institute of Technology
May 1994

The author hereby grants to MIT permission to reproduce and to distribute publicly paper and electronic copies of this thesis document in whole or in part.

Signature of Author. . . . . .

Certified by . . . . . .
Ronald M. Latanision, Professor of Materials Science
Department of Materials Science and Engineering
Thesis Advisor

Certified by . . . . . .
Koichi Masubuchi, Kawasaki Professor of Engineering
Department of Ocean Engineering
Thesis Reader

Accepted by . . . . . .
Carl V. Thompson II, Professor of Electronic Materials
Chair, Departmental Committee on Graduate Students

Accepted by . . . . . .
A. Douglas Carmichael, Professor of Power Engineering
Chair, Departmental Committee on Graduate Students

DISCLAIMER NOTICE

THIS DOCUMENT IS BEST QUALITY AVAILABLE. THE COPY FURNISHED TO DTIC CONTAINED A SIGNIFICANT NUMBER OF COLOR PAGES WHICH DO NOT REPRODUCE LEGIBLY ON BLACK AND WHITE MICROFICHE.

AD NUMBER	DATE 8/23/94	DTIC ACCESSION NOTICE
1. REPORT IDENTIFYING INFORMATION		REQUESTER:
A. ORIGINATING AGENCY 93943 NAVAL POSTGRAUTE SCHOOL, MONTEREY, CA		1. Put your mailing address on reverse of form. 2. Complete items 1 and 2.
B. REPORT TITLE AND/OR NUMBER PRELIMINARY CORROSION STUDIES OF CANDIDATE MATERIALS FOR SUPERCRITICAL WATER OXIDATION		3. Attach form to reports mailed to DTIC.
C. MONITOR REPORT NUMBER M.I.T. BY: JOHN ORZALLI MAY 94 THESIS		4. Use unclassified information only.
D. PREPARED UNDER CONTRACT NUMBER N00123-89-G-0580		5. Do not order document for 6 to 8 weeks.
2. DISTRIBUTION STATEMENT APPROVED FOR PUBLIC RELEASE; DISTRIBUTION UNLIMITED		DTIC: 1. Assign AD Number. 2. Return to requester.

DTIC Form 50 DEC 91 PREVIOUS EDITIONS ARE OBSOLETE

PRELIMINARY CORROSION STUDIES OF CANDIDATE MATERIALS FOR SUPER TICAL WATER OXIDATION REACTOR SYSTEMS

by

John Clarke Orzalli

submitted to the Departments of Ocean Engineering and Materials Science and Engineering on 6 May, 1994 in partial fulfillment of the requirements for the Degrees of Naval Engineer and Master of Science in Materials Science and Engineering.

ABSTRACT

An experimental test facility has been designed and constructed for investigation of the corrosion behavior of candidate materials in a supercritical water oxidation environment. The high temperatures (500°C) and high pressures (300 atm) required in this process, made the experimental apparatus construction and control a complex engineering problem.

The facility consists of two systems. The first is an exposure autoclave ,internal volume 850 ml, with associated monitoring and control systems for conducting long term exposure testing of test coupons and U-bends. The second is an electrochemical cell with a potentiostat and frequency response analyzer for conducting Electronic Impedance Spectroscopy (EIS) in the supercritical water environment.

Exposure testing of three candidate materials; Inconel 625, Hastelloy C-276 and 316 stainless steel was conducted at three temperature regimes corresponding to three locations in a SCWO waste treatment system. Preliminary results are presented in an environment of demineralized water as a control.

Experimental results indicate evidence of a film on the materials characterized by slight weight gain. Light and confocal laser light microscopic evaluations revealed the presence of localized pitting corrosion on the Inconel 625.

Thesis Supervisor: Dr. Ronald M. Latanision

Title: Professor of Materials Science

TABLE OF CONTENTS

TABLE OF CONTENTS (Continued)

TABLE OF CONTENTS (Continued)

LIST OF ILLUSTRATIONS AND FIGURES

LIST OF TABLES

ACKNOWLEDGEMENTS

This experimental facility has been a joint effort between the members of the H. H. Uhlig Corrosion Laboratory and the Chemical Engineering Department. The design and construction of the system was possible due the technical expertise and guidance of chemical engineers Matt DiPippo, Phil Marrone, Brian Phenix, CPT Jerry Meyer, U.S. Army, and CPT Russ Lachance, U. S. Army. Steve Attanasio of the Materials Science Department helped to devise sample preparation and evaluation techniques, in addition to tolerating my presence in his laboratory.

Haynes International, specifically Galen Hodge, provided not only the sample material but also technical advise which was invaluable. The laboratory of Professor Ron Ballinger and technical advise of Martin Morra were essential in the preparation of quality samples.

The machine shops at the Massachusetts Institute of Technology were instrumental in accomplishment of this project. Not only did they train me in operation of the equipment, but they were willing to help out to ensure the work was completed properly. For this I am grateful to Mike Aloisi and his crew in the Laboratory for Nuclear Science machine shop, and Guenter Arndt in the Materials Science and Engineering Department machine shop.

The Energy Laboratory has been a source of constant support, not only technically but emotionally. The constant encouragement of Professor Jeff Tester has helped me to see the practical aspects of the project and made me wonder why I am not a chemical engineer. His support staff of Rosemary Fleming and Beth

Ann McCain walked me through the details of the procurement process, without which this project would still be in the design stage.

The technical advice, and encouragement from the Ocean Engineering Department has been instrumental in meaningful results for this project. Gokhan Goktug graciously took the time to train me in the use of the special microscopes used for sample evaluation. The encouragement and helpful suggestions of Professor Koici Masubuchi, have allowed me remain focused throughout this effort.

Professor Ronald Latanision, my thesis advisor, has consistently provided the direction needed to see the project through to fruition. His ability to diagnose and provide the "cure" for the ailments which tend to derail an experimental project were key in the success to date. His staff of Connie Beal and Kelly Fischer have provided administrative support surpassed only by their cheerful attitudes and smiles which have been greatly appreciated.

The majority of the work documented here is a collaboration between Dr. D. Bryce Mitton and myself. His technical expertise, wise counsel, and attention to detail are not only evident by his design of many of the special components of the system, but also were key in production of documents such as this thesis. His daily interest in my progress, has been the consistency which has ensured the completion of my portion of this project. I leave, knowing the project is in his able hands.

The individuals in the Navy Academic Office have been outstanding in their support. Jennifer Liable administrative support and untiring efforts to make the Navy students' lives bearable is gratefully noted. LCDR Jeff Reed's interest in the project,

from faithful attendance at briefings on the subject, to even monitoring of the initial approach to supercritical conditions, falls into above and beyond the call of duty category. His positive approach to everything rubs off, and it is evident in this project. Without CAPT Alan Brown, this project would never have started. His insight into future Navy and environmental needs, allowed me to pursue a project in which I had high interest. Throughout the course of this research, his encouragement and reinforcement of Navy interest has kept me moving towards the goal.

I am indebted to my fellow classmates, especially the members of my design team; CDR Mark Lusted, LCDR Greg Thomas, and LT Dave Fox. Their flexibility in scheduling, and untiring effort has made my work on this project possible.

My motivation and inspiration to study Naval applications of corrosion phenomena stem from my high school chemistry teacher in McLean Virginia, Mrs. Marjorie Green. My interests in engineering applications of materials, and my motivation to pursue an advanced engineering degree were instilled by Professor Dennis Hasson, at the United States Naval Academy. The confidence they showed in me at an early age has propelled me to do better.

Success of this project is also due, in part, to my computer repairman who just happens to be my father, Jack Orzalli. He and my mother, Myrtle, have supported me in all my efforts and instilled in me the desire for excellence. Their encouragement has kept me focused on the important qualities of life rather than the day to day trivialities that tend to bog one down. Additionally, my thanks are due to my mother-in-law, Peggy McComas, who has come to the rescue many times in sitting with the

children because their father was always studying. She also has helped me maintain the proper perspective for this thesis.

Without the support, and encouragement of my children, this thesis would not have been possible. Sarah, Ian and Robbie have looked at their fathers back too long as I have spent countless hours in front of the computer screen. They have been told to be quiet more often than any children should be. They have even eaten meals in the lab on the weekends just to be with me. Their tolerance, and constant love has lifted me through this effort.

No acknowledgement would be complete without heartfelt thanks, and love to my wife, Dale. Without her devotion, patience, tolerance and flexibility, this thesis would never have happened. Her ability to get all us kids off to school has been remarkable. She has sacrificed too many of her own opportunities to allow me to take advantage of mine. I only hope I can somehow make it up to her. Her love and support has sustained me throughout this effort, for which I am thankful.

Finally I must acknowledge the gifts I have been given by God. The love he has expressed through his son, Jesus Christ, has been my strength through this project. The knowledge that through Him, I can do anything, has been a constant in the completion of this thesis and the course of study at MIT. For these gifts, I am ever grateful.

DEDICATION:

To Dale, this project is as much yours as it is mine.

Chapter 1

Introduction

Details of the impact of man's industrialization of the planet earth are being revealed at an alarming rate. What is becoming clearer with each discovery is that we, as a civilization must learn not only to monitor our impact, but develop new technologies to limit production of harmful effects or efficiently eliminate haz products before they are released to our environment.[1] Ships at sea, especially Naval Ships, have historically had exemptions from even the limited environmental regulations in effect.[2] In the future for the United States Navy to have access to the oceans of the world, we must develop technologies to eliminate dumping of any material over the side.

From a ship designer's perspective, elimination of overboard dumping creates a significant stowage space requirement unless there is a waste processing capability on the ship.[3] Any processing plant must be able to handle a wide variety of wastes, in a marine environment, safely and efficiently utilizing a minimum amount of space. As the principle mission of U. S. Navy Ships is warfare, any support system which occupies a large volume, reduces the weapons systems the ship can carry.[4]

The supercritical water oxidation (SCWO) process is an emerging technology which may be a solution for destruction of shipboard wastes at sea. The waste destruction technology utilizes water above the critical point (374°C, 218 atm) as a solvent for organic compounds and oxygen. Unlike water below the critical point, the solubility of organic materials is almost complete in supercritical water. By

introduction of oxygen into this environment, complete destruction of the compounds to basic components of water, carbon dioxide and nitrogen rapidly occurs. Inorganic compounds are insoluble in the conditions such that they can be precipitated out and removed.[5]

Pilot scale and laboratory plants have demonstrated this technology on a wide variety of compounds. The resultant destruction efficiency and short residence times of this process make it a serious alternative to incineration for treatment of many hazardous waste.[6] Additionally due to the relatively low temperature of this process, off gassing of nitrous oxides are not a problem as in incineration.[7] These properties have resulted in investigation and development of SCWO reactors for use in biological waste collection and processing in the space program.[8]

The potential for application on ships seems unlimited. Vessels could be installed with small plants capable of processing large amounts of not only biological and food wastes but also plastics, black and grey water and bilge water contaminated with oil. This would effectively reduce dumping without large capacity on board tanks. Additionally current ship designs, which have holding tanks for these types of waste, would be able to reduce their capacity. Future Navy ships have been envisioned, which would be outfitted with a SCWO reactor for waste processing .[9] Figure 1-1 is a conceptual design of a Destroyer/Frigate (DDG/FFG) with emphasis on minimizing overboard discharge of water. Experiments in destruction of Naval wastes have been conducted[10] and there is currently an effort to develop large scale land based SCWO reactors for processing of Navy wastes by the Civil Engineering Corps.[11]

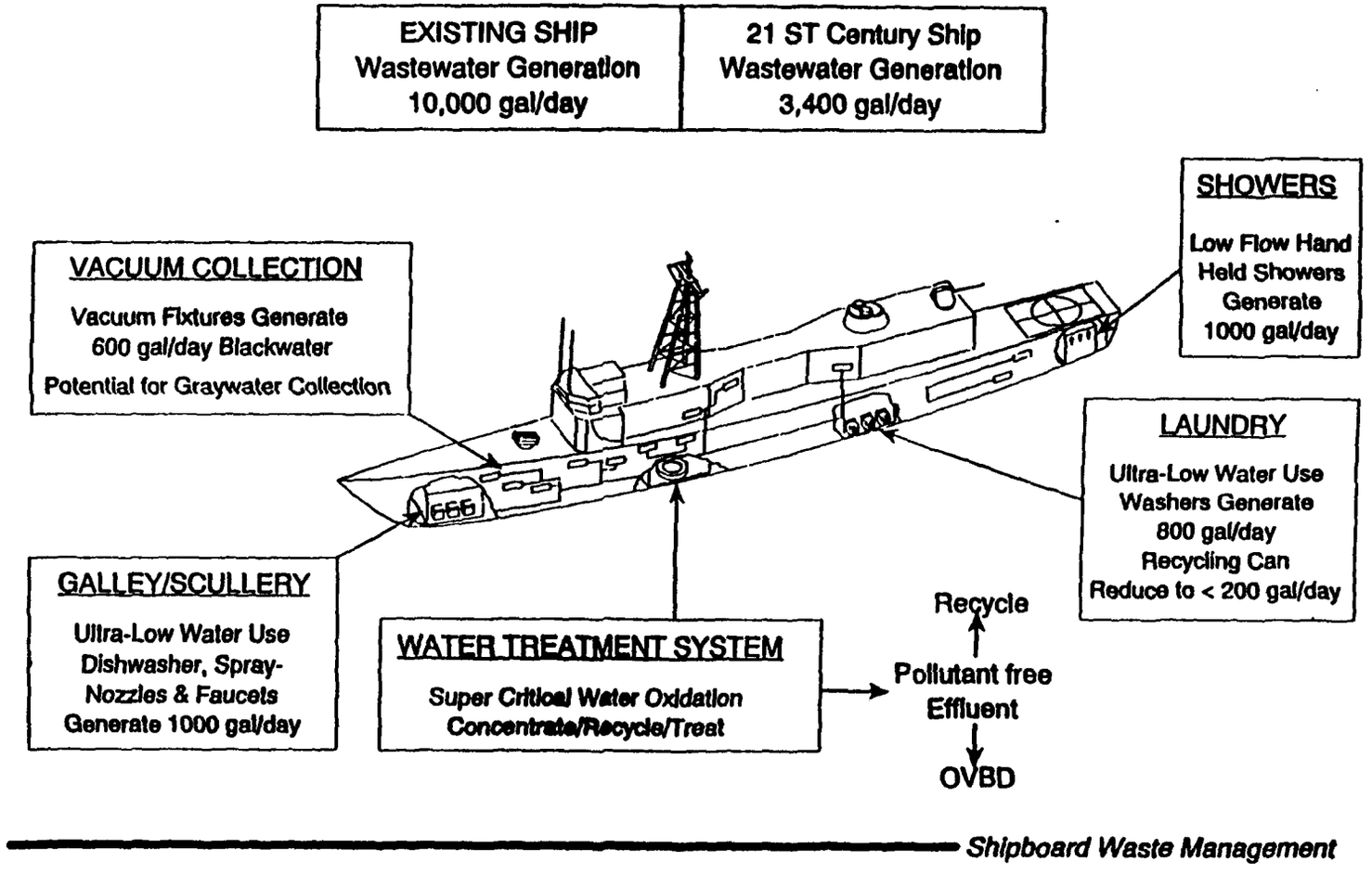

FIGURE 1-1 Concept of Future Navy Ship

The application of this technology for any use, however, hinges on an investigation not only of the kinetics of the reaction process, but also of the materials of construction of the reactor system. As the potential waste streams include a wide range of hazardous materials including chemical weapons, the behavior of the reactor materials must be clearly understood prior to building full scale operational plants.

Current research in this area at the Massachusetts Institute of Technology is sponsored by the U.S. Army Research Office as part of a University Research Initiative for developing chemical weapons destruction technology. The goal of this preliminary research was to develop a testing apparatus, determine test materials and test solutions, and run initial corrosion testing of a limited number of materials to demonstrate the operability of the system.

Chapter 2

Background Literature Survey

The supercritical water oxidation process for the destruction of hazardous wastes is a relatively recent technological development.[12] Numerous compounds have been tested to determine destruction efficiency of the process, but very limited specific corrosion testing has been accomplished. The difficulty in performing corrosion testing at high temperatures and pressures, as well as the relatively small size of many test reactors contributes to this lack of data. As different components in the SCWO process experience a wide range of temperatures and pressures, some corrosion data from other high temperature and high pressure environments may help to evaluate material performance of certain sections of the reactor system.

2.1 Basic Description of Cycle.

An understanding of the basic SCWO cycle is necessary to address corrosion problems in the different sections. Figure 2-1 is a representative schematic diagram of one of the processes currently in use.[6] The components of the process are similar in the many different variations of the system. The basic cycle consists of seven major steps [13]:

1) Feed preparation and pressurization
2) Preheating
3) Reaction
4) Salt Formation and Separation
5) Quenching, cooling and energy/heat recovery
6) Pressure Letdown and phase disengagement
7) Effluent water polishing

While there are seven identifiable subprocesses in the system, for the purposes of

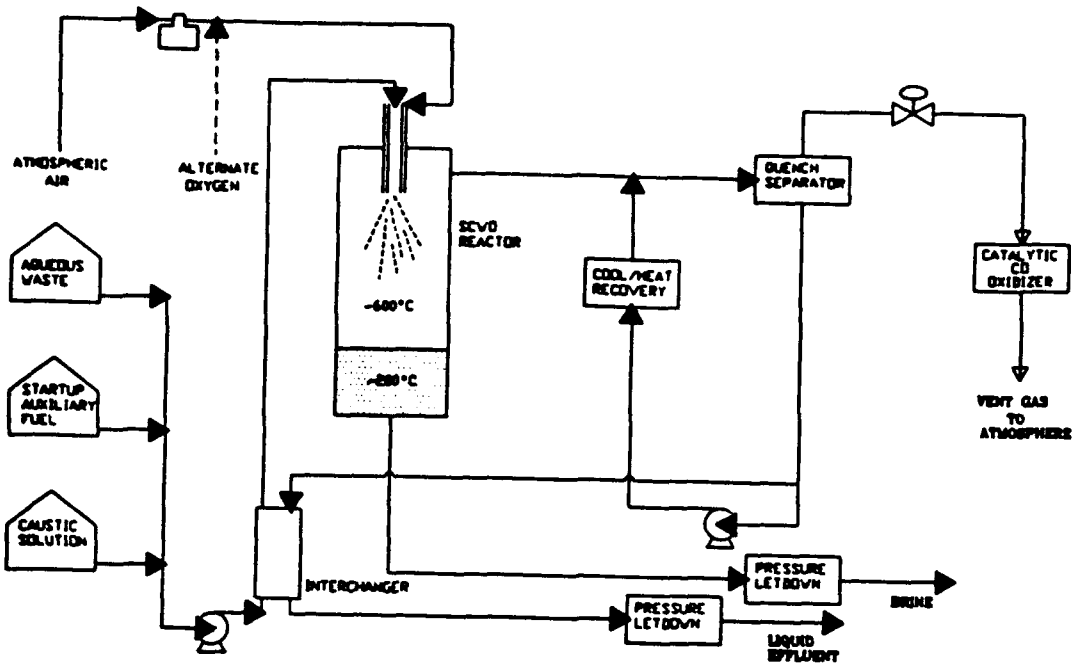

FIGURE 2-1 MODAR SCWO Process. From Tester et. al [13]

identifying and analyzing corrosion problems three general areas are addressed. The pretreatment region where water, waste and oxidant are mixed, pressurized and heated to supercritical or near supercritical conditions. The materials in this region see, at different times, a wide range of temperatures, pressures, and chemical environments. The reactor region itself experiences supercritical conditions while operating and a range in temperatures during heat up and cool down. Salt insolubility in the supercritical region may result in sticky salt deposits[14] which could affect material performance of the reactor itself. Finally, the letdown or cool down section is exposed to a wide range of temperatures as well as pressures. Concentrated brine of redissolved salts can occur at subcritical temperatures[15], thus, adding to the complexity of the corrosion environment in the letdown section. Understanding the material

properties in each of these sections under the operating conditions is a critical component in the selection of the best material for the specific application.

2.2 Theoretical Background.

2.2.1 Basic Corrosion Principles. Corrosion itself is a chemical or electrochemical reaction between a metal and its environment.[16] In a specific environment, the change in the Gibbs free energy determines thermodynamically whether chemical reactions can occur. In the following example:

$$Cu + H_20\ (l) + 1/2O_2(g) \rightarrow Cu(OH)_2(s) \qquad \Delta G^o = -28{,}000\ cal$$ [16]

The large negative value of ΔG^o indicates the reaction will occur as written at standard conditions of 25°C, although it does not indicate a rate of reaction. The change in Gibbs free energy can be equated to a specific electromotive force, (emf) by use of the relationship $\Delta G = -EnF$. Where E is the emf, n is the number of electrons and F is the Faraday. Any electrochemical reaction can be written as the sum of two half cell reactions each with an associated Gibbs free energy and therefore an emf with each half cell reaction. Values of emf for various reactions are available at standard conditions of temperature, pressure and concentration. In order to modify standard values to existing conditions, the Nernst equation must be applied. For a given reaction of the form: $lL + mM + \ldots \rightarrow qQ + rR + \ldots$

$$E = E^{o} - \frac{RT}{nF}\ln\frac{a_Q^q \cdot a_R^r \cdots}{a_L^l \cdot a_M^m \cdots}$$

Where the activity a_M is expressed as concentration in molality times an activity coefficient. R is the ideal gas constant and T is the absolute temperature. For reactions in aqueous solutions which involve the reduction of hydrogen or oxygen as the cathodic half cell, the concentration of hydrogen ion is a critical factor in determining the overall emf and thus the thermodynamic tendency to corrode. pH is defined as - log (H^+), the hydrogen half cell emf is reduced as pH increases by the following relationship in an environment of 1 atmosphere of hydrogen.[17]

$$2H^+ + 2e^- \rightarrow H_2 \qquad E_{H_2} = 0 - \frac{RT}{2F}\ln\frac{p_{H_2}}{(H^+)}$$

$$= \frac{(8.314\ J/^{\circ}\cdot mole)(298.2^{\circ}K)}{2 \cdot 96500\ C/eq} \cdot ln10 \cdot \log[\frac{1}{(H^+)}]$$

eq is the equivalent number of moles of the ion, C is a coulomb

$$E_{H_2} = 0.0592 \cdot \log(H^+) \quad = -0.0592 \cdot pH$$

Direct application of the Nernst equation and the Gibbs free energy associated with various compounds of a metal leads to development of the Pourbaix diagram,[17] which plot the potential versus pH at a given temperature. Figures 2-2 and 2-3 depict pH versus potential diagrams for iron and chromium at 25°C.

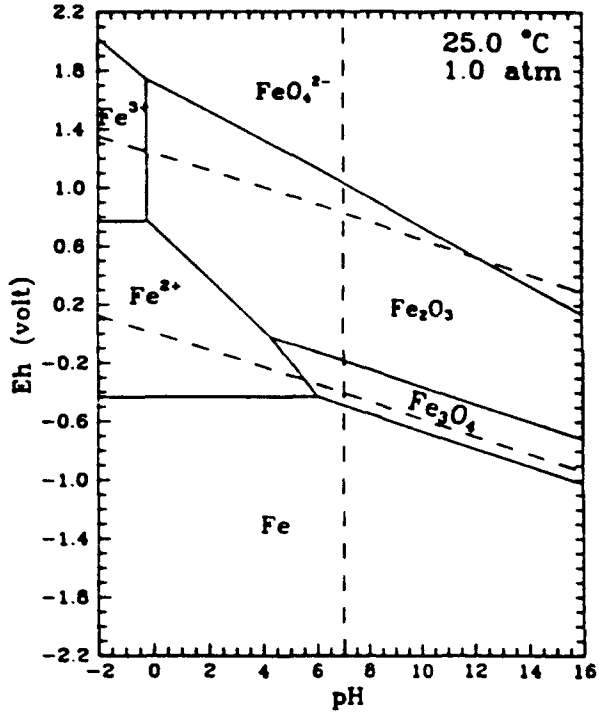

FIGURE 2-2 Pourbaix Diagram For Iron at 25°C. From Huang et. al. [18]

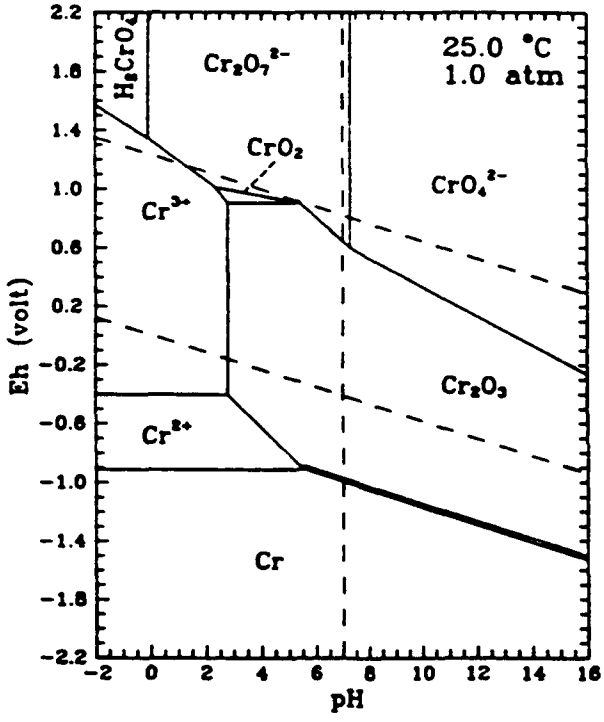

FIGURE 2-3 Pourbaix Diagram For Chromium at 25°C. From Huang et. al. [18]

While helpful in predicting the thermodynamic tendency for corrosion mechanisms to occur, the Pourbaix diagram is not kinetically based, thus rates of corrosion are not available from this tool. To determine corrosion rates, polarization or Evans diagrams are necessary. These curves are developed at low temperatures and pressures, using a test apparatus similar to Figure 2-4. The apparatus measures values of current from a working electrode at various applied emf values. The resultant plots can provide a value for the corrosion current density. See Figure 2-5. The corrosion current density can then be directly converted to weight loss of the metal if the surface area in contact with the electrolyte is known.

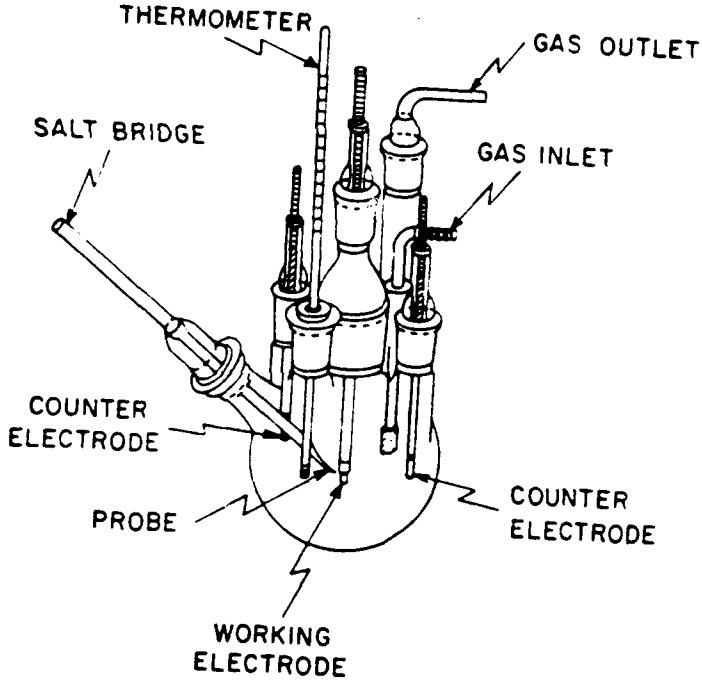

FIGURE 2-4 Schematic of Commonly Used Polarization Cell (Annual Book of ASTM Standards)[19]

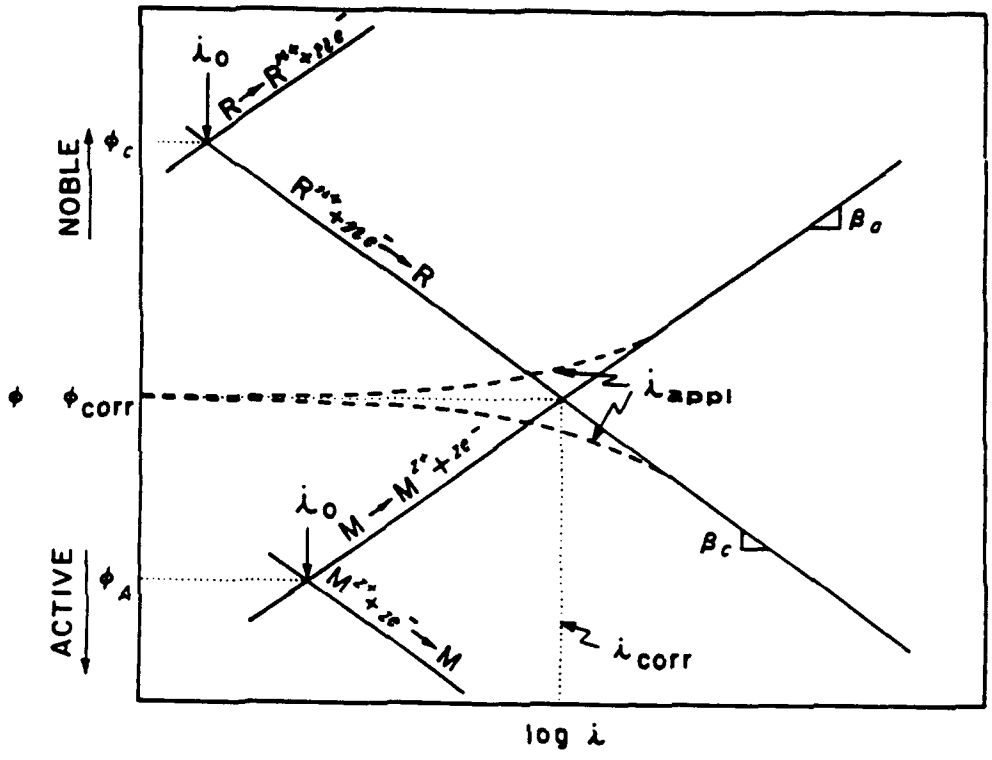

FIGURE 2-5 Polarization Diagram . From Uhlig, Corrosion and Corrosion Control[16]

2.2.2 Properties of Supercritical Water. Development of meaningful data in the supercritical region is dependent on understanding the properties of the environment. Those properties which allow dissolution and subsequent oxidation of organic wastes and precipitation of inorganic and ionic compounds, create corrosive environments which may not be described in strictly aqueous terms. The dielectric constant of water is drastically reduced in the supercritical state and ionic species are virtually non-existent. The density of the fluid, though significantly higher than steam, is much lower than water, such that frequency of molecular interactions may prohibit aqueous corrosion modeling. Figure 2-6 depicts some of the physical properties of water as it transitions to the supercritical region.[12]

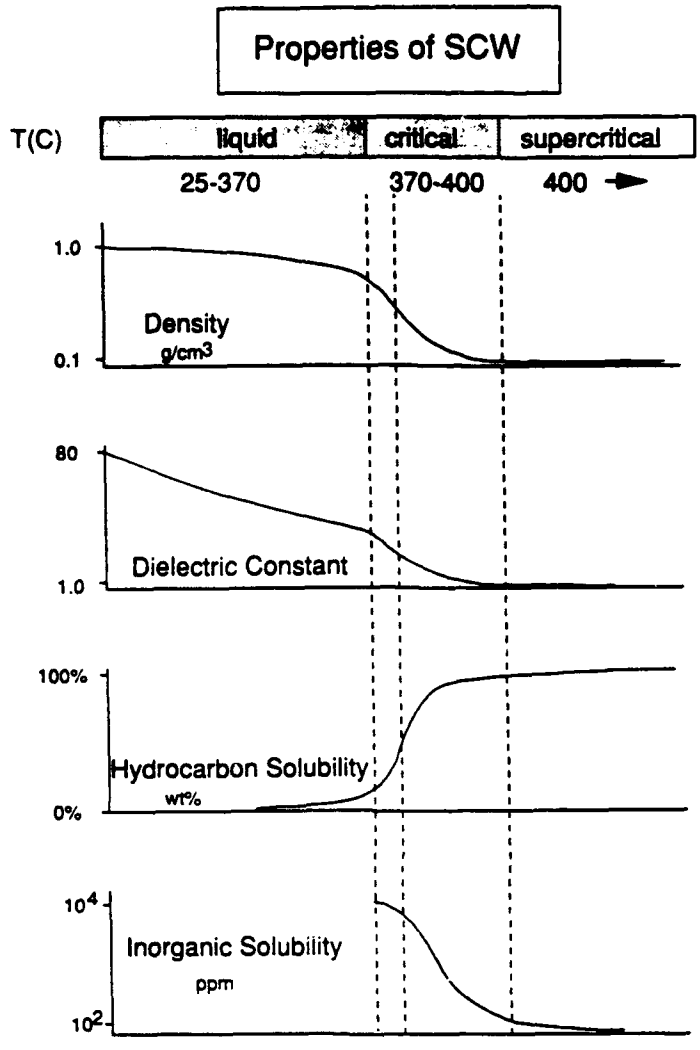

FIGURE 2-6 Properties of Water in the Supercritical Region for Pressure Range of 218 to 300 atm. Michael Modell, MODAR, INC.[12]

2.2.3 Supercritical Electrochemical Studies. Thermodynamic models of the supercritical water environment which can be utilized to help analyze corrosion behavior are limited.[18] The lack of electrochemical measurements in the supercritical region has made development of a reasonable model very difficult. Huang et. al.[18], developed Pourbaix diagrams for iron and chromium based upon a computer model of

extrapolation of chemical potentials to dissolution temperature and pressure conditions. Figures 2-7 and 2-8 depict the results of these calculations. For clarity in discussion, the Pourbaix diagrams for iron and chromium at room temperature were included as Figures 2-2 and 2-3. The Pourbaix diagrams for iron and chromium at the critical point reveal some interesting results. Neutral pH is 7.2 at the conditions depicted (374.1°C, 217.8 Atm). The potential region for the stable phase of iron (Fe_2O_3) in neutral pH, is much narrower than at ambient conditions. It also encompasses negative potentials. Even more significant, is the observation that chromium does not exhibit passivity in the neutral and basic pH ranges at supercritical conditions which indicates potential for pitting or other attack in this region.

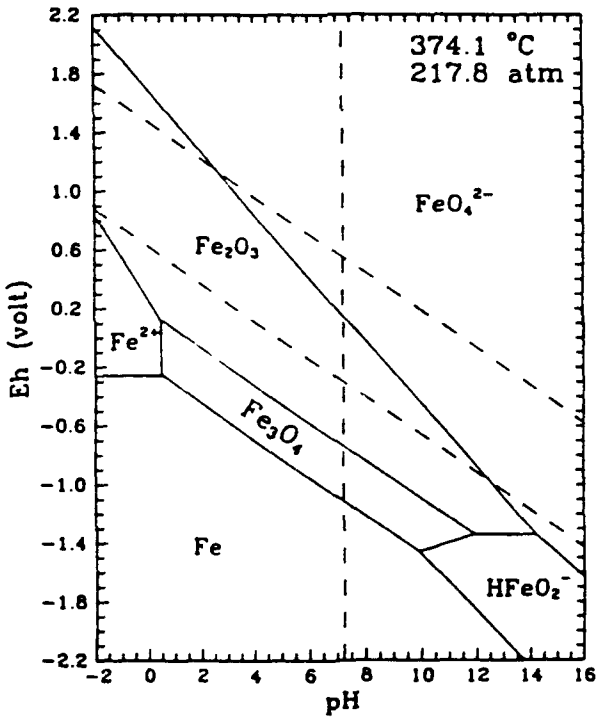

FIGURE 2-7 Pourbaix Diagram For Iron at the Critical Point. From Huang et. al. [18]

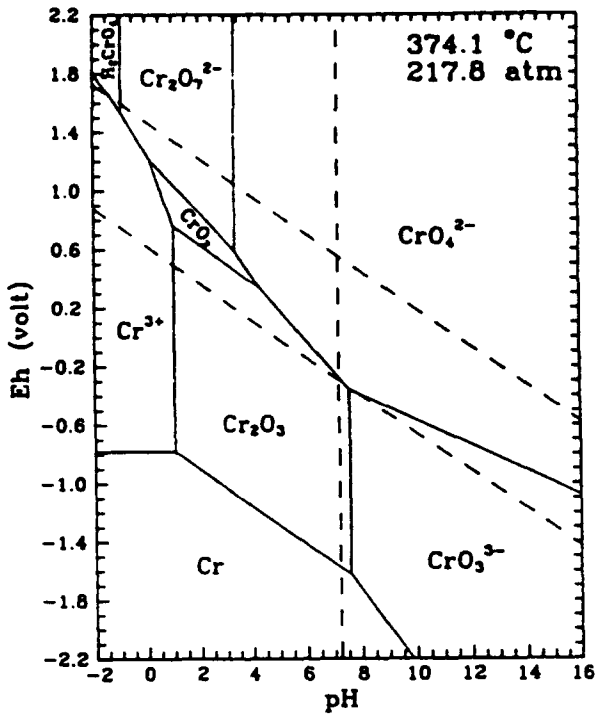

FIGURE 2-8 Pourbaix Diagram For Chromium at the Critical Point. From Huang et. al.[18]

Measurements of electrochemical properties of iron in supercritical water and in dilute (0.005 moles/liter) sodium sulfate also have interesting results[20]. A polarization plot , Figure 2-9, and plot of exchange current density versus temperature, Figure 2-10, reveal insight into the validity of the Pourbaix diagrams presented above. Specifically, the passivity of 304 stainless steel appears to be lost at about the critical point. Also of note is the significantly higher exchange current density at dissolution temperature and pressure conditions. The current density drops off after reaching supercritical conditions, indicating a possibility of decreased corrosion in this region.

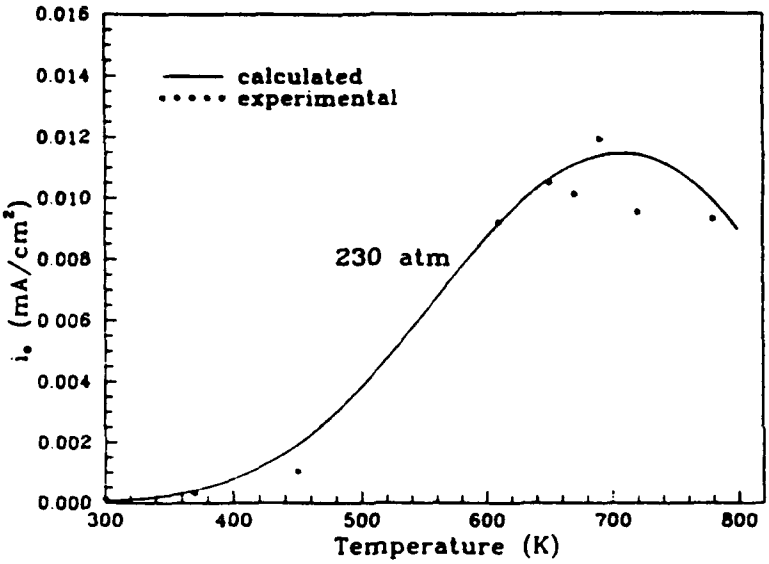

FIGURE 2-9 Polarization Curves for type 304 Stainless Steel in Pure Water and 0.005 mol/l Na_2SO_4

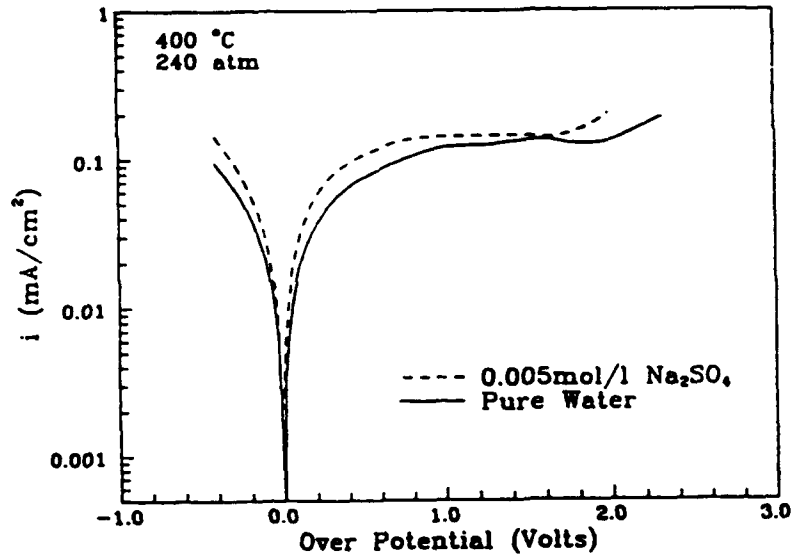

FIGURE 2-10 Temperature effect on exchange current density of 304 S.S. in pure water. From Huang et. al.[20]

The information available from supercritical conditions for iron is limited, but is beneficial to help evaluate the potential effects in a supercritical water environment.

The effects of contaminants, complex alloys and the unique properties of the supercritical state make extrapolation of proven technology from the subcritical region, suspect in the supercritical region.

2.3 Possible Corrosion Mechanisms.

An examination of materials in high temperature environments in other applications is beneficial for determining the types of possible corrosion mechanisms in the SCWO reactor system. Significantly more data exists in lower temperature conditions found in the preheater and letdown sections. Based upon experience in sour gas wells, and currently utilized materials in SCWO systems[12], high nickel alloys and stainless steels are examined for behavior in various conditions which might be similar to those found in the three sections of the system. Alloying compositions of metals discussed in this section are listed in Appendix A for reference.

2.3.1 Uniform Attack. Nickel is inert in deaerated water at room temperature. It also exhibits passive behavior in aerated solutions. The passive layer however for nickel is not as stable as that for chromium.[16] The high temperature behavior of nickel based alloys however is of most interest. Nickel alloys have numerous applications in high temperature environments due to the stability of the passive layer. The SCWO process is nominally aqueous, at least in all but the reactor section, thus high temperature data in this environment is considered pertinent. General corrosion rates have been obtained in a gaseous environment of 60% H_2O, 40% HCl[21]. Table 2-1 summarizes the results of these tests for some candidate materials. Of particular note, is that nickel alloys are not normally resistant to chloride solutions, but these alloys include

molybdenum which improves the resistance to the pitting condition.[16] In this environment passivity occurs due to formation of a film on the surface.

	Corrosion Rate (μm/y)		
Temperature °C	316L SS	Inconel 625	Hastelloy C-276
500	483	132	-
400	15	-	-
380	-	13-23	-
375	-	10-15	-
365	-	13	-
350	-	8-15	-
315	-	8	-
310	-	0	-
300	3	-	-
290	-	-	1
260	-	8	-
200	7	-	-
195	-	0	0
190	5	0	0
180	4	0	1
175	9	-	-
170	10	0	1
160	27	-	-
155	-	3	3
140	-	112	91
115	-	869	315
110	485	-	307
100	-	2200	1600
95	12100	-	-

- indicates no data taken

Table 2-1 Corrosion in 60% H_20, 40% HCl, From Carter et. al.[21]

The above samples were either rubbed or acid cleaned to remove the corrosion products prior to weighing. In addition the samples were examined by Auger electron

spectroscopy to determine the composition of the film following the attack. No characterization of the type of attack was provided, but the mechanism appeared to be HCl attack thinning the passive oxide layer.

Though the HCl environment is a single data point, there are a wide range of chlorinated compounds, which are candidates for destruction by SCWO technology. In this specific environment (150 - 400°C at ambient pressure), which is significantly lower in pressure than the SCWO process, the resistance to general corrosion of nickel based alloys is excellent. The specific environments of the SCWO system covers a wide range of temperatures and based upon these results it is evident that a material that exhibits good general corrosion properties at one temperature may have drastically different properties at a different temperature. Localized corrosion phenomena however may occur in these materials at different temperature and pressure conditions, and was not addressed in this study.

2.3.2 Stress Corrosion Cracking The wide variety of conditions in the various sections of the SCWO system increase the probability of stress corrosion cracking. High stresses exist in potentially susceptible materials due not only to high pressures but also to thermal gradients. The multitude of chemical environments seen by reactor materials may create the combination necessary for initiation of stress corrosion cracking.

High nickel alloys have been utilized in pressurized water reactors with a relatively pure water environment. In certain conditions in this environment, stress corrosion cracking has been observed, although nickel alloys are not as susceptible as

stainless steel originally utilized in this application.[22] The presence of oxygen, inherent in the SCWO process, is also a key contributor to conditions for stress corrosion cracking. The high nickel alloys, including Inconel 625, experience stress corrosion cracking in oxygenated water when crevices are present[22]. Critical potential ranges over which stress corrosion cracking exists at ambient temperatures[16], seem to exist for high temperatures as well. Development of electrochemical procedures for analysis of this phenomenon in the dissolution temperature range seems a vital area for investigation. Development of curves similar to Figure 2-11, may help to predict the onset of cracking behavior in any environment including the supercritical region.

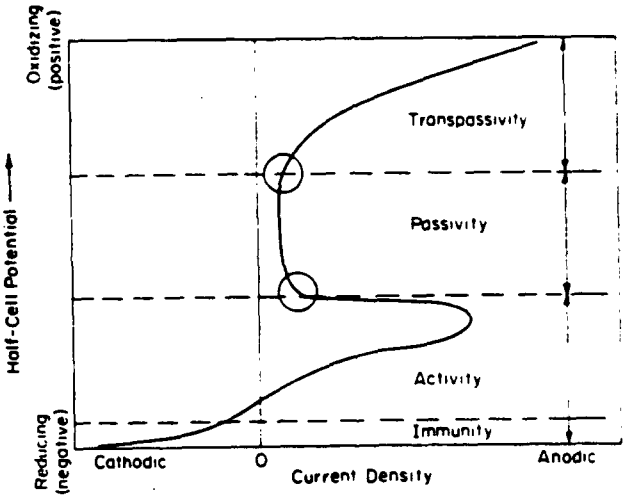

FIGURE 2-11 Schematic Polarization Curve of Fe-Cr-Ni Alloy in an Environment that Might Promote Stress Corrosion Cracking. From Berry[22]

In this representation, the two circled regions are areas susceptible to cracking. The first is the region just above the anodic peak where the passive layer is not completely formed, and the second at the beginning of the transpassive region where breakdown of the passive film initiates[22]. Development of environmentally specific curves for potential waste streams in a similar manner would help to define the susceptibility of

a particular material to stress corrosion cracking in that environment and aid in determining material/waste stream compatibility. This task would be immense, but investigation by exposure testing may present candidate combinations for examination by this method.

2.3.3 Hydrogen Embrittlement. The various wastes expected to be processed by this technology include compounds containing oxygen, chloride, ammonia, sulfate , fluoride phosphate and carbonate.[23] The materials technology developed for sour gas (H_2S) wells is therefore beneficial in analyzing the effect of exposure to this potential hydrogen rich environment. One material in common use in these wells is Hastelloy C-276 which is also a material of construction of many SCWO reactors[24] . This material has demonstrated susceptibility to hydrogen embrittlement. Of particular note, with increased cold working, and subsequent heat treatment, the susceptibility of the material to hydrogen embrittlement increases.[24] The redistribution of impurity elements (phosphorus) to the grain boundaries during heat treatment, results in and increased susceptibility to hydrogen embrittlement. Since the temperatures encountered in SCWO reactors are at or above the aging temperatures (149 - 482°C) examined by Berkowitz [24], any cold working of the reactor piping would in effect increase its susceptibility to hydrogen embrittlement in a similar environment. In related studies of another high nickel based alloy(MP35N), the effects of migration of impurities to the grain boundaries could be reduced by heat treatment at higher temperatures (732 - 816°C) than experienced in SCWO reactors.[25]

Cold work and heat treatments thus plays a significant role in the susceptibility of these materials to hydrogen embrittlement. Of note, these tests were conducted at room temperature. Normally effects of hydrogen embrittlement are reduced at elevated temperatures as the diffusivity of hydrogen increases. Operating procedures in heat up and cool down of the SCWO system would be significant in reduction of the risks of this type of attack. In essence, the materials should be at a high temperature before introduction of a hydrogen rich environment, thus reducing the effect of hydrogen embrittlement.

2.4 Monitored Effluent Surveys

A majority of corrosion studies in SCWO reactors to date have been monitoring of effluent streams for the presence of materials of construction of the system. This method may help to determine whether a particular waste stream causes corrosion, but it does not aid in determination of the mechanism of corrosion or the portion of the system under attack. Table 2-2 lists some of the effluent monitoring of SCWO reactions.

The presence of reactor materials in the effluent is not encouraging if one desires a system that will last any significant period of time. The wide range in reported values is somewhat misleading as neither the waste concentration or reactor residence time is universally reported. Additionally there is very little correlation of corrosion products in the effluent to a specific temperature of reaction. The results of Buelow et. al.[27] detailed in table 2-3, present both the concentration of the feed stock, the flow rate and the temperature of the reaction in addition to the chemistry of the

effluent. This data is helpful in identifying conditions which amplify corrosion rates, but is not helpful in determining the mechanisms in which operate. In addition to monitored effluent samples, many researchers note colored effluents, some with particulate. [28] These qualitative findings help stress the need for further research

Reactor Material	Waste Stream	Effluent Sample	Source
Hastelloy C-276	Ammonium Perchlorate 400-600°C	Cr (130 ppm) Mo (54 ppm) Ni (39 ppm)	Dyer, et. al., 1992 Reference 26
Gold Lined 316 SS Acidified	Ammonium Perchlorate 400-600°C	Au (1622 ppm) Cr (3.36 ppm) Fe (65.38 ppm) Ni (55.04 ppm)	Dyer, et. al. 1992 (26)
Gold Lined 316 SS Alkaline	Ammonium Perchlorate 400-600°C	Au (0 ppm) Cr (0.99 ppm) Fe (0.99 ppm) Ni (3.73 ppm)	Dyer, et. al. 1992 (26)
Inconel 625	Methanol 472-574°C	Ni (none detectable) Cr (0.07-.3 ppm)	Rice et. al. 1993 (10)
Inconel 625	Methyl Ethyl Ketone 445-568°C	Ni (none detectable) Cr (1.01 ppm)	Rice et. al. 1993 (10)
Inconel 625	Acetic Acid 441-533°C	Ni (none detectable) Cr (3.01 ppm)	Rice et. al. 1993 (10)
Inconel 625	Methylene Chloride 447-570°C	Ni (30.7 ppm) Cr (0.02 ppm)	Rice et. al. 1993 (10)
Inconel 625	Trichloroethane 409-474°C	Ni (49.0 ppm) Cr (0.55 ppm)	Rice et. al. 1993 (10)
Inconel 625 Hastelloy C-276	NaCl Various Temperatures	Ni (0.359 ppm) Cr (0.036 ppm) Mo (0.093 ppm) Fe (0.124 ppm) Nb (0.043 ppm)	Armellini and Tester, 1993 (15)
Inconel 625 Hastelloy C-276	Na_2SO_4 Various Temperatures	Ni (0.042 ppm) Cr (0.534 ppm) Mo (0.429 ppm) Fe (0.017 ppm) Nb (0.043 ppm)	Armellini and Tester 1993 (15) Represent Average Values of 15 runs
Hastelloy C-276	Distilled Water 450°C for 60 minutes	Mo (4.80 mg/liter) Cr (6.75 mg/liter) Ni (2.60 mg/liter)	Takahasi et. al. 1989 (8)
Hastelloy C-276	Ammonium Hydroxide and Acetic Acid 450°C for 60 minutes	Mo (18.1 mg/liter) Cr (11.5 mg/liter) Ni (15.0 mg/liter)	Takahasi et. al. 1989 (8)
Hastelloy C-276	Human Waste Feed 400°C for 60 minutes	Mo (45 mg/liter) Cr (8.4 mg/liter) Ni (7.4 mg/liter)	Takahasi et. al 1989 (8)

Table 2-2 Effluent Samples of Various Waste Streams in SCWO reactors

into the corrosion mechanisms at work in this unique environment and have led to more sophisticated specific corrosion testing.

Feedstock	Flow Rate	Temp °C	Cr (ppm)	Mo (ppm)	Ni (ppm)
0.1 M Ammonium Perchlorate	2 ml/min	500	59	10	26
0.1 M Ammonium Perchlorate	4 ml/min	500	130	54	39
0.1 M Ammonium Perchlorate	8 ml/min	500	101	48	35
0.1 M Ammonium Perchlorate	2 ml/min	400	4.4	9.6	<0.4
0.1 M Ammonium Perchlorate	8 ml/min	400	1.2	3.8	<0.4
0.16 M Nitromethane	2 ml/min	500	<0.4	<0.4	<0.4
0.16 M Nitromethane	8 ml/min	580	<0.4	<0.4	<0.4
Water	8 ml/min	580	<0.4	<0.4	<0.4

Table 2-3 Effluent Samples of Ammonium Perchlorate and Nitromethane Feedstock in Hastelloy C-276 Reactor. From Buelow et. al.[27]

2.5 Exposure Studies

Exposure studies in supercritical water oxidation reactors are difficult. Most of the experimental work, even some of that devoted specifically to materials evaluation occurs in plug flow tubular reactors with a relatively small diameter tubing as the reactor itself.[29] There simply is not enough room for standard sized exposure samples in these types of reactors. There have been limited tests performed in larger reactors many of them stimulated by the results of effluent samples of either analytical or visual nature.

Brownish, and golden colored effluents indicative of ionic iron and chromium, with some solid material present, prompted researchers to place long witness wires into an operating SCWO reactor. The witness wires were removed after testing and cut into pieces. Subsequently the surface of the wire was analyzed by various methods. The witness wires were exposed to the environment in each of the three system areas and,

thus, provide an indication of the corrosion present in that section[28]. Table 2-4 summarizes the results of this experiment.

Wire Material	Waste Material	Section of Reactor	Results
Inconel 625	Hanford	Preheater Upper Temp Zone	Reduction in Nickel and Chromium concentrations and deposition of Iron
Inconel 625	Hanford	Reactor Inlet	Deposition of Iron and feed solution metal
Inconel 625	Hanford	Reactor Outlet and Cool down	Dissolution of Chromium/ Molybdenum
Inconel 625	Hanford/ $NaNO_3$	Preheater Upper Temp Zone	Dissolution of Chromium
Inconel 625	Hanford/ $NaNO_3$	Reactor Inlet	Dissolution of Chromium- some Iron deposition
Inconel 625	Hanford/ $NaNO_3$	Reactor Outlet and Cool down	Dissolution of Chromium but to a lesser degree
Hastelloy C-276	Hanford/ $NaNO_3$	Reactor after Max Temp	Drastic dissolution of Molybdenum, Tungsten and Chromium
Titanium	Hanford/ $NaNO_3$	Preheater Upper Temp Zone	Chromium and Nickel deposition
Titanium	Hanford/ $NaNO_3$	Reactor	Chromium and Nickel Deposition

Table 2-4 Corrosion of Witness Wires in SCWO Processing Stream. Bramlette et. al.[28]

These results indicate a change in surface composition within identifiable regions of the reactor system. Since the Hanford waste simulant is a combination of a variety of compounds (Appendix A), the mechanism of corrosion is difficult to infer. Visual analysis was performed on the wire sections, but damage to wires as a result of removal from the system masked some of the results. Most of the wires which exhibited depletion were described by the author as being etched on the surface[28], indicating the possibility of some localized form of corrosion.

Standard corrosion coupons have been tested in SCWO reactors for limited materials in some waste streams. Results from early tests on the MODAR bench scale

plant indicated no evidence of corrosion in the Inconel 625 and Hastelloy C-276 system after several hundred hours of operation in a variety of waste streams. Prestressed coupons were exposed to chloride levels of 5000-10000 ppm by oxidation of trichloroethylene, and then examined by microscopic and metallurgical methods. Corrosion of the Inconel 625 reactor vessel was termed insignificant while considerable corrosion was evident in the letdown region.[13]

Coupons of high grade alloys were tested in industrial sludge at the University of Texas Center for Research in Water Resources[30]. A temperature profile up to a maximum of 457°C within the reactor presented different conditions for the samples. Twelve different combinations of sludge concentration, feed rate and oxygen concentration were introduced to the single set of samples. Some samples were removed after 67.5 hours as the system was opened for clearing of blockage. The samples were subjected to heat up and cool down in each of the twelve runs. Table 2-5 summarizes the results of this test in which the maximum exposure time was 106.5 hours.

The table represents the maximum value calculated from six coupons of each metal exposed to sludge at a range of temperatures from 250°C to 457°C. The weight loss was determined following cleaning in a light acid solution with non-metallic brushes. The author summarized the findings stating that corrosion rates were highest in the hottest portion of the reactor. When analyzed in some detail, specifically for Inconel 625, it is noted that the maximum corrosion rate was measured on a sample placed in one of the coolest sections of the reactor, and that at the maximum

temperature, Inconel 625 had one of the lowest values of corrosion rate (-1.1 mpy). Additionally, the characterization of pitting and crevice corrosion was only observed on the points of attachment. For this experiment every point of attachment failed, possibly due to multiple heat up and cool down cycles.

Alloy	Corrosion Rate	Types of Corrosion
SS 316	5.9 mpy	Pitting, Crevice
SS 316L	7.6 mpy	Pitting, Crevice
2205	0.2 mpy	Uniform, Crevice
20CB3	7.1 mpy	Severe Pitting
C-276	1.1 mpy	Uniform
C-22	2.6 mpy	Uniform
Inconel 625	1.7 mpy	Pitting, Crevice
Inconel 825	12.0 mpy	Pitting, Crevice
G-3	6.5 mpy	Pitting, Crevice
G-30	2.2 mpy	Pitting, Crevice
Titanium Grade 9	0	None detectable
Titanium Grade 12	-0.2 mpy	None detectable

Table 2-5 High Grade Alloy Corrosion Study Results. From Thomas and Gloyna[30]

These results indicate further analysis is needed even with this environment. The high corrosion rate noted on a single sample of Inconel 625 in a lower temperature region, contrary to the trends of all the other data, indicates the possibility of an erroneous data point. In weight loss calculations, multiple samples in similar environments would identify abnormalities as well as some statistical distribution. Additionally, weight loss results with negative corrosion rates suggests that removal of scale is not complete and these values should be questioned. Finally, characterizing corrosion by weight loss when there is evidence of localized corrosion may be

misleading, as the actual penetration in the vicinity of the attack may be much higher. A pitting factor would be appropriate to report as well in instances of localized attack.[16] (Figure 2-12)

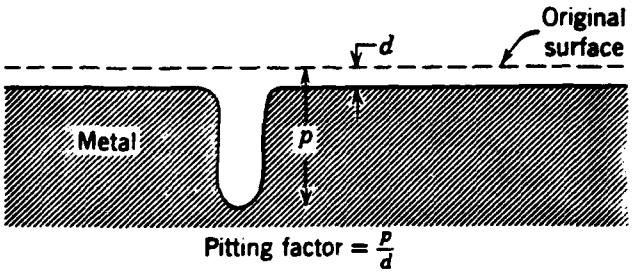

FIGURE 2-12 Sketch of Deepest Pit with Relation to Average Metal Penetration and the Pitting Factor. From Uhlig, Corrosion and Corrosion Control. [16]

Other corrosion studies have been conducted[31], but the results are proprietary and are not available for comparison.

2.6 Areas for further investigation. Based upon the research published to date, there is a great need for investigation into the material properties in SCWO reactor systems. Not only is a relatively large exposure vessel needed which can hold larger samples, but also such a vessel needs to be dedicated to corrosion studies. Specific waste streams at different temperatures as well as exposure times need to be examined. Additionally electrochemical methods to determine polarization curves or provide other data would be very beneficial. Finally Electrochemical Impedance Spectroscopy (EIS) could help to characterize the mechanisms of corrosion if parallel exposure studies were performed for validation of the results.[32]

Chapter 3

Experimental Apparatus

The experimental apparatus for this research was designed and constructed as part of the project. The actual research is part of a larger corrosion testing program, such that the design discussed here includes some equipment which has yet to be tested. The overall corrosion testing program for SCWO at the Massachusetts Institute of Technology will attempt to address the issues presented in the previous chapter of this thesis. Specifically, when all systems are operational, D.C. electrochemical measurements, as well as A. C. Electrochemical Impedance Spectroscopy (EIS) will be conducted in the SCWO environment in addition to the companion testing in the exposure autoclave currently in use. The SCWO environment includes a temperature range of 25°C to 600°C as these temperatures are experienced in the operational cycle. For discussion purposes, the exposure autoclave system will be addressed in detail, then differences in the electrochemical system design will be mentioned separately. As the goal is to have comparable environments for each of the systems, a majority of the components are identical in the two systems.

3.1 Basic System Design.

For corrosion testing, a simple SCWO system was needed. The primary purpose of the system is to determine the mechanisms and conditions leading to corrosion of candidate materials of construction. A test system apparatus similar to that currently employed in a salt study[14], was chosen to achieve the required conditions. Figure 3-1 is a schematic of the developed corrosion testing system.

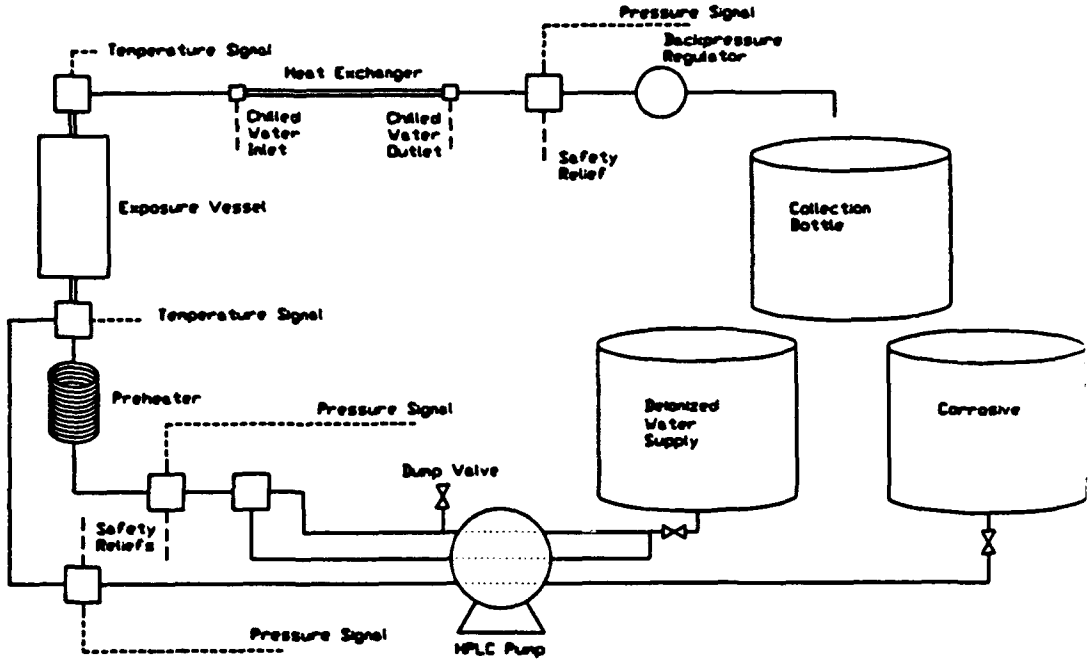

FIGURE 3-1 Schematic of Exposure Autoclave System

The simplicity of the system becomes evident when compared with Figure 2-1. The corrosion testing system does not have an oxygen source, a heat recovery system, or much of the effluent monitoring and processing equipment. For a laboratory apparatus, the requirement was for simplicity in construction and maintenance. The design, procurement and testing of the system components required almost 15 months, and reflects a majority of the effort of this project to date. Table 3-1 lists the components of the system which will be addressed in this document. A complete material list appears as Appendix B.

Exposure Vessel	Tubing/Fittings	Preheater
Heat Exchanger	Heaters	Pumps
Insulation	Sensors	Control System
Safety Features	Sample Holder	Support Systems
Electrochemical Equipment	Omitted Equipment	

TABLE 3-1 System Components

3.2 General Guidelines.

The corrosion testing loop was designed for ease of construction and maintenance. A single material of construction, Inconel 625, was chosen, based upon the high temperature strength characteristics, corrosion experience of other researchers[13,14,33], and availability of the material at a reasonable cost. The use of a single material was desired to minimize the possibility of any galvanic action, and to limit the effects of differences in thermal coefficient of expansion on fittings. For certain applications, components were not manufactured out of Inconel 625. Components of other materials were chosen, and the system designed to ensure that such a component did not experience a high temperature, high pressure condition. Additionally, to reduce the probability of leaks, the system was designed minimizing the overall number of high temperature fittings. Unlike previous SCWO testing schemes which require an operator, this system is required to function unattended for long periods of time. For long term corrosion studies, even those of days in length, a system which can safely be left unattended was required. Equipment previously proven in the SCWO research environment was preferred, but as noted earlier, research in the area has been limited, thus , some components are new to this application.

3.3 Exposure Vessel.

The exposure vessel is a modification of a design currently in use at MODAR for testing of corrosion in the effluent section of the pilot scale reactor system.[33] The vessel, manufactured by REFLANGE Inc. of Houston Texas and designated as R-CON 4, is shown schematically as figure 3-2. The vessel has openings at both ends to

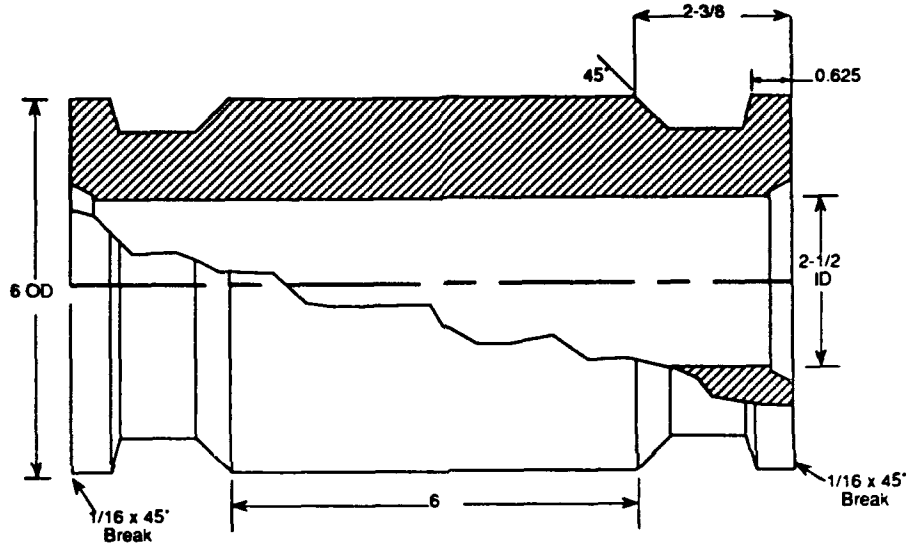

FIGURE 3-2 Exposure Vessel Drawing

facilitate inspection, and if necessary, to marry to additional cylinder for an increased internal volume capability. The wall thickness of the vessel is nominally 1.75 inches with a constriction to 1.25 inches at the clamp seating surface. The vessel heads, shown in figure 3-3, are attached with a double clamp assembly and four bolts. Photographs of the vessel, the heads and the clamps appear in Appendix C for clarity. The mechanical seal is made with a diamond shaped seal ring also made of Inconel 625. When assembled the vessel has an internal volume of 850 ml, and a total dry

weight of vessel, heads and clamps of approximately 180 pounds. Connections to the heads at the top and bottom are with HF-6, ⅜ inch high pressure fittings manufactured by High Pressure Equipment Corporation.

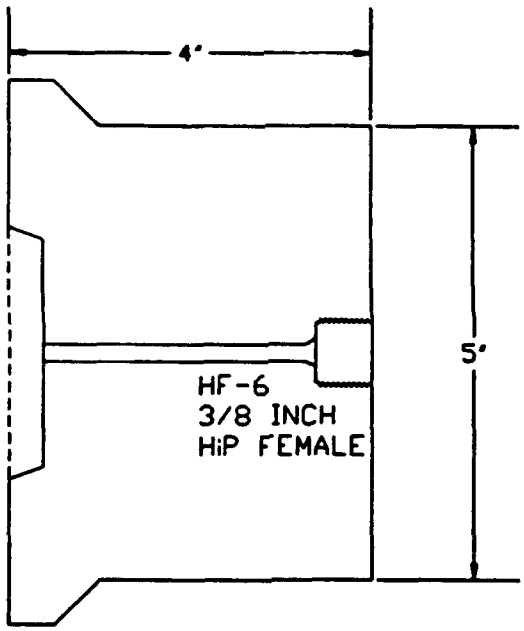

FIGURE 3-3 Exposure Vessel End Closure

3.3.1. Vessel Design Calculations. The vessel was designed to operate in an environment of 5000 psi (340 atm) at a temperature of 600°C. Stresses in the vessel were calculated using thick walled pressure vessel theory.[34] The resultant stress field is three dimensional, therefore a Mises equivalent stress was calculated as the maximum resolved stress[35]. With a distinct possibility of corrosion requiring machining of the vessel walls, a corrosion allowance was included. The following calculations for the vessel were utilized to specify the system design.

$$\sigma_{\theta\theta} = P \cdot \frac{[(\frac{r_o}{r_i})^2 + 1]}{[(\frac{r_o}{r_i})^2 - 1]} \qquad \sigma_{zz} = \frac{P \cdot r_i}{2 \cdot t} \qquad \sigma_{rr} = -P$$

P = 5000 psi **r_o = 2.5 inches** **r_i = 1.25 inches** **t = 1.25 inches**

$\sigma_{\theta\theta}$ = 8333.3 psi **σ_{zz} = 2500 psi** **σ_{rr} = -5000 psi**

Where $\sigma_{\theta\theta}$ is defined as the hoop stress, σ_{zz} is the axial stress and σ_{rr} is the maximum radial stress which occurs at the inside vessel wall. The Mises stress is defined as:

$$\sigma_e = \sqrt{\frac{1}{2}[(\sigma_{rr} - \sigma_{\theta\theta})^2 + (\sigma_{rr} - \sigma_{zz})^2 + (\sigma_{zz} - \sigma_{\theta\theta})^2]}$$

σ_e = 11577 psi

The yield strength of Inconel 625 at 600°C is 60000 psi.[36] Thus the calculated factor of safety is about 5. Additional calculations were performed to determine, with a factor of safety of 4, that the corrosion allowance is .373 inches, almost ⅜ inch. Some sample calculations appear in Appendix D.

In addition to failure by yielding, the vessel was designed to leak before fracture. For analysis purposes, the worst case crack geometry of an elliptical crack was assumed. The crack is one in which crack depth is the same dimension as half of the major axis dimension. Figure 3-4 shows the crack geometry and a flaw shape parameter.[37]

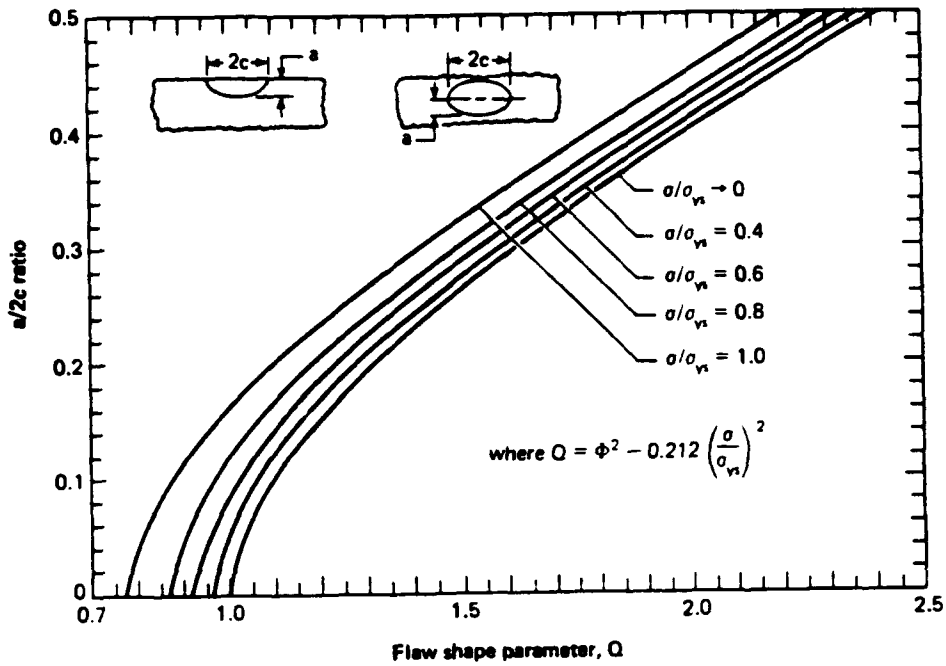

FIGURE 3-4 Graph of Crack Geometry versus Flaw Shape Parameter. From Application of Fracture Mechanics[37]

The a/2c parameter is 0.5 in this worst shape crack situation. The other entering argument for this curve is the ratio of applied stress to the yield stress of the material. The ratio in this case is 11577/60000 or 0.19. The value of Q from the graph is 2.38. The flaw shape parameter, Q, is then converted to critical crack size using the following equation.[37]

$$K_{IC} = 1.1\sigma_e\left[\frac{\pi a}{Q}\right]^{1/2} \qquad a = 29.89 \text{ inches}$$

A lower end value of 80000 psi $\sqrt{\text{in}}$ was estimated for K_{IC} of Inconel 625. The actual value is probably much higher, but sample testing of tough materials is not routinely performed.[38] When compared to the wall thickness of 1.25 inches, it is

evident the vessel will leak long before a crack of 30 inches is formed. These calculations demonstrate that the vessel is adequately designed and should a crack develop, the vessel will leak before fracturing.

3.3.2 Vessel Testing and Certification. In order to meet Massachusetts Institute of Technology Safety Office and insurance company standards, the vessel was required to be tested. The vessel does not meet the size requirements for ASME code section VIII, as: (1) the internal volume is less than one liter (2) there are no welded seams, and (3) the pipe size is less than six inches[39]; thus no state certification was required. As there is no applicable code for the size and construction of the vessel, the insurance company and, thus, the safety office, required that the vessel should be tested to the satisfaction of those operating it. To meet this objective, the vessel was tested to ASME CODE VIII section 1, as the requirements could be met. For the vessel to be certified to 5000 psi (P_{600C})at 600°C, the maximum hoop stress ($\sigma_{\theta\theta}$) must be less than the code allowable stress at this temperature. The allowable stress is 19,300 psi[36] ($\sigma_{allow\ 600C}$) at this temperature, and the maximum hoop stress is 8333.33 psi. Testing was accomplished at room temperature where the maximum allowable stress is 25000 psi[36] ($\sigma_{allow\ room\ temp}$). The test pressure was determined by the ratio:

$$TestPressure = \frac{\sigma_{allow\ room\ temp}}{\sigma_{allow\ 600C}} \cdot P_{600C} = \frac{25000}{19300} \cdot 5000 = 6477$$

The limiting component for this vessel is, in fact, the closure clamp assembly which has an allowable vessel pressure at room temperature of 6480 psi.[40]

The vessel was tested at Thielsch Engineering, Inc. in Cranston Rhode Island

on 15 December 1993, with no noted leakage. Coupled with additional safety features, the vessel and system was certified for use by the MIT Safety Office on 19 January 1994.[41]

3.4 Fittings and Tubing Selection.

An extensive search for available Inconel 625 tubing revealed it would have to be manufactured to order. This significantly increased the cost, as all companies have a minimum order requirement to mill a specific lot of tubing. Seamless tubing was required to minimize the possibility of corrosion at the welded seams. An outside diameter of 0.125 inches and a wall thickness of 0.040 inches were selected. The maximum tubing size considered was ¼ inch because of the need to be able to bend the tubing into a coiled preheater heat exchanger within the lab. When comparing ⅛ inch tubing and fittings to ¼ inch components, the cost differential was significant, which was an additional factor in the ultimate selection of the ⅛ inch diameter. A single tubing size was needed throughout the exposure system, and the concurrent search for a pump selected one with discharge fittings ⅛ inch outer diameter. Smaller diameter tubing was not considered sturdy enough for the exposure testing system. The maximum inside diameter was selected to allow for a corrosion allowance given recent experience with preheater tubing failure.[42]

The fittings chosen for the system are of High Pressure Equipment design and are manufactured out of Inconel 625 where possible. Two basic types of blocks were utilized. Low temperature blocks, which were placed in the system upstream of the heaters and down stream of the heat exchanger, have wetted components manufactured

of Inconel 625, with the remaining parts manufactured of 316 stainless steel to reduce cost. High temperature blocks have both wetted and non wetted parts constructed of Inconel 625 to minimize the effects of differences in thermal expansion. Rather than have a series of adapters to attach the various inlets to the blocks, each block was specially designed and ordered for the application. This, in fact reduced the cost, as all parts would have been special ordered because of the required material of construction. Figure 3-5 is a schematic of the low temperature fitting, while Figure 3-6 is a schematic of the high temperature fitting.

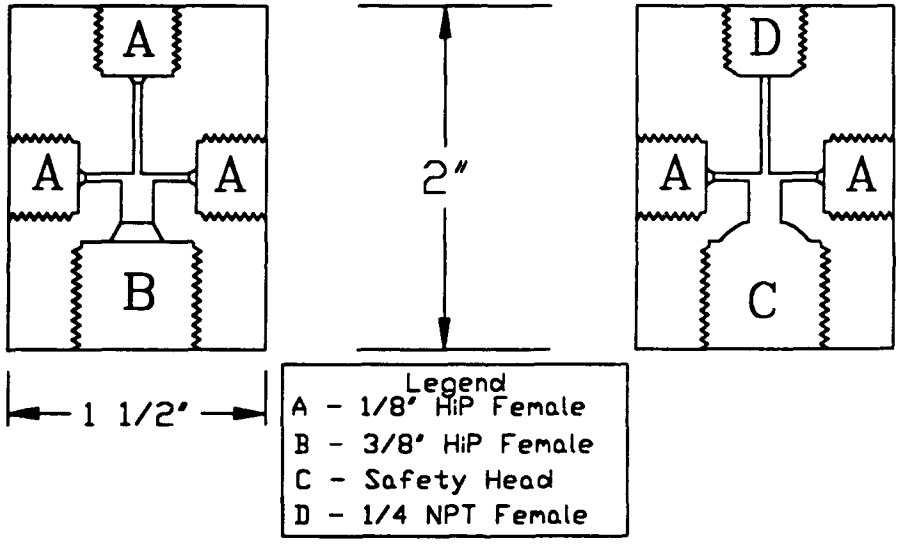

FIGURE 3-5 Low Temperature Block FIGURE 3-6 High Temperature Block

Inlet and outlet fittings for the reactor are ⅜ inch High Pressure Equipment fittings vice ⅛ inch. This larger size was selected due to concern for possible blockage in the ⅛ inch tubing from salt deposits after introduction of the corrosive into the system. These deposits are anticipated due to the reduction in solubility of ionic compounds at supercritical conditions. The ⅜ inch High Pressure Equipment

type seal housing was machined into the vessel heads.

The ends of the tubing were coned and threaded using High Pressure Equipment dies and SULFLO® cutting compound. The mechanical seal is made by threading a collar over the end of the tubing and then tightening a backing nut into the threaded portion of the fitting. For the low temperature fittings, the collar and backing nut, which experience no liquid, are manufactured out of 316 stainless steel. Figure 3-7 is a schematic of the mechanical seals.

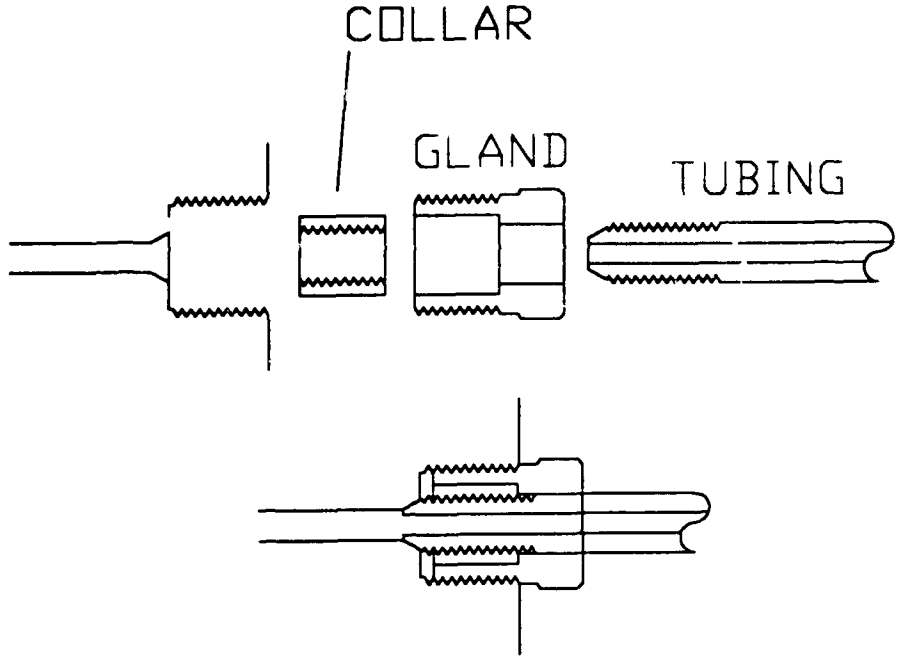

FIGURE 3-7 Mechanical Seal Detail

3.5 Preheater

To raise the temperature of the water feed from ambient to maximum temperature conditions, a preheater is utilized. The preheater was fabricated by rolling a 24 foot section of ⅛ inch tubing around a cylinder on a slowly turned lathe. The resultant coil was then checked to ensure it fit inside the radiant heaters. Elastic

deformation of the Inconel 625 material was significant, such that a coil wound around a four inch cylinder, expanded to five and one half inches upon removal. The wound coils were then subjected to a post cold working heat treatment of 1725°C for 15 minutes and then a vacuum cooled by Hooven Metal Treatments Incorporated of Ipswich, MA. The heat treatment was performed because of prior knowledge of increased corrosion rates in high nickel alloys following cold working[24.25].

3.6 Heat Exchanger.

The system does not attempt to recover any of the heat from the heaters or the destruction process. Commercial applications of this technology would naturally require a heat recovery system for reduction of costs. For corrosion studies, preheating the water inlet with reactor effluent added complexity to the design. A regenerative heat exchanger would have required an additional size of tubing for the shell, and would have required a high pressure, high temperature seal of the outer tubing to the inner tubing. Experience with regenerative heat exchangers in operating nuclear power plants, indicates this arrangement would lead to reduced system reliability.

The cool down heat exchanger used in the system was manufactured with ⅜ inch stainless steel tubing and Swagelok® mechanical fittings. Swagelok® fittings are acceptable as the pressure of the cooling water supply is only that of the building chilled water system. Bored through, reducing fittings allow a mechanical seal on the outside of the ⅛ inch Inconel 625 tubing. Both ends of the heat exchanger are formed by ⅜ inch union tees allowing cooling water to flow around the hot discharge

piping. A detailed drawing of the heat exchanger appears as Figure 3-8. A throttle valve was added to the building chill water supply outlet to allow control of flow and thus temperature of the system outlet.

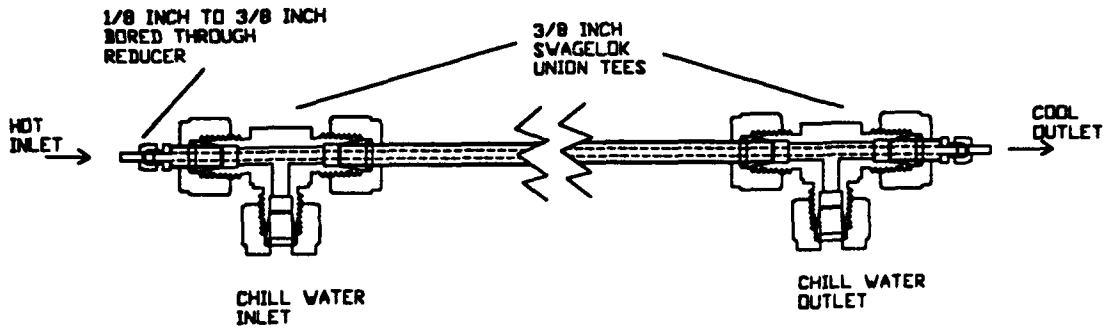

FIGURE 3-8 Heat Exchanger Detail

3.7 Heaters.

The heaters are placed around the preheater tubing and around the vessel. The heaters are Omega ceramic radiant heaters. The preheater is cylindrical and rated at 1350 watts, up to a temperature of 1100°C. To ensure the preheater tubing coil does not touch the heating elements, strips of insulation were cut and placed at the four quadrants of the heaters. Contact with the heater would cause the elements to short out. The coil diameter is slightly larger than ideal for the heaters due to the spring back of the coil following bending mentioned previously. The vessel heater consists of two semicylindrical sections rated at 950 watts each. The inside diameter of the heater pair is seven inches allowing for the ideal distance of ½ inch from heater element to heating surface.[43] All heaters are supplied with 220 volt AC from the building power supply. Appendix C contains photographs of the heating elements.

3.8 Pumps.

The pump in the exposure system is a three head HPLC (High Pressure Liquid Chromatograph) model manufactured by Eldex Inc. Three inlet and outlet ports are equipped with ⅛ inch Swagelok stainless steel fittings. The outlet fittings are connected to the Inconel 625 tubing. The pump is a positive displacement pump with adjustable stroke pistons. Each piston has a micrometer with a locking ring for accurate control of output volume per stroke. The maximum capacity of the pump is 100 ml/min. Pump wetted parts are manufactured of 316 stainless steel with Kel-F® seating surfaces. Two pump outlets are combined into the inlet of the preheater. These two pump heads are utilized for distilled water only. The third pump head is configured for corrosive solution and the outlet is piped directly into the mixing block just prior to the vessel inlet. A three way valve was placed on the outlet of one pump head to allow for rapid depressurization of the system, if necessary, from outside the vessel enclosure. The pump power supply is 120 volt AC from the building power supply. Appendix C contains photographs of the pump connections.

3.9 Insulation.

To minimize heating losses, reduce electrical costs, and reduce temperature of the shielded enclosure, insulation was added to the system. Fiberglass tape is wrapped around the reactor inlet piping and the inlet junction block. Insulating bricks form the pedestal on which the preheater rests. Ceramic fiberboard is used under the vessel, and as a support for the vessel heaters. The remainder of the heated portions of the system are wrapped with one to three inches of Kaowool® ceramic fiber cloth.

Photographs in Appendix C detail some of the insulation. Though necessary for heat loss considerations, the insulation made it difficult to discover leakage locations during the initial testing and subsequently during experiments.

3.10 Sensors

The requirement to maintain the system unattended lead to the selection of pressure and temperature sensors. Sensors were selected with voltage outputs which can be converted to digital signals for computer processing. The potential for plugging of the system,[14,15,30] led to three pressure sampling points. Temperature is sampled inside the reactor, at the outlet of the preheater, and against the outer wall of the exposure vessel. Leads of up to 15 feet in length are required to provide signals to the read and control circuitry as it was placed in the adjacent room for safety considerations. The signals are scanned and converted to temperature and pressure readings by LABVIEW® a computer instrument developed by National Instruments Corporation.

3.10.1 Pressure. The pressure transducers are a model PX613 manufactured by Omega Engineering. A separate 24 Volt DC unregulated power supply is required for excitation of the transducer. With excitation, the output voltage ranges from 1 to 5 volts corresponding to 0 to 5000 psi. Detectors were chosen with volt range output vice current or millivolt output to minimize the impact of electrical noise on the signals from the nearby power supply voltages of the heaters and pumps. The detector is connected to the power supply and the scanning circuitry by a 4 pin twist type connector and 4 wire cable. A schematic of the electrical connection appears in

Figure 3-9. (Note: one of the wires in the cable is not utilized). The maximum working temperature of the detectors is 80°C, such that low temperature fluid is a necessity. The low temperature junction block fittings have one port machined with a ¼ inch 18 National Pipe Thread (NPT) female connection. The pressure sensor has male ¼ NPT threads. A pressure snubber is installed between the junction block and the pressure detector to minimize fluctuations due to the pulsing of the positive displacement pump. The wetted parts of the pressure transducer are made of 17-4 PH and 300 series stainless steels. Signals produced by the transducers are scanned by the LABVIEW® software and then converted to pressure output signals.

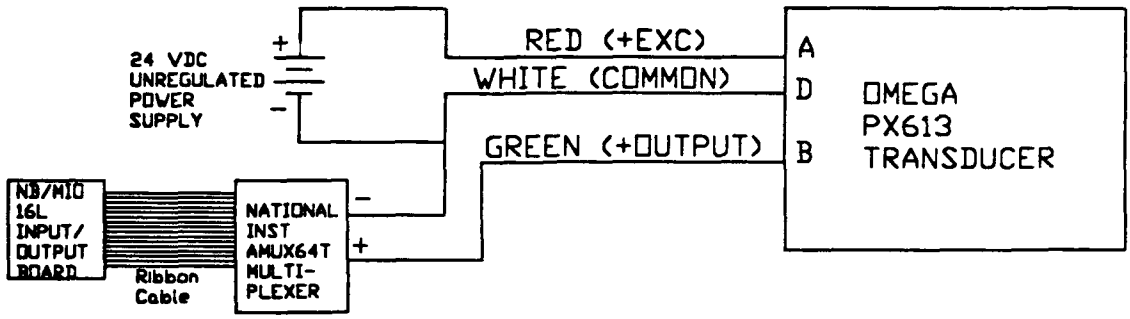

FIGURE 3-9 Pressure Detector Sensing Circuit

3.10.2 Temperature. The temperature detectors are the 1/16 inch K type, chromel-alumel subminiature thermocouple manufactured by Omega Engineering. The selected thermocouples are ungrounded and have an Inconel 600 sheath. The K type thermocouple was selected because it covers the temperature range of -200°C to 1200°C, and for commonality with other projects in the SCWO research initiative. Ungrounded thermocouples were selected for improved accuracy and compatibility with the data acquisition system. High temperature block fittings provide junctions for

the thermocouple adapter fittings. The thermocouple at the preheater outlet is positioned in one of the side ports of the lower block. It extends to the center of the block. The thermocouple at the top of the vessel passes through the high temperature block, and the ⅜ inch tubing into the top of the pressure vessel. To clear the sample holder this thermocouple is positioned slightly off center. High Pressure Equipment thermocouple adapters provide the pressure seal around the thermocouple sheath. The vessel external thermocouple was installed after commencement of operations due to concern that the exterior of the vessel may be reaching excessive temperatures. Millivolt signals are carried by chromel/alumel thermocouple wire through the Lexan® shielding to the input of the read and control computer. The voltage output of the thermocouples is amplified, scanned and converted to temperature readings by the LABVIEW® software package.

3.10.3 Sensor Output Processing. The voltage sensors for the three temperature and three pressure instruments are connected to an input/output board on a Macintosh® IIvx computer via a multiplexer board which quadruples the number of input signals that can be processed. The thermocouple output is in millivolts such that the signal is amplified by the software prior to processing. The pressure signal requires no amplification. The signal processing is a series of virtual instruments assimilated specifically for this application.

LABVIEW® software allows the user to interactively create virtual instruments for a wide variety of uses. The virtual instrument is one developed within the software using a icon driven menu. The software can display a front panel with

desired information. Additionally, the software can show signal flow paths in wiring diagrams. In the SCWO sensor system, the temperature read virtual instrument is a modification to a sample instrument provided with the software. The pressure read instrument, however was developed from basic components. Schematics of the software virtual instruments developed for this project are included as Appendix E.

The thermocouple processing is automatically temperature compensated by a temperature probe on the multiplexer board. The temperature output is an average reading of sixteen samples read over a 100 millisecond period. The output of the temperature instrument is an input to an alarm circuit, a heater control circuit and a system shutdown circuit.

The pressure readout is an average of 10 successive pressure signals over a 100 millisecond period. The output of the pressure instrument is an input to an alarm circuit, a pump control circuit and a system shutdown circuit. The alarms of the individual temperature and pressure monitoring points appear as a red light on the read out panel and an audible alarm. The frequency of the audible alarm was programmed to provide a different tone for each of the different alarm conditions to aid in recognition.

3.11 Control

Primary pressure control of the system is provided by a back pressure regulator at the low temperature outlet of the system. Temperature control is provided by control virtual instruments developed in the LABVIEW® system. Backup pressure control is provided by virtual instrumentation in LABVIEW® as well. Individual

pressure and temperature controllers were considered, but with the total number of sensing functions required for both the exposure and electrochemical corrosion testing loops, and the control functions desired, the LABVIEW® system was in fact less expensive, and provides data recording functions as well as control functions.

3.11.1 Back Pressure Regulator. Pressure is controlled by an adjustable back pressure regulator at the exit of the cool down heat exchanger. A TESCOM model 26-1722 rated up to 6000 psi is installed. The wetted parts of the back pressure regulator are 300 series stainless steel with Kel-F-81® seats. Both the inlet and outlet are ¼ inch - 18 NPT female threaded ports. A ⅛ inch high pressure fitting to ¼ inch NPT adapter made of Inconel 625 provides the transition into the back pressure regulator. The outlet port is a ¼ inch NPT to ⅜ inch Swagelok® adapter made of 316 stainless steel. The remainder of the discharge piping is 316 stainless steel. The back pressure regulator is directly mounted to the Lexan® protective barrier with the valve bonnet and control screw accessible from the side of the enclosure. A locking nut is also installed to secure the position of the control screw.

3.11.2 Temperature Control System. A virtual instrument was developed on the LABVIEW® software to control the temperature. Control signals from the software are sent via a digital input/output board to a relay board. The relays provide a power path for 220 volt AC current to the heater elements. The preheater outlet temperature is compared to a preheater control set point. If the temperature is lower than the setpoint, a signal is sent to maintain the preheater relay closed. If the temperature is higher than the setpoint, the signal opens the relay. To prevent rapid cycling of the

breaker, once the setpoint is reached, the relays will not reclose until a temperature drop of 20°C is sensed. The vessel heater circuit is similar except both the clamshell heaters work together based upon the internal vessel temperature. The vessel heaters also only have a 3 °C temperature drop for the heaters to re-energize. The large vessel and large internal volume is such that even with only a 3°C temperature drop, the cycle time (heaters off until next cycle of heaters off) is about 30 minutes. The temperature overshoot past the setpoint is insignificant on the preheaters, and is 2-3°C with the vessel heaters. The temperature response lags as well once the heaters turn back on such that the total cycle temperature band of the vessel is only 7-9°C.

3.11.3 Backup Pressure Control. Should the back pressure regulator fail, a LABVIEW® virtual instrument was added to secure the pump if the pressure exceeds an operator selected setpoint. The control mechanism is similar to the heaters except the relays control the 120 volt power to the pump. This is not the preferred method of pressure control because the pump cycling on and off reduces both relay and pump life; however, the backup system allows the corrosion test facility to remain operational before reaching a pressure shutdown criteria. The pressure control setpoint is normally 150-250 psi higher than the desired back pressure regulator control pressure. During the heat up cycle, at high pump flow rates, the pressure excursion at the pump outlet occasionally causes the pump to cycle off momentarily. Unlike the temperature circuitry in which a cycle band is present to prevent rapid cycling of the relays, no pressure band was placed in the pump control circuitry. During the sensing interval of 1 second with the pump secured, pressure is reduced rapidly such that the

pump would come back on even with a control band. As this is not the primary means of pressure control, the complexity of the circuit is not necessary. Detailed schematics of both the pressure and temperature LABVIEW® virtual controller instruments appear with the other LABVIEW® instruments in Appendix E.

3.12 Safety Features

A primary concern of the design of the system was operator and equipment safety. The large internal volume at high temperatures and pressures contains a significant amount of stored energy. Rapid release of this energy could seriously injure the operator or destroy the equipment. Safety of the system is a multilevel approach. The system design was conservative, in fact over designed in many components. The LABVIEW® system was programmed with system shutdowns when operator selected setpoints are reached. A safety head pressure relief system is included should other systems fail to control the pressure. And finally the system is surrounded by a high strength Lexan® shield.

3.12.1 Component Design. As mentioned in many previous descriptions, most components are designed for larger stresses than should be experienced in the system. Specifically, even with a safety factor of 4, the vessel still has a corrosion allowance of ⅜ inch. The vessel is designed to leak before fracture. All high pressure fittings are rated to at least 30,000 psi. The tubing has been tested to 11000 psi. The back pressure regulator is rated to 6000 psi. The pumps and pressure detectors are only rated to 5000 psi (340 atm), but the maximum pressure expected in the system is about 4400 psi (300 atm).

3.12.2 LABVIEW® Control Shutdowns. A temperature signal greater than an operator selected setpoint will shut down both the heaters and the pump. If a shutdown condition exists, a subsequent reduction in the temperature signal will not cause the heaters or pumps to restart. This programming was incorporated to prevent the system from coming back on and causing system damage by cycling back to a shutdown condition. Normally the operator selected high temperature shutdown is set at 550°C as read on the vessel internal and preheater temperatures. The external vessel temperature sensor was installed for information only and is not part of the high temperature shutdown circuitry. A high pressure shutdown is also included. It is normally set 200 psi lower than the pressure at which the burst disks will rupture, and controls both the pumps and the heaters. A low pressure shutdown was added after the initial test run. If a leak occurs in the system, which unfortunately has occurred, the pressure is rapidly reduced to the saturated conditions for the temperature of the fluid. To ensure the system shuts down in the leak scenario, during the startup once the system is at operating pressure, the operator depresses a button on the virtual instrument front panel which activates the low pressure shutdown. Depending on the operating temperature, the amount of pressure drop necessary to cause a shutdown can be adjusted. The drop is normally 1000 - 1500 psi below the operating pressure, such that small pressure fluctuations will not cause a shutdown. To alert the operator to a potential problem, audible and visual alarms on the front panel are initiated based upon proximity to the shutdown alarm setpoints. Thus, the pressure alarms sound when within 100 psi of the shutdown condition, while the temperature alarms sound

when within 10 °C of the shutdown temperature condition. Detailed schematics of the shutdown virtual instruments are included in Appendix E. Upon loss of power to the computer, the relays controlling the heaters and the pump de-energize which interrupts power to and results in a shut down of the system. Upon regaining computer power, the relays will not re-energize without operator action.

3.12.3 Safety Heads. The low temperature blocks which contain the pressure sensors also have a High Pressure Equipment safety head machined into one end. The safety head consists of a rupture disk and a seating ring in addition to a threaded outlet port. The installed rupture disks are rated at 4660 psi and are manufactured of Hastelloy C-276 as they were not available in Inconel 625. The outlet port is a 316 stainless steel ⅜ inch NPT female thread into which a 316 stainless steel adapter to ⅜ inch Swagelok® fitting is connected. The outlet of the three safety heads are piped with ⅜ inch stainless steel tubing to form a combined discharge path into the upper section of the lab ventilation hood. All connections are 316 stainless steel Swagelok® fittings. The ventilation hood should be running continuously while the system is operational. Thus if a disk ruptures, the exhaust steam will not enter the room but will be vented outside the building. Figure 3-10 shows details of the safety head.

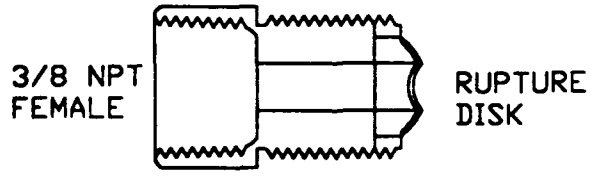

FIGURE 3-10 Safety Head Detail

3.12.4 Shielding. All portions of the system which contain high temperature, high pressure fluid are surrounded by one inch of Lexan® shielding. This material, sometimes referred to as bulletproof glass, provides a barrier to a projectile if one was created during a casualty. The only high pressure component not inside the shield is the HPLC pump due to the requirement to adjust the micrometer stroke controls during operation. As the pump only experiences the low temperature fluid, it does not need to be inside the shield from a safety perspective. The shielding consists of two layers of ½ inch Lexan® panels which were cut from 4' by 8' sheets. The panels are attached to framing with either ½ inch bolts with nuts or with 5/16 inch bolts into threaded angle fittings. The threaded fittings were utilized for the panels which are routinely removed for access to the system. All panels could not be fastened with nuts and bolts because when installing the final panel, the nuts would not be accessible to hold while tightening. The panel routinely removed for access is 4' by 2' and has a weight of 50 pounds. Penetrations through the shielding are limited to the holes for the hold down bolts, back pressure regulator bonnet, pump discharge tubing, heat exchanger cooling water supply, and the system discharge stainless steel tubing. All power and control leads are introduced into the shielded area through the holes in the framing. The shield is not pressure tight, nor is it required to be. The shield limits projectile flight, and would knock down a stream of steam from a leak. The total volume of the system is not such that steam in the room would be an issue.

The control system computer components are in the adjacent room separated by a single layer of ⅜ inch Lexan® . Holes are drilled through this viewing window for

power and sensor leads. Normal operation of the system has the operator inside the inner room only for adjustment of the back pressure regulator, pump flow rate, to refill the fluid supply bottles, or to empty the collection bottle. Otherwise the operator can observe and control all functions outside a total of 1 ⅜ inches of shielding.

3.13 Sample Holder.

The sample holder utilized is a modification to a design developed by Metal Samples Incorporated . As Inconel 625 components were not available, the holder is manufactured out of Hastelloy C-276. There are no welded parts, a requirement, given the experience of welded sample holders of Thomas and Gloyna[30] in industrial sludge. The holder consists of two end plates separated by threaded rods covered by zirconia insulators. A center threaded rod holds the samples, which are separated by ⅛ inch zirconia washers. Both U-Bend and flat coupon samples can be supported by the sample holder. If fully loaded, the holder can support 17, ⅛ inch coupons and 11 U-Bend samples. A smaller number of samples can be held snugly by using more than a single spacer between samples. The sample holder sets into the vessel and rests on the nuts holding the support rods. The end plates are cutout such that only a small section of metal remains for attachment of the support rods, and flow can pass without difficulty. Figure 3-11 is a drawing of the sample holder assembly.

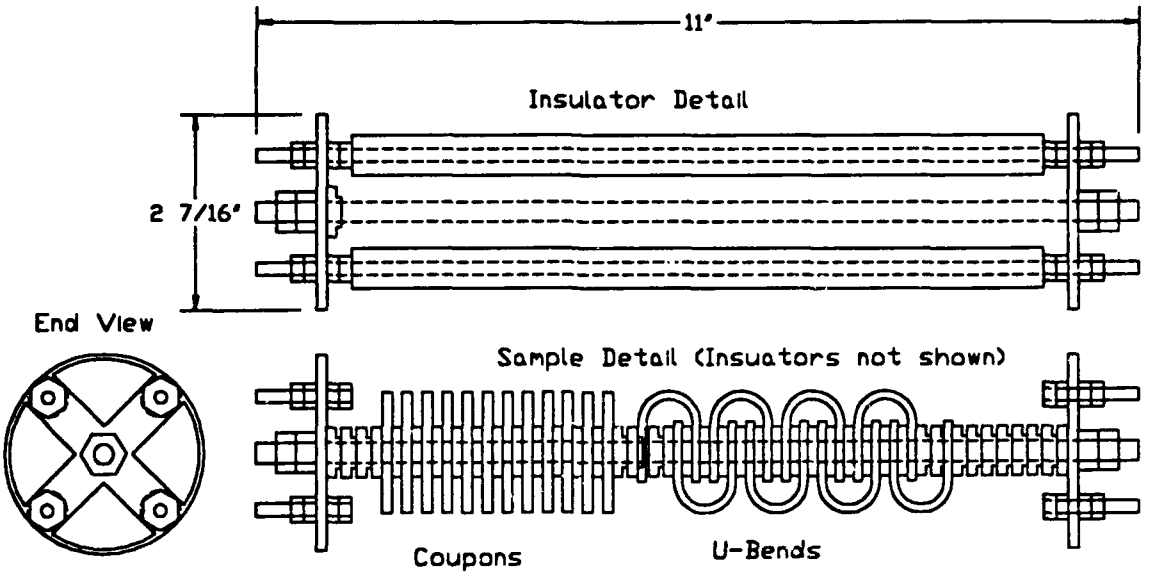

FIGURE 3-11 Sample Holder Assembly

3.14 Support Systems

The corrosion testing loop requires specific support systems and equipment not only for operation but also for analysis of results. For the purposes of discussion, the support systems are divided into four areas. Special equipment and tools were required for the system. A special enclosure was constructed to support the testing facility and protective shielding. The fluids utilized as a test medium have specific equipment requirements for storage and analysis. Finally some unique equipment was utilized in sample analysis which warrants more detailed description.

3.14.1 Tools Coning and threading tools were purchased for preparation of tubing ends to make the high pressure mechanical seals. The strength, toughness and hardness of the Inconel 625 alloy presented problems when trying to machine the

tubing. The dies and cutters degraded rapidly such that replacements were required during the construction process. During operation of the system, leaks developed at some of the unions due to temperature differences associated with the cool down. The steam leaks resulted in damage to the mechanical seal seating surface. Reseating tools were purchased to repair this damage. Finally, the closure clamps have a torquing requirement of 160 foot-pounds, requiring purchase of a large torque wrench and box end wrench to anchor the bolts when tightening..

3.14.2 Enclosure. Construction of a sturdy enclosure to hold not only the test equipment but also the shielding was a significant part of the project. The enclosure is a box 3 ft 7 ½ inches wide and 5 feet long. The total height of the enclosure is 7 feet 1 inch. All of the supports are made of UNISTRUT®, 1000 (1 ⅝ inch) channel , except the top section which is 4000 series (¾ inch) channel. The channel is connected with UNISTRUT® fittings to form two major sections of the enclosure. The first section is enclosed by shielding, the second is open and holds the pump as well as the supply and collection bottles. On first appearance there seems to be more space than required, but room was provided for future growth if needed and the serviceable temperature (180°C) of the shielding is such that it cannot be in close proximity to any of the heated components. Figure 3-12 shows the details of the enclosure.

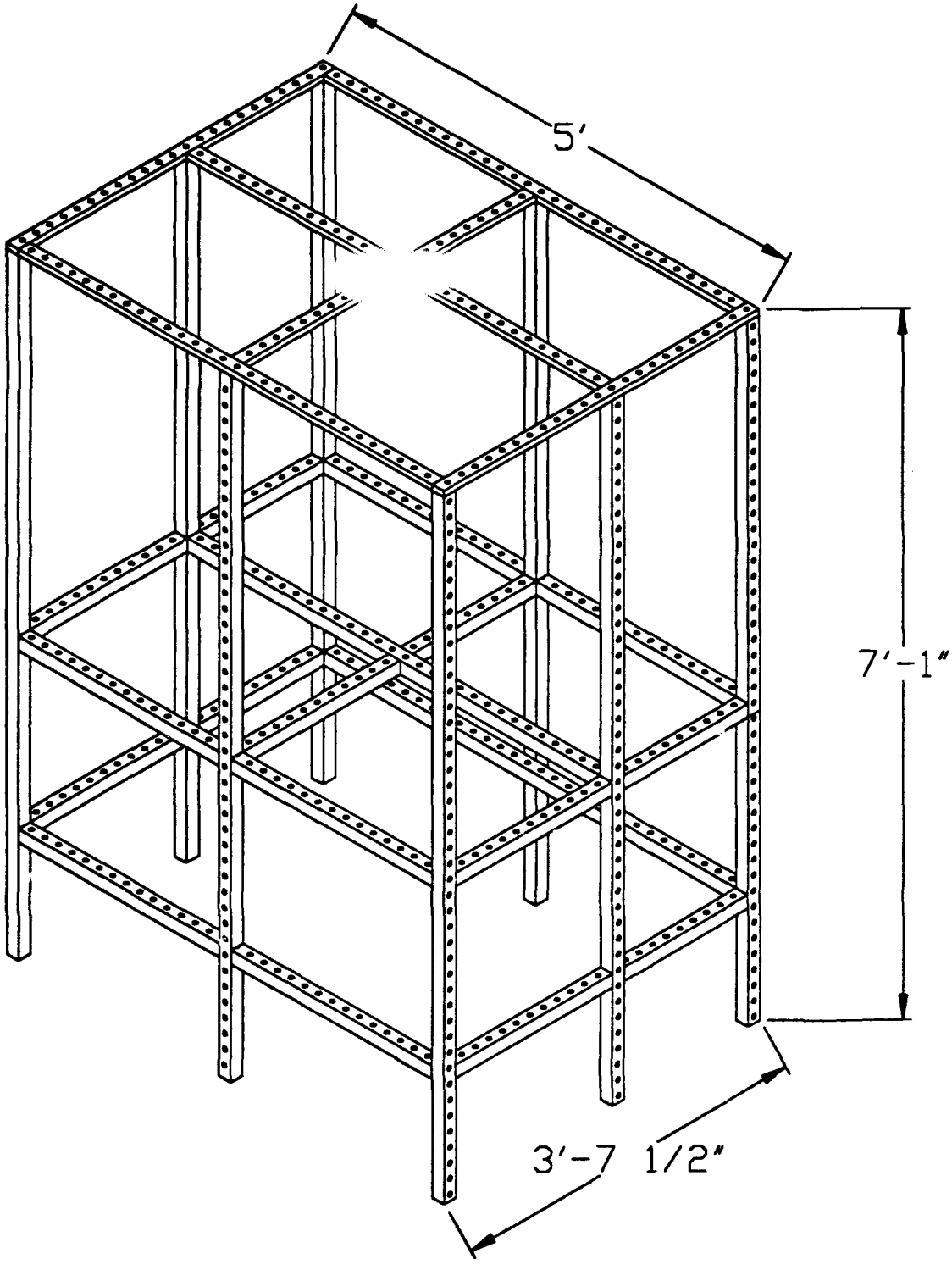

FIGURE 3-12 UNISTRUT® Enclosure Detail

3.14.3 Fluid Support. Deionized water must be supplied to the pump suction. Due to the length of time the system can run, the limitation on length of unattended operation is determined by the size of the supply and collection bottles. To ensure adequate Net Positive Suction Head (NPSH) to the pump, the supply bottles are placed above the pump. This prevents difficulty in priming the pump on initial fill, and allows gravity fill of the system as the pump does not prevent flow through when secured. The supply containers are 20 liter Nalgene® bottles which are connected to the ⅛ inch stainless steel suction tubing with ⅜ inch polyethylene tubing through Swagelok® adapters. The bottles have shut off valves installed. The collection bottle is also of the 20 liter Nalgene® variety. It is located under the discharge piping such that the effluent is allowed to drip into it.

No sample analysis equipment has been installed in the effluent stream as in many SCWO reactors. A Corning Model 340 pH meter was purchased for effluent batch sampling. More detailed analysis have been performed for dissolved metal ions by taking samples to the Massachusetts Institute of Technology, Industrial Hygiene Laboratory.

3.14.4 Sample Support Equipment. The details of the procedure on sample preparation will be described in the next chapter, but some of the specific equipment utilized for analysis needs further explanation. The optical tools utilized to characterize the nature of the surface of the samples include a fiber optic microscope and a laser confocal light microscope. The fiber optic microscope, manufactured by Hirox, provides a clear color image of the surface with magnifications up to 250 X.

The output of the microscope is connected to a digital color printer allowing rapid recording of surface sample images. A drawing of components of the microscope is included as Figure 3-13. The laser confocal microscope, manufactured by LASERTECH, allows magnification up to 6000 X without surface preparation requirements. The laser allows for precise focusing, and the controller has the ability to scan a view and store the highest response for each pixel on the screen. In this way the output is a composite image with each pixel in focus even though the surface may not be smooth.[44] Additionally the microscope has the ability to determine depth while scanning by correlating focus intensity to position of the lens. In this way a profile of a surface can be obtained. A simple schematic of the laser focused microscope is included as Figure 3-14.

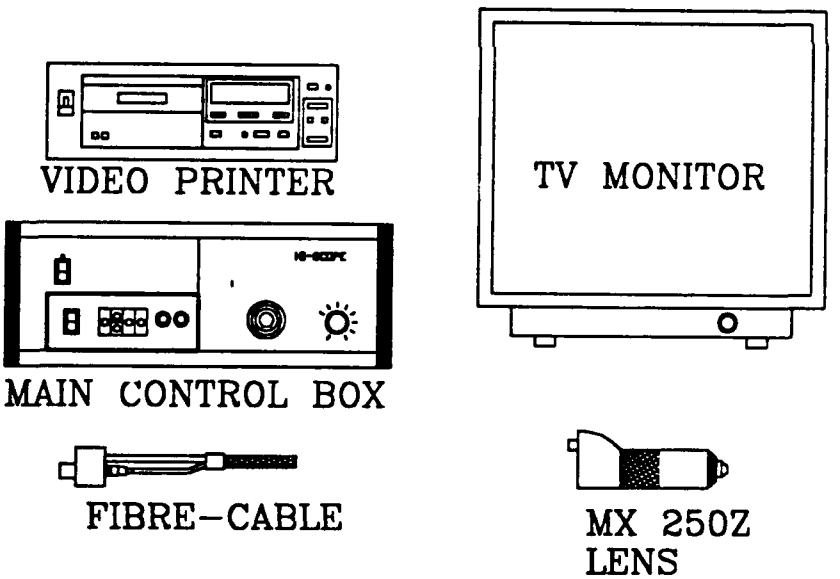

FIGURE 3-13 Fiber Optic Microscope Components

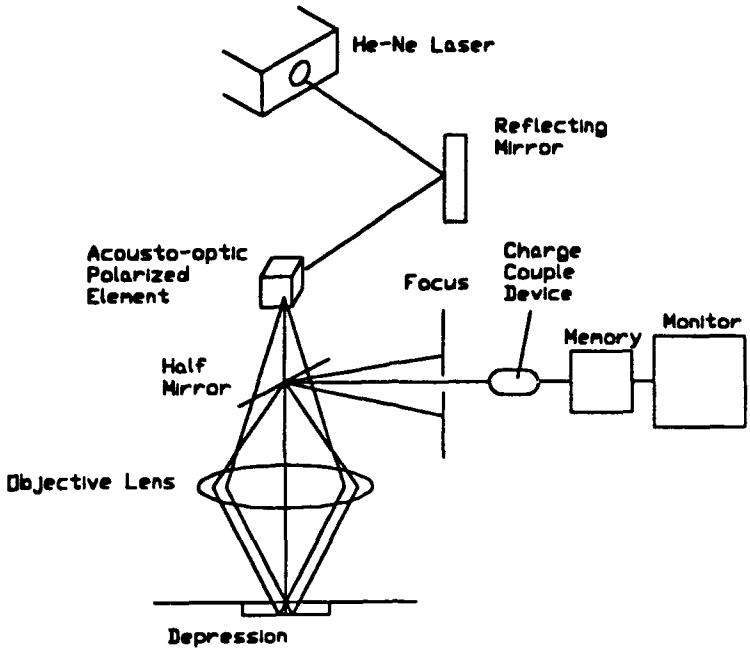

FIGURE 3-14 Laser Confocal Microscope Schematic

3.15 Electrochemical System Differences

The electrochemical corrosion testing system was designed concurrently with the exposure system. The system is currently under construction in the same laboratory. Most of the components are identical to the exposure system, but there are a few differences worthy of note. Some of the changes are simply different sized components as the electrochemical autoclave required volume is significantly less than the exposure autoclave. Other differences are due to the different purpose of the system and include additional equipment requirements.

3.15.1 Component Sizing Differences. The electrochemical system autoclave internal volume is approximately 30 ml requiring smaller components. Specifically, the capacity of the HPLC pump is 15 ml/min and it has only two heads. This requires an

adapter from the 1/16 inch outlet tubing to the ⅛ inch system tubing size. The heaters required for the preheater are reduced to 900 watts and the vessel heaters are reduced to 850 watts each. The reduced size of the autoclave also allows for reduction in the shielding to ½ inch Lexan®, and the support structure is reduced to 4000 (¾ inch) series UNISTRUT®.

3.15.2 Different Equipment. The electrochemical autoclave is drastically different from the exposure autoclave. The autoclave was designed by Dr. D. Bryce Mitton of the H. H. Uhlig Corrosion Laboratory at MIT. It has connections for a reference electrode, as well as a working electrode. Thermocouples are installed at the inlet and outlet of the autoclave. The externally cooled reference electrode has been developed at Penn State University[45] for use in supercritical water power generation plants in Europe. The electrochemical system also has additional analysis equipment in a Sclumberger 1286 potentiostat and 1260 Frequency Response Analyzer for performance of EIS. Sketches of the electrochemical autoclave and reference electrode appear as Figures 3-15 and 3-16.

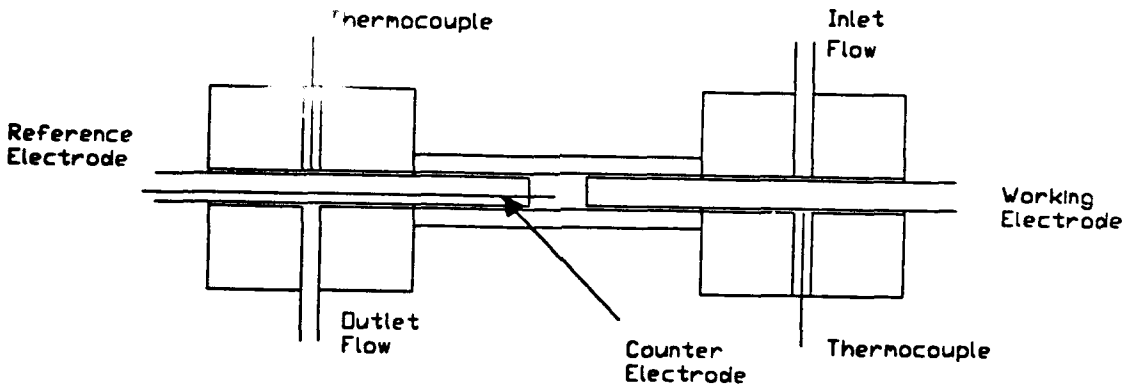

FIGURE 3-15 Electrochemical Autoclave (Schematic of design by D. Bryce Mitton)

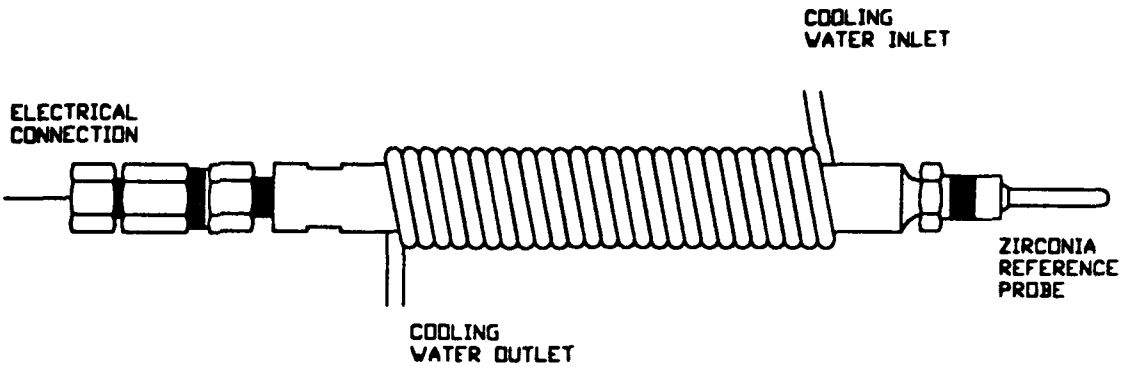

FIGURE 3-16 Externally Cooled Reference Electrode, developed from Macdonald.[45]

3.16 Omitted Equipment

The original corrosion testing system design is without an oxygen source, although one will need to be added at a later time to allow a wider range of environments to be studied. Dissolved oxygen in the feed water can be enough to oxidize some waste streams without the added complexity and cost of an oxygen supply.[46] Testing of The SCWO process for waste destruction nominally monitors the effluent for waste concentration to determine efficiency and adjust the operational parameters of the system. The corrosion test system does not monitor the effluent for residual of waste inlet. Only compounds for which destruction efficiency and kinetic data are available will be tested in the corrosion loop. The only testing performed on the effluent will be to determine the presence of metallic ions for indication of corrosion, and to meet requirements for disposal.[47]

Chapter 4

Description of Experiment

The exposure autoclave is designed for long term corrosion studies. The first series of experiments were initiated to test the operability of the system in addition to testing some metal samples. The experiment basically consists of three distinct procedures. Sample preparation, exposure and sample analysis.

4.1 Sample Selection and Preparation.

To demonstrate operability of the system, samples were selected of the three materials of construction; Inconel 625, Hastelloy C-276 and 316 stainless steel. Samples were provided free of charge from Haynes International but had to be modified to fit inside the exposure vessel. Specifically, the provided samples, shown in Figure 4-1, were ⅛ inches thick, 1 ½ inches wide and 2 ½ inches long. A weld bead was present through the center of the sample, and a ⅜ inch hole was drilled in one end. Modifications to the samples to allow placement into the sample holder, included stamping with a material identification code, cutting along the width and drilling additional ⅜ inch holes. Figure 4-1 also contains the resultant sample size. The cutting and drilling were accomplished in the Laboratory for Nuclear Science machine shop. The final sample size is ⅛ inch thick, ¾ inches wide and 1 ½ inches long with a ⅜ inch diameter hole drilled in the center.

Prior to placement into the sample holder, the samples were prepared in accordance with procedure G-4 of ASTM Standards[48]. The samples were hand polished on a grinding wheel with 320 grit carborundum grinding paper. After the

initial two runs the finish was modified to 800 grit to reduce the interference from the grinding lines during visual analysis. The samples were then measured with a micrometer. Following polishing and measuring, the samples were cleaned in an ultrasonic bath with ALCONOX detergent , Acetone and then demineralized water. The samples were rapidly dried in forced air. Pre-exposure visual images were obtained on some of the samples as a reference. The samples were then weighed with a precision balance. After polishing, the samples were maintained in a desiccator except for the small amount of time when being weighed, measured or photographed.

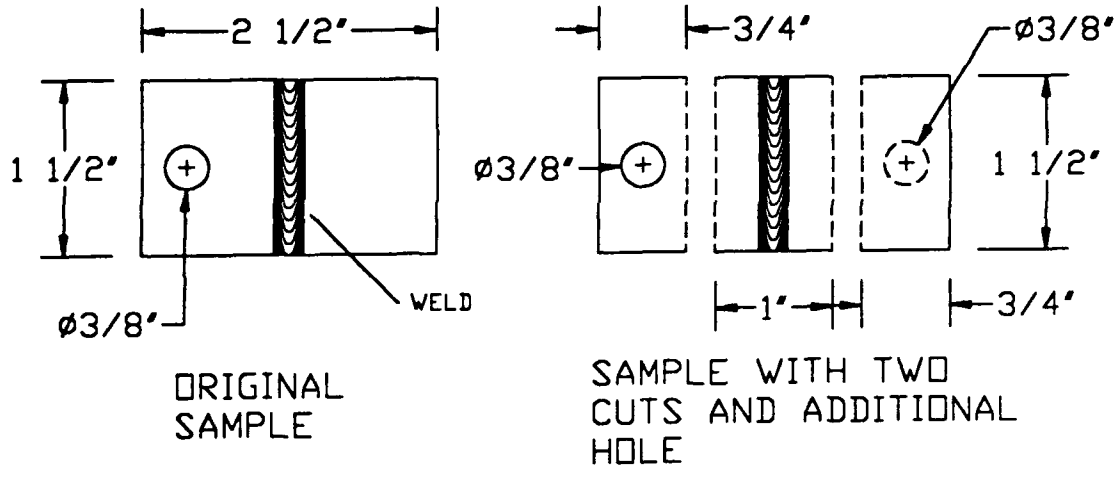

FIGURE 4-1 Sample Initial and Final Configuration

For the initial test runs, the entire capacity of the sample holder was not utilized. The samples were placed on the center rod of the sample holder separated by three to five ceramic washers. Double nuts on the ends of the rod were tightened and the sample holder immediately placed in the vessel.

4.2 Exposure Testing

To insert the samples into the exposure autoclave, some portions of the system must be disassembled. The sequence of events following insertion of the samples includes reassembly of the system, pressurization and heat up, exposure testing, cool down and depressurization, disassembly and finally sample removal.

4.2.1 System Reassembly. When the samples are placed inside the vessel, the lower head is already tightened to the required torque. The upper head is lowered onto the vessel cautiously to ensure the thermocouple clears the sample holder. Ideally the only connection broken between testing runs is the top head clamp assembly such that the discharge piping is attached to the upper head when it is lowered onto the vessel. Testing in more aggressive environments, however may require complete removal of the vessel for adequate inspection between each sample run. The upper head is torqued to the required 160 foot pounds alternately on the four bolts. There is a tendency for the clamp to get hung up on the angled exterior of the vessel; therefore, the clamp must be tapped with a hammer to ensure the clamps are properly seated.

Once the clamps are in place, the system can be filled. The supply valves to the pump from the deionized water source are opened and the LABVIEW® controller is turned on with a control pressure set 150-250 psi above the target pressure for the specific run. The pump will operate continuously until that pressure is reached. When water appears at the discharge tubing, the system is full, and the back pressure regulator is adjusted slowly until the desired pressure is reached. The lock nut is tightened to prevent drifting of the back pressure regulator. As the lagging covers

indications of problems, the system is monitored for leakage before all of the lagging is installed.

With the system satisfactorily operating at pressure, the clamshell heaters are installed around the vessel. Installation prior to this time could cause damage to the heaters especially during the torquing process, as the clearances are small and the vessel moves slightly during tightening. The heaters should be approximately ½ inch from the vessel and then connected electrically with spade type connectors. The external thermocouple is placed at the upper end of the vessel against the wall and held in place with the lagging. The remainder of the lagging on the top of the vessel is then installed.

4.2.2 System Heat up The heater power cord is plugged into the 220 volt outlet, and the LABVIEW® heater controller is set to the desired temperature on the preheater and the vessel heaters. Proper operation of the heaters is verified by rising temperature on the preheater outlet thermocouple and the exterior vessel thermocouple. Once proper operation of the heaters is verified, the Lexan® shielding removed for access to the vessel, is replaced and tightened down. The shielding should be in place before temperature in the vessel exceeds 100 °C so that an unobstructed steam jet would not be released into the room should a failure occur. Cooling water to the heat exchanger is initiated prior to vessel temperature reaching 80°C, to protect the pressure sensors and back pressure regulator. The temperature of the effluent is maintained cool by controlling the flow of the cooling water.

The system heats up to operating temperature without required action from the operator. Effluent flow rate can be monitored, but it is not accurate during the heat up due to the changes in density of the fluid. Once the system is cycling around the desired temperature, the level in the collection bottle can be monitored to determine a flow rate. A discrepancy between this value and the flow rate from pump piston micrometer settings can be an indicator of leakage in the system.

4.2.3 Exposure Testing Once the system is at temperature, the flow of the corrosive fluid can be initiated. Since there is a volume of distilled water which must be displaced, the actual time of initiation of the corrosive media is calculated based upon pump flow rate and volume of the system upstream of the exposure vessel This method may not be exact, but with testing runs which are days in length the error becomes insignificant. Similarly, at the end of the run once the corrosive is secured, the system is operated long enough to purge the system prior to commencing the cool down. The only action required of the operator once at temperature is to monitor the level of fluid in the supply bottle and the collection bottle. Depending on the flow rate, the system has been left unattended successfully for periods of up to 44 hours.

4.2.4 Cool down and Depressurization. The cool down is the most critical portion of the operational cycle. Temperature gradients can cause differences in thermal expansion, resulting in mechanical seals failing to hold pressure. This condition was experienced on two occasions in the proof testing phase and was remedied by maintaining the preheaters energized for portions of the cool down cycle. To commence cool down, the control setpoint for the vessel heaters is reduced to 0 °C.

The controller for the preheaters is adjusted as necessary to prevent temperature differences of 100°C from developing between the vessel and the preheater outlet. In this way cold water is not pumped into the vessel, causing the inlet fitting to leak.

Once the temperature of the vessel is less than 100°C, all heaters are secured, and the 220 volt receptacle is unplugged. The Lexan® shield is removed and lagging and the clam shell heaters are carefully opened up to expose the vessel to additional air. The suction hose from the ventilation hood can also be rigged to evacuate the air around the vessel. This helps significantly in reducing the temperature of the vessel. When the vessel temperature is less than 80 °C the pressure is relieved by setting the control pressure to 0, switching off the pump, and fully opening the back pressure regulator. The pump must be shut off because the pressure instruments sometimes register negative pressure when the system is at ambient, and the controller would turn the pump on if the switch was not turned off.

4.2.5 Disassembly and Sample Removal. Once the vessel temperature is less than about 45 °C and lagging and the clamshell heaters are removed, the upper head clamps can be removed and the vessel upper head removed. The thermocouple adapter fitting is also removed to allow the vessel head to be placed on a platform adjacent to the vessel. The sample holder is removed from the vessel without draining the standing water. To minimize exposure to the atmosphere, the samples are immediately removed from the sample holder, dried using forced air, and then placed in sample boxes inside a desiccator. The samples, and sample holder are handled with rubber gloves or plastic forceps at all times to maintain cleanliness.

4.3 Sample Analysis Techniques

The samples are analyzed by weight loss and visual methods. For the initial operability testing, weight loss measurements were taken but no attempts to remove corrosion products were conducted, though they may be in future testing. The visual evaluation is by multiple means.

The appearance of the samples with the unaided eye was noted and recorded with a camera. The samples were then examined with the fiber optic microscope described in the previous section. The laser confocal microscope was then utilized to examine specific areas identified in the previous examinations. A profile map of areas of concern was utilize the level of the surface. A light microscope was also utilized to obtain more detailed photographs of some of the samples as the video printer associated with the laser and optical microscopes does not present the same detail. Finally specific samples were mounted in epoxy and examined in cross section to determine the nature of the surface layer.

Chapter 5

Experimental Results and Discussion of Results

The exposure autoclave system achieved supercritical conditions at 1230 on 2 March 1994. No samples were in the vessel during this initial cycle, and only deionized water was utilized. The system operated well and reached conditions of 500°C at 3550 psi (241.5 atm). An initial series of tests in deionized water at three temperature regions was conducted to demonstrate the functionality of the system and develop a methodology for sample preparation and evaluation. The three temperature regions were chosen to represent the subcritical (300°C) range, the low supercritical (400°C) and the higher supercritical range (500°C). Table 5-1 details the conditions for the testing sequence.

Run No.	Temp	Pressure	Samples	Flow	Medium	Duration
1	500°C	341.5 atm	Inc 625 C-276 316 SS	8 ml/min	DI Water	96 hours
2	300°C	341.5 atm	Inc 625 C-276 316 SS	8 ml/min	DI Water	96 hours
3	400°C	341.5 atm	Inc 625 C-276 316 SS	8 ml/min	DI Water	24 hours

Table 5-1 Sample Testing Conditions

The third run was truncated from the desired 96 hours due to development of a steam leak at the high temperature block at the vessel inlet which subsequently required repairs.

5.1 Visual Observations

The overall general appearance of the samples was noted following removal from the vessel. All samples displayed some degree of discoloration with marked changes at the area around the insulating washer. Table 5-2 details the results of the visual observations of the samples.

Run	Material	Visual Observation
1	Inconel 625	Patchy bronze colored appearance over exposed region, area under insulator washer is not as dark in color.
1	Hastelloy C-276	Greyish uniform appearance over the entire exposed surface. Area under the insulator is somewhat lighter and shinier.
1	316 SS	Surface has a blue tint. Area under the insulating washer is shiny.
2	Inconel 625	Very Patchy bronze colored surface, area under insulating washer is still shiny similar to conditions prior to exposure.
2	Hastelloy C-276	Grey appearance over exposed surface, with shiny area under insulator.
2	316 SS	Surface has a blue tint with many splotches of brownish color, the area under the washer is not as shiny as pre-exposed metal.
3	Inconel 625	Relatively uniform bronze colored surface with slightly lighter and shiny area under the insulator.
3	Hastelloy C-276	Milky grey uniform appearance over the entire exposed surface. Area under the insulator is somewhat lighter and shinier.
3	316 SS	Bluish tint is not as apparent as in previous samples. Area under the insulator is shiny with patches of brown.

Table 5-2 Visual Sample Results

The visual observation though not precise in nature, allows a basis for comparison of one sample to another. Of note, 2 samples of each material were

placed into the vessel. In each case, the visual observation of the two samples was either the same or of the same character. Observed changes were slightly intensified for the sample located higher in the vessel. It appears the higher position corresponds to a somewhat higher temperature due to discoloration of the vessel.

Following visual observations, the samples were weighed. Details of the weighing are presented in Appendix F. For each of the samples in this series, a slight weight gain of 0.0001 to 0.0016 gram was experienced. This is probably attributable to the formation of the previously mentioned film on the surface of each of the samples. The procedure of determination of weight change is one requirement of the experimentation process.

5.2 Fibre Optic Microscopic Observation

Each of the samples was examined with the 250 x fibre optic microscope. The colors and details presented by this tool, help to identify anomalies on the surface to facilitate further investigation. Some of the images of this microscope, in a black and white form, are presented in Appendix G. These images were produced with a video printer, such that the 250 x available on the local monitor is reduced to 100 x on the hard copy output. Table 5-3 summarizes the observations made with this microscope. Of particular note are the colors of the surface and the apparent masking of the polishing lines by a film on the surface. Additionally, the photographs of the areas around the insulating washer show not only a characterization of the surface in both the exposed and masked areas, but also a detail of the transition region. The slight differences between samples of the same material at different heights in the reactor are

noticeable in these views. The degree of tightness of the washer in addition to the probable temperature differences may contribute to the slightly different nature of the surfaces of similar materials in the same basic environment.

Run	Material	Visual Observation
1	Inconel 625	Dark Brown appearance with shiny patches and dark spots covering the entire exposed surface. No polishing lines remain in the exposed area. The transition region to the area under the insulation washer shows polishing scratches. The area under the insulator has a lower density of shiny spots, and has a bluish color. Polishing lines are barely present under the insulated area. (G - 1)
1	Hastelloy C-276	Greyish appearance with small shiny spots over the entire exposed surface Area under the insulator is brownish with some evidence of polishing lines remaining. (G - 2)
1	316 SS	Polishing lines on the surface are detailed, similar to preexposed sample. The area under the insulator is somewhat grey in nature with softened polishing lines.
2	Inconel 625	Brown appearance on exposed region, with some evidence of polishing lines. There are no dark spots noted. The area under the insulating washer is shiny and shows polishing scratches similar to conditions prior to exposure.
2	Hastelloy C-276	Brownish appearance over exposed surface, with some evidence of polishing scratches. The area under the insulator is similar to preexposed conditions.
2	316 SS	Exposed area is dark with slight evidence of polishing scratches. The area under the washer is shiny with polishing scratches but also contains areas of brown material. (G - 3)
3	Inconel 625	Similar in appearance to run 1 sample, but the shiny patches are not as pronounced or numerous.
3	Hastelloy C-276	Similar in appearance to run 1 sample.
3	316 SS	Similar in appearance to run 1 sample.

Table 5-3 Fibre Optic Sample Observations (250 x)

5.3 Laser Confocal Microscope Observations

The sample surfaces were observed at magnifications up to 6000 x using the laser confocal microscope. The images were compared to preexposure images to note differences. The preexposed images were dominated by polishing scratches, but were focused without difficulty. For the exposed samples, the difficulty in focusing the microscope, especially in the higher magnifications, demonstrated the irregular nature of the surface. The ability of the microscope to form a composite focused image, was beneficial in characterizing the surface, but the images were sometimes still not clear because of the surface irregularity. Table 5-4 summarizes the results of the laser microscope survey. The video printer output produces an image with a maximum magnification of 2000 x . A sample image of this survey appears in Appendix G.

The laser images themselves, while interesting, did not present any conclusive evidence as to the characterization of the surface or the irregularities. Additionally, the lack of color in these images made identification of differences in the nature of the surface difficult.

Run	Material	Visual Observation
1	Inconel 625	There is a dark covering over most of the exposed surface. Shiny spots and darker spots are present. Insulated area has dark areas in an otherwise polishing scratch background. Unable to get a good representation at higher magnification due to irregularity of surface.
1	Hastelloy C-276	Uniform dark surface without evidence of polishing lines. The surface is not smooth however. Under insulation polishing scratches are partially masked by dark circles.
1	316 SS	Surface has some evidence of polishing scratches, some areas more prevalent than others. There are some dark patches within and around shiny spots. The area under the insulator shows few dark spots.
2	Inconel 625	Image is dominated by polishing lines with some evidence of dark spots distributed over the surface. (G - 4)
2	Hastelloy C-276	Surface is somewhat uniform in appearance with a few dark spots and minor evidence of polishing scratches.
2	316 SS	Polishing scratches appear partially filled in with rough material, rather than circular spots.
3	Inconel 625	The surface is somewhat uniform, free from scratches but has numerous shiny spots as well as dark spots.
3	Hastelloy C-276	The surface is free from scratches, and spots but is not smooth as indicated by difficulty in focusing.
3	316 SS	The surface has some evidence of polishing scratches which are masked by a dark rough material.

Table 5-4 Summary of Laser Images

5.4 Light Microscope Analysis

The samples were examined using a light microscope to determine if the nature of the surface irregularities could be classified. The clarity and color of the light images allowed identification of raised portions and pits on the surface of some samples. Table 5-5 is a summary of the results of the light microscope observations.

Run	Material	Visual Observation
1	Inconel 625	There was evidence of raised shiny patches and some pitting in addition to some raised spots on the surface. (G - 5)
1	Hastelloy C-276	The sample shows a uniformly bumpy surface with no evidence of pits or raised spots.
1	316 SS	The image presents a relatively uniform surface with some slight remnant of polishing scratches. No evidence of pitting or raised spots.
2	Inconel 625	The surface shows some evidence of polishing scratches remaining. The surface has few raised spots and no evidence of pitting. (G - 6)
2	Hastelloy C-276	There is no evidence of pitting or raised spots, only remnants of polishing scratches.
2	316 SS	Polishing scratches seem to be intensified in some regions indicating the possibility of some localized attack. (G - 7)
3	Inconel 625	There is evidence of pitting and raised spots. The pitting seems more prevalent than in 500°C sample. (G - 8, G - 9)
3	Hastelloy C-276	The sample appears similar to the 500°C sample.
3	316 SS	The sample appears similar to the 500°C sample.

Table 5-5 Light Microscope Sample Results

5.5 Laser Surface Profiling

Following identification of pits and raised portions on the surface of some of the samples, attempts to measure the dimensions of the irregularities were performed using the profiler on the laser confocal microscope. Figure 5.1 depicts the profile of a pit in the surface of an Inconel 625 sample which was exposed to deionized water for 24 hours at 400°C and 241.5 atm. The cursers on the image indicate a pit width of 12 μm and a depth of 3.7 μm. The remainder of the surface is fairly level in this view. Figure 5.2 shows the same pit without the interference of the profiling lines.

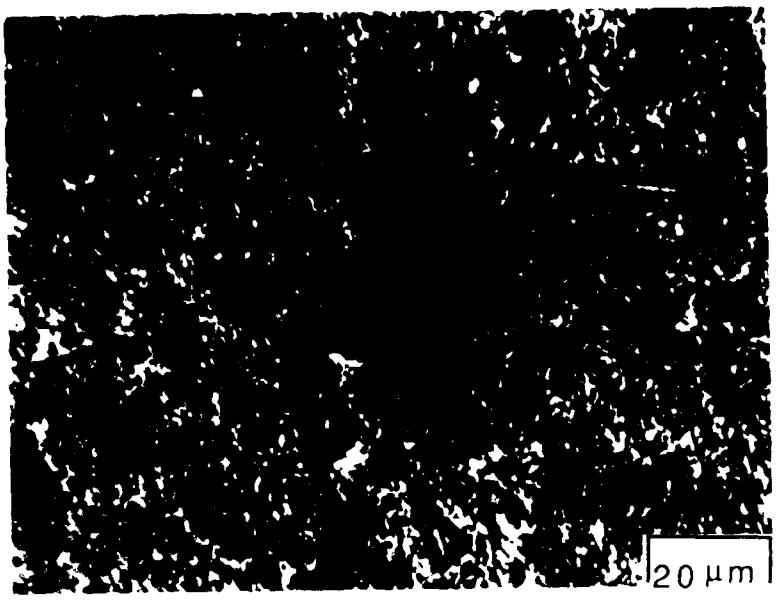

Figure 5 - 1 Confocal laser microscope surface profile of Inconel 625 exposed to deionized water at 400°C, 241.5 atm; for a period of 24 hours. (800 x)

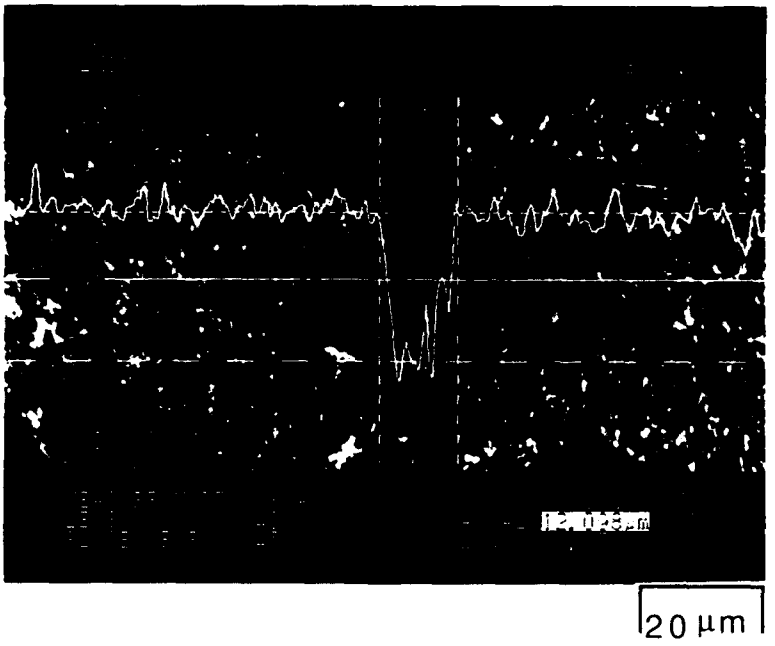

Figure 5-2 Confocal laser microscope image of Inconel 625 exposed to deionized water at 400°C, 241.5 atm; for a period of 24 hours. (800 x)

Of the pits profiled, the width was in the range of 8 - 14 μm, with a depth of 2 - 4 μm. In addition to pits, the dark circular raised spots were profiled. These spots ranged from 8 - 20 μm in width with a height in the same dimension as the pit depth. Additionally the large shiny areas on the Inconel 625 samples exposed at 500°C were profiled. They have a height in the 1 - 2 μm range with widths up to 80 μm. On one occasion an irregularity was profiled with half being raised, the other half being indented into the surface.

The surface of the 316 stainless steel exposed to the 300°C environment was profiled. The surface is very irregular in the darkened region, but some areas are raised while others are depressed. Finally a Hastelloy sample which had experienced a supercritical environment was profiled, revealing a very rough surface as expected from previous observations. Profile plots appear in Appendix G. (G - 10,11,12,13,14)

5.6 Cross Sectional Analysis

A single sample of Inconel 625 from the 400°C run was mounted and polished to allow a cross sectional analysis. The surface was polished down to a 1 μm finish with diamond paste. Due to the relatively rough surface finish of the original sample, microscopic analysis of the surface revealed no conclusive evidence of pitting . Attempts were made to etch the sample as well, to determine if grain boundaries could be correlated to surface irregularities. This effort to etch was not successful.

5.7 Discussion of Results

The weight change and visual results indicate some sort of layer is formed on the surface of the three metals exposed to the deionized water environment. The

appearance of the surface is different in the three materials. As the only environment tested was deionized water, any conclusions as to acceptability of a particular material for use in another SCWO environment would be premature.

5.7.1 316 stainless steel The stainless steel samples seemed to form a surface layer more readily in the subcritical environment. Specifically the polishing scratches, are more evident in the supercritical samples, and the appearance of the subcritical sample has large irregularities on the surface. There appears to be no evidence of pitting in this environment of deionized water.

5.7.2 Hastelloy C-276 The C-276 samples appeared to form a relatively complete rough surface layer in the supercritical region. The surface layer as evidenced by remaining polishing scratches, is not formed as readily in the high subcritical condition.

5.7.3 Inconel 625 In the supercritical environments, Inconel 625 forms a surface layer, but is also susceptible to pitting. Finding, what may be a partially filled in pit indicates the pits are probably related to raised spots which also form on the surface. Either the pits form under the spots, and then the raised portion is knocked off, or the pit fills up to form the raised area. Cross sectional views were unable to determine the composition of the area under the raised spots. Large shiny raised areas were also evident on the 500°C samples. In the subcritical environment, the layer on the Inconel 625 surface does not seem to form as readily as evidenced by remnants of polishing scratches.

Chapter 6

Conclusions and Considerations for Future Work

An exposure corrosion test facility is in operation in the H. H. Uhlig Corrosion Laboratory at the Massachusetts Institute of Technology. The ability of the system to achieve and maintain supercritical water conditions for extended periods of time has been demonstrated and selected samples have been tested in various temperature regimes. The system now serves as a prototype for a companion electrochemical facility nearing completion. When in operation the two systems will provide the ability to test a wide variety of materials in a matrix of chemical and temperature environments. The results of these tests will be crucial in the design and selection of materials for use in developing large scale SCWO hazardous waste destruction facilities.

6.1 System Performance

The exposure test facility has worked well in service to date. Differences in temperature at mechanical fittings have lead to steam leaks requiring repairs on two occasions. Modifications to the operating procedure to limit temperature differences should improve the reliability of the system. Additionally the control system is conservatively based, such that a single erroneous signal can cause a system shutdown. With experience, it should be possible to modify the system to provide more reliability for continuity of operation.

The system, as constructed, functioned properly from the beginning. Minor modifications were made to improve system operation. Specifically the heat exchanger

was moved about 20 cm further away from outlet high temperature block. This was done to allow some ambient heat loss from the effluent before being cooled by the heat exchanger. The stainless steel Swagelok fitting on the heat exchanger inlet was becoming discolored due to the excessive temperature. Moving the heat exchanger has resolved the problem. Additionally, a thermocouple was added to monitor the exterior temperature of the vessel, to ensure maximum material temperatures are not exceeded. Finally additional insulation was added to limit the heat loss and reduce the heater breaker cycling times.

The system is simple to use as was the intention and control of the operation is essentially automatic during operation. The heat up can proceed without operator action once all system components are assembled and adequate cooling water is flowing through the heat exchanger. At the test temperature and pressure, only replenishment of the fluid supply and discarding of effluent are required operator actions. The cool down process requires some monitoring to ensure large temperature differences do not exist which might cause mechanical fittings to leak. Loading and unloading of samples is a somewhat cumbersome task, requiring partial system disassembly and removal of the vessel head.

6.2 Materials Evaluation

The three significant materials of system construction were tested in a deionized water environment. All materials formed a layer, as yet to be identified, on the surface in one or more of the conditions tested. The Inconel 625 apparently exhibited shallow pitting behavior at the supercritical temperatures. This is a concern

because all of the elevated temperature strength bearing portions of the system are constructed of this material.

The fibre optical and laser confocal microscopes provide additional insight into the characterization of the surface of the samples. The profiling capability on the laser microscope, provides a relatively accurate surface topography without elaborate sample preparation requirements. The fibre optic microscope, in addition to being employed in an initial observation of the sample, was utilized to examine the interior of the vessel for the presence of localized corrosion following discovery of pitting on the samples. Only the end regions of the vessel are accessible with the microscope, and no conclusive evidence of pitting on the vessel was observed.

6.3 Considerations for future work

This facility can provide a significant amount of information required to help answer the questions of material selection and design of SCWO reactors. There are improvements in the tools and methodology which should be incorporated into the subsequent testing schemes. A matrix of test solutions and materials should be developed for evaluation in this reactor. Finally corresponding tests with this reactor and the electrochemical reactor should be performed to better understand the mechanisms of the corrosion processes.

6.3.1 Improvements The system can provide additional information than was obtained from the initial runs of system proof testing even in the same environments. The initial sample run at 500°C may have had some contamination of the system due to materials utilized in the construction process. Specifically the SULFO® cutting fluid

contains a variety of compounds which could have affected the initial sample results. The initial run should be repeated to determine if contamination was a factor for the first samples.

Samples should be polished to a finer finish prior to placement in the cell. The polishing scratches, though helpful in determining the evidence of a surface film, prevent identification of small surface irregularities when viewed in a cross section. The apparent pitting identified on the Inconel 625 surface had depths in the 2-4 μm range, which cannot easily be discerned from polishing scratches made with 320 or even 800 grit paper. Additionally, the polishing scratches may provide initiation sites for some of the corrosion processes. It could be argued that any components placed in service will not be polished, thus the results obtained using polished specimens would not accurately reflect of susceptibility of the metal to an environment. The purpose of the testing is to determine mechanisms and conditions leading to corrosion, and polishing scratches may interfere with this determination. Finally, the electrochemical testing, which will be performed concurrently with this facility will have polished samples, thus correlation would be more accurate.

An evaluation of the layer on the surface of the samples might be beneficial to determine its chemical composition. The layer may in fact be a beneficial oxide. If that is the case, a period of time of preconditioning in a deionized water environment to establish the oxide layer prior to introduction of more aggressive solution, might be beneficial, establishing some operational parameters for a large scale system. Preconditioned samples may be utilized in some future materials testing matrix.

The operating procedures need to be evaluated over a longer period of time to determine the extent of damage to the vessel and piping. During periods of long term inactivation, the system should be flushed and purged to limit the concentration of potentially damaging solutions. Other operational limitations and restrictions may become apparent as experience with the system is obtained.

6.3.1 Testing matrix A wide variety of materials and solutions can be tested in the corrosion facility. In addition to the flat sample coupons, creviced samples and stressed samples should be included. The use of witness wires in other portions of the system may be a possibility, to obtain a general indication of corrosion in another temperature regime. Initial test solutions should be limited to those for which kinetic studies have been performed, to reduce the potential of inadvertently employing a solution which could severely damage the system. The materials to be tested should include not only metallic alloys, but also ceramic materials and other possible liners. A high pressure oxygen source may ultimately need to be added to allow testing of all environments expected in a SCWO reactor hazardous waste destruction system.

6.3.3 Electrochemical corrosion test facility Lessons have been learned from the construction and operability testing of the exposure test facility which can be incorporated into the electrochemical system. The development of high temperature reference and working electrodes for use in the cell provides an additional area of challenge. Once the joint facility is operational, materials can be evaluated in both systems in similar environments, such that results can be compared to gain a better understanding of corrosion processes.

Appendix A

Composition of Alloys and Waste Streams

Composition of Alloys of Interest (%):

Austenetic Stainless Steel

Alloy	C	Fe	Ma	P	S	Si	Cr	Ni	Mo	Source
316 Stainless	0.08	62-69	2.00	0.045	0.03	1.00	16-18	10-14	2-3	(49)

Nickel-Based Alloys

Alloy	C	Fe	Nb	Si	Cr	Ni	Mo	W	Source
Inconel 625	0.1	5.0	4.0	0.5	21.5	62	9.0	--	(49)
Hastelloy C-276	0.01	5.5	--	0.08	15.5	57	16	4.0	(49)

Nickel-Cobalt Based Alloy

Alloy	C	Fe	S	Cr	Ni	Mo	Co	Ti	P	Source
MP35N	0.005	0.90	0.004	20.34	33.75	9.35	34.85	0.80	0.001	(25)

Composition of Waste Stream, From Bramlette et. al [28]

Hanford Mixed Waste Simulant (Neutralized by NaOH)

Component	Weight Percentage	
H_2O	98	
HNO_3	0.63	
$NaNO_3$	0.46	
Na_2CO_3	0.20	
NaOH	0.40	
$Na_xH_y(EDTA)$	0.19	(x = 3,4; y = 1,0)
$Na_3C_6H_5O_7$	0.03	
$Al(NO_3)_3$	0.06	
$Fe(NO_3)_3$	0.02	

Other additives <0.01%: Oxalic Acid, $Ca(NO_3)_2$, KNO_3 , $Mg(NO_3)_2$, $Mn(NO_3)_2$, $Zn(C_2H_3C_2)_2$, NaH_2PO_4 , NaCl , $Na_2B_4O_7$, $La(NO_3)_3$, $Nd(NO_3)_3$, $Ce(NO_3)_3$

28.

Appendix B

Parts List

Manufacturer	Description	Part Number	Application
Reflange	6" OD Vessel	R-CON-4	Pressure Vessel
Omega Engineering			
	24 VDC Power Supply	U24V101	Pressure Inst.
	6 Pressure Transducers	PX-613-5KG1	Pressure Inst.
	Ceramic Heater	CRFC-66/240	Preheat (EXP)
	Ceramic Heater	CRFC-46/240	Preheat (EC)
	2 Ceramic Heaters	CR[illegible]240	Vessel Heat
	Twist Lock Connector	PT[illegible]	Pressure Inst
	Shielded Cable	TX-4-10'	Pressure Inst.
	10 K-Type Thermocouples	KMQIN-062-U-12	Temp Inst.
	6 Pressure Snubber	PS-4D	Pressure Inst.
	100 ft Thermocouple wire	GG-K-20	Temp Inst.
	Hole, Fish Spine (1000)	FS-110-20	Heater Wire
Metal Samples			
	C-276 Sample Rack	Special Order	Sample (EXP)
	Zirconia Spacers	905	Sample (EXP)
Apple Computer			
	Macintosh IIvx	M1358	Control
	RGB Monitor	M0297	Control
	Monitor Stand	M0403	Control
	Apple Ext. Keyboard	M0142	Control
Eldex Laboratories			
	100 ml/min HPLC Pump	BBB-4	Pump (EXP)
	10 ml/min HPLC Pump	AA-100s	Pump (EC)
National Instruments			
	LABVIEW for Macintosh	ver 2.2.1	Control
	Analog Input/Output board	NB-MIO-16L-9	Control
	Analog Multiplexer	AMUX-64T	Control
	Digital Input/Output board	NB-DIO-24	Relay Control
	Cable Adapter	SC-2051	Relay Control
	Relay Module	SC-2062	Power Control
	PID Control Software		Control (EC)

National Instruments (continued)			
	Rack Mount Kit	181080-2	Control
Tube Methods	200 ft Inconel 625 Tubing	0.125 OD/ 0.040 ID	Tubing
Swagelok			
	4 Bored Through Reducers	SS-200-R-6-BT	Heat Exch
	4 Union Tees	SS-600-3	Heat Exch
	2 Union Tees	SS-600-3	Safety piping
	2 ⅜ to ¼ NPT adapters	SS-600-1-4	BPR Outlet
	4 ⅜ to ⅜ NPT adapters	SS-600-1-6	Safety piping
	3 ⅛ to ⅜ reducers	SS-600-6-2	Pump suction
	10 ⅜ tube inserts	SS-605-4	Poly Tube
	4 ⅜ Union elbows	SS-600-9	Safety Piping
	3 ⅜ Unions	SS-600-6	Chilled Water
Northeast Engineering			
	2 Backpressure Regulators	TESCOM 26-1722	Press Control
Eagle Stainless Steel	100 ft ⅜ stainless steel tube	316 seamless	Heat Exch Safety Piping
Cole Parmer Instrument			
	pH meter with probe	G-58903-10	Sample outlet
Unistrut Northeast Corporation			
	8 U brackets	P-1047	Support Box
	4 Post braces	P-1887	Support Box
	8 Z shaped fittings	P-1736	Support Box
	1 Flat plate fitting	P-1925	Support Box
	1 Flat plate fitting	P-1953	Support Box
	28 Winged shape fittings	P-2223	Support Box
	4 Winged shape fittings	P-2227	Support Box
	4 Wing shape fittings	P-2345	Support Box
	200 Spring nuts	P-1010	Support Box
	100 Hex head nuts	HHXN050	Support Box
	200 Flat washers	HFLW050	Support Box
	300 Hex head bolts	HHCS050094	Support Box
	22 90 degree braces	P-1026	Support Box
	100 ft 1 ⅝" channel	P-1000HS	Support Box
	110 ft ¾" channel	P-4000HS	Support Box
	8 Z shaped fittings	P-1734	Support Box
	8 U brackets	P-1732	Support Box
	80 Spring nuts	P-4010	Support Box

Unistrut Northeast Corporation (continued)			
	80 Hex head bolts	HHCS050175	Support Box
	40 Hex head bolts	HHCS031125	Support Box
	40 Flat washers	HFLW031	Support Box
High Pressure Equipment Corporation			
	Special Equipment	Safety Heads	Low T Block
	Special Equipment	Thermocouple	High T Block
	Special Equipment	Electrochemical Cell	(EC)
	⅛ female HiP to ¼ NPT	30-21HF2NMB	BPR Inlet
	3 way valve	30-13-HF2	Dump Valve
	Coning Tool	2HF2	Pipe Joints
	Threading Tool	2MHF2	Pipe Joints
	T - Inconel wetted parts	60-23HF2	Pump disch
	6 spare gland nuts	60-2HM6	Spares
	6 spare collars	60-2H6	Spares
	Reseating tool ⅜"	RTHF6	Repairs
	Spare cutter	2-HF2L	Coning
	Spare collet	2-HF2P	Coning
	Spare threading die	⅛" - 40LH	Threading
	Reseating tool ⅛"	RTHF2	Repairs
	6 Thermocouple adapters	1521AF1HM2-T	Temp
	12 Rupture Disks	C-276: 4500 psi	Safety Head
	Cutter ⅜"	2-HF6L	Coning ⅜"
	Collet ⅜"	2-HF6P	Coning ⅜"
MODAR	3 ⅜" Inconel nipples	None	Head inlet/ outlet
MIT Physics Stockroom			
	Miscellaneous wires connectors and cables		Heater control
Morgan Thermal Ceramics			
	Insulating Brick	OLS 131740	Preheater base
	Kaowool fiber board		Insulation
	Kaowool Ceramic Blanket		Insulation
Sears Roebuck - Craftsman Tools			
	0 - 250 ft-lb torque wrench		Tighten clamp
	1 7/16 socket		
	⅜ to ½ " adapter		
	1 7/16 " box end wrench		
Nalge company	5 Nalgene bottles	20 Liters	Water supply

General Electric Plastics Division			
	9 4' x 8' Lexan sheets	MR-5	Shielding
MIT Office of Lab Supplies			
	Tygon Tubing	⅜ inch	Chilled Water
	Poly Tubing	⅜ inch	Pump suction

Notes:

EXP - Component is present in Exposure System Only
EC - Component is present in Electrochemical System Only

Trademark Listings

Kel-F® and Kel-F-81® are registered trademarks of the 3M company

UNISTRUT® is a registered trademark of the Unistrut Company

LABVIEW® is a registered trademark of National Instruments

Kaowool® is a registered trademark of Morgan Thermal Ceramics Company

Lexan® is a registered trademark of General Electrics, Plastics Division

Swagelok® is a registered trademark of the Swagelok Company

Macintosh® is a registered trademark of the Apple® Computer Company

Nalgene® is a registered trademark of the Nalge Company

SULFLO® is a registered trademark of SULFLO Inc.

Appendix C

Photographs of System Components

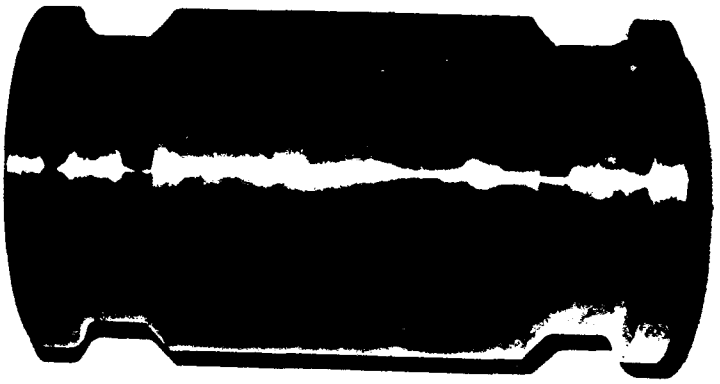

Figure C-1 Pressure Vessel Side View

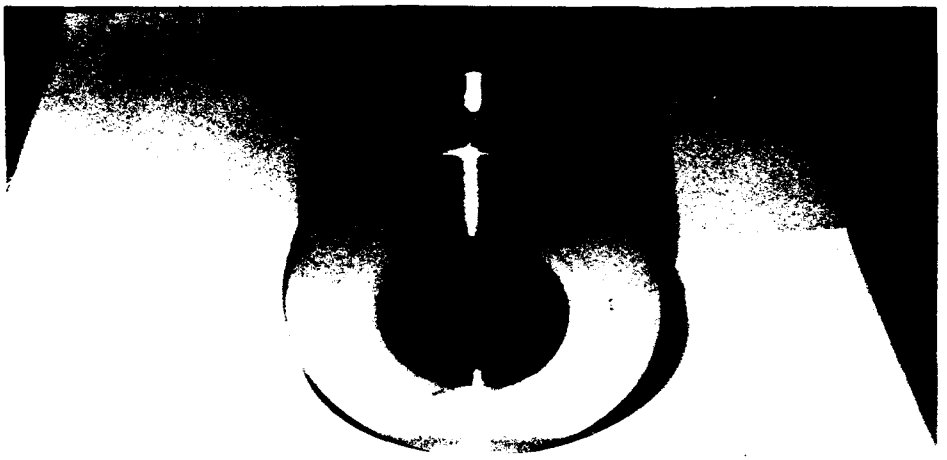

Figure C-2 Pressure Vessel End View

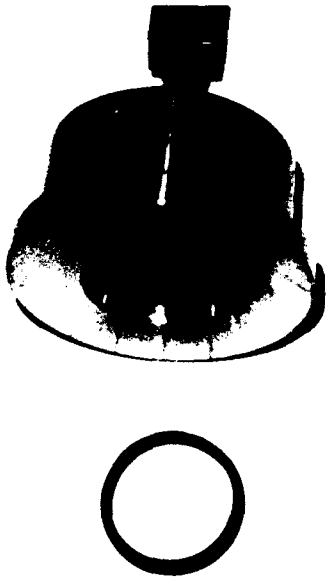

Figure C-3 End Closure and Seal Ring

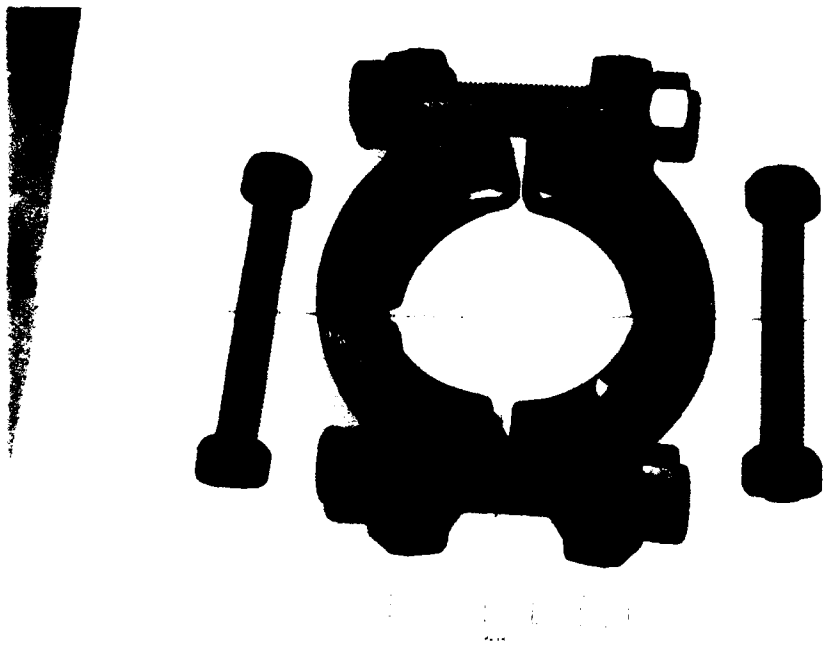

Figure C-4 Clamp Assembly

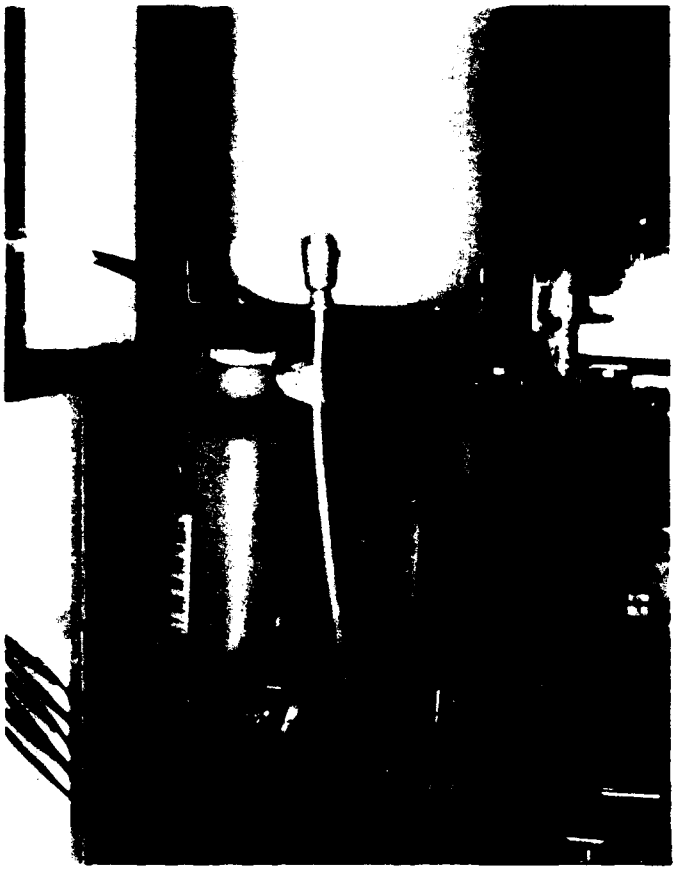

Figure C-5 Pump Connections

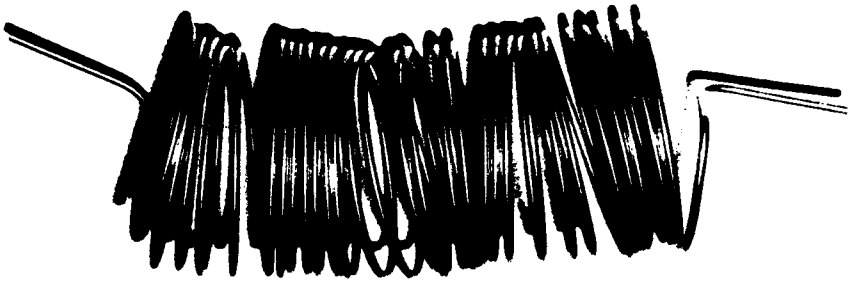

C-6 Preheater Coil

C-7 Heater Element

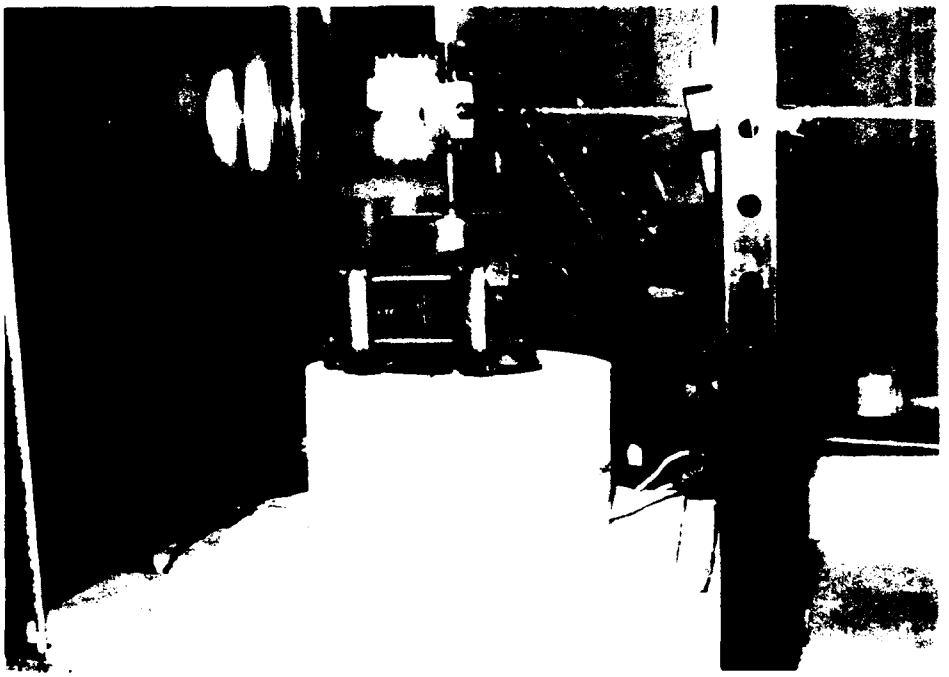

C-8 Vessel Heaters and Partial Insulation

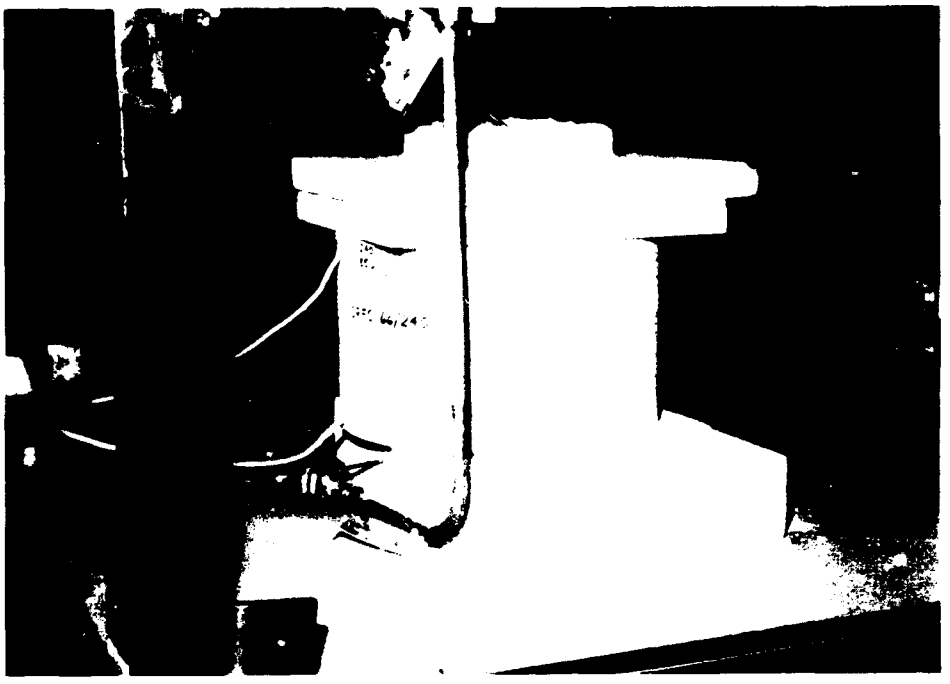

C-9 Preheater Heater and Partial Insulation

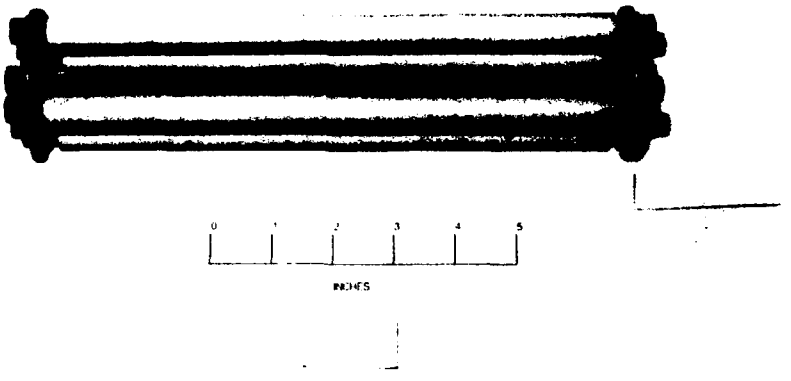

C-10 Sample Holder with Sample

Appendix D

Strength Calculations for Pressure Vessel

From Thick Walled Theory:

$P := 5000 \cdot psi \qquad r_i := 1.25 \cdot in \qquad r_o := 2.5 \cdot in \qquad t := 1.25 \cdot in$

$$\sigma_{zz} := \frac{P \cdot r_i}{2 \cdot t} \qquad \sigma_{\theta\theta} := P \cdot \left[\frac{\left(\frac{r_o}{r_i}\right)^2 + 1}{\left[\left(\frac{r_o}{r_i}\right)^2 - 1\right]} \right] \qquad \sigma_{rr} := -P$$

$\sigma_{zz} = 2.5 \cdot 10^3 \cdot psi \qquad \sigma_{\theta\theta} = 8.333 \cdot 10^3 \cdot psi \qquad \sigma_{rr} = -5 \cdot 10^3 \cdot psi$

$$\sigma_{ys} := 60000 \cdot psi \qquad \sigma_e := \sqrt{\frac{1}{2} \cdot \left[(\sigma_{rr} - \sigma_{zz})^2 + (\sigma_{rr} - \sigma_{\theta\theta})^2 + (\sigma_{zz} - \sigma_{\theta\theta})^2 \right]}$$

$$\frac{\sigma_e}{\sigma_{ys}} = 0.193 \qquad S_F := \frac{\sigma_{ys}}{\sigma_e} \qquad S_F = 5.183$$

For Corrosion Allowance: Iterate until Safety Factor is 4.

$P := 5000 \cdot psi \qquad r_i := 1.623 \cdot in \qquad r_o := 2.5 \cdot in \qquad t := r_o - r_i$

$$\sigma_{zz} := \frac{P \cdot r_i}{2 \cdot t} \qquad \sigma_{\theta\theta} := P \cdot \left[\frac{\left(\frac{r_o}{r_i}\right)^2 + 1}{\left[\left(\frac{r_o}{r_i}\right)^2 - 1\right]} \right] \qquad \sigma_{rr} := -P$$

$\sigma_{zz} = 4.627 \cdot 10^3 \cdot psi \qquad \sigma_{\theta\theta} = 1.228 \cdot 10^4 \cdot psi \qquad \sigma_{rr} = -5 \cdot 10^3 \cdot psi$

$$\sigma_{ys} := 60000 \cdot psi \qquad \sigma_{eca} := \sqrt{\frac{1}{2} \cdot \left[(\sigma_{rr} - \sigma_{zz})^2 + (\sigma_{rr} - \sigma_{\theta\theta})^2 + (\sigma_{zz} - \sigma_{\theta\theta})^2 \right]}$$

$$\frac{\sigma_{eca}}{\sigma_{ys}} = 0.25 \qquad S_F := \frac{\sigma_{ys}}{\sigma_{eca}} \qquad S_F = 4$$

Thus the corrosion allowance is .373 inches or about 3/8 inch.

Leak before break criteria

From the graph with a/2c = .5 and ratio of equivalent stress to yield strength of 0.19 the value of Q is 2.38. $Q := 2.38 \cdot in$ $K_{IC} := 80000 \cdot psi$

Critical Crack Size:

$$a := \left(\frac{K_{IC}}{\sigma_e}\right)^2 \cdot \frac{Q}{1.21 \cdot \pi} \qquad a = 29.897 \cdot in$$

Appendix E

Labview Virtual Instrument Schematics

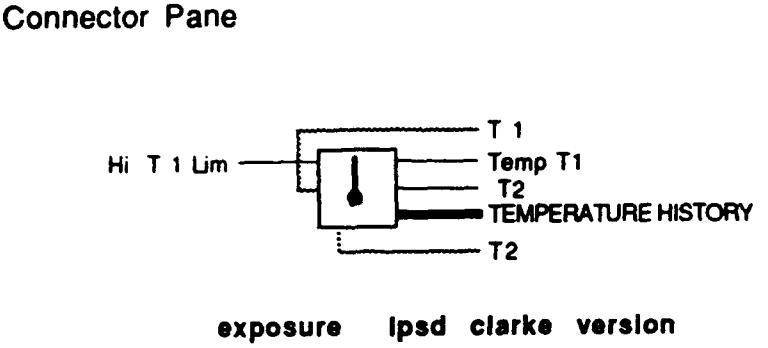

Figure E-1 Labview® Exposure System Controller

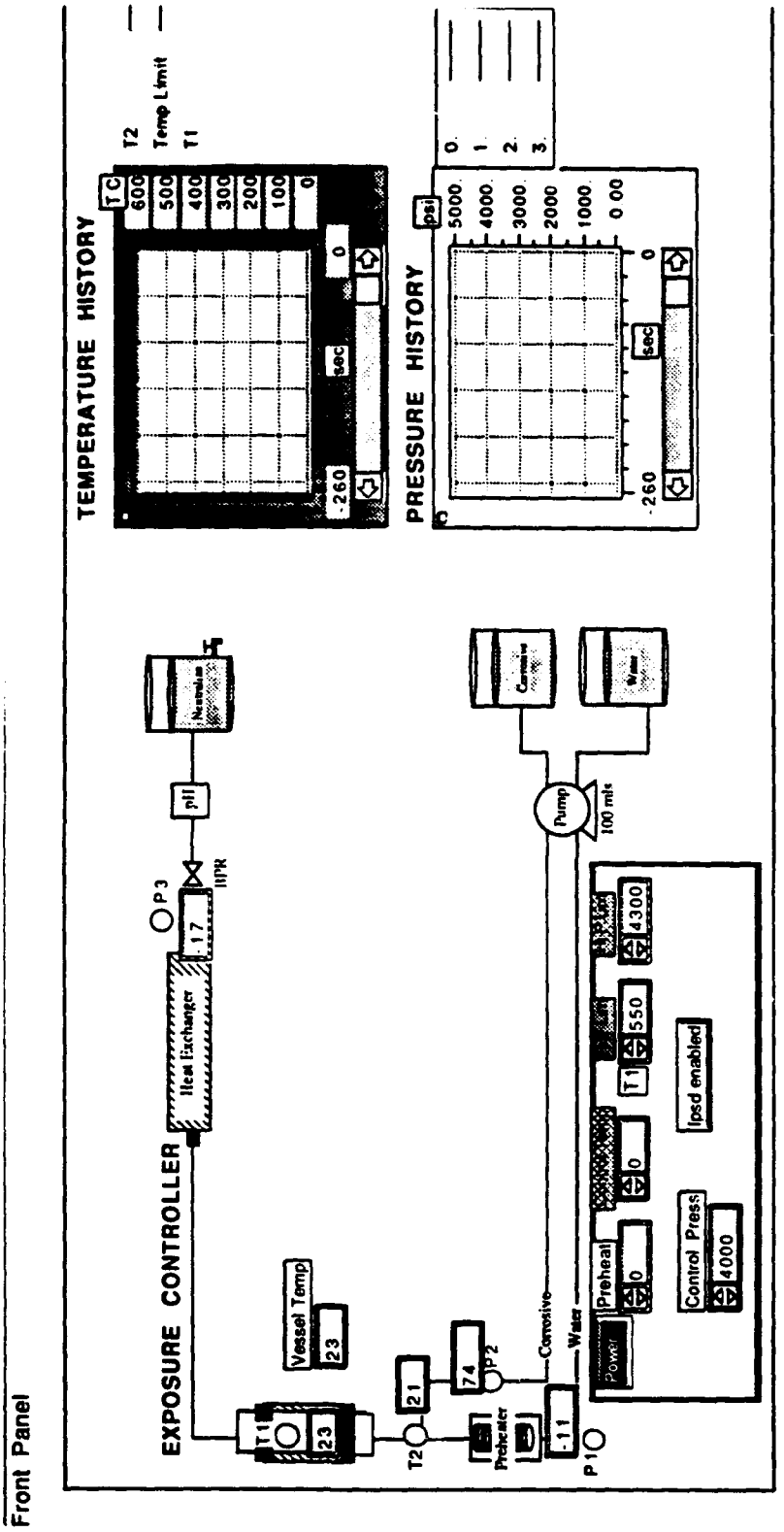

Figure E-1 Labview® Exposure System Controller (continued)

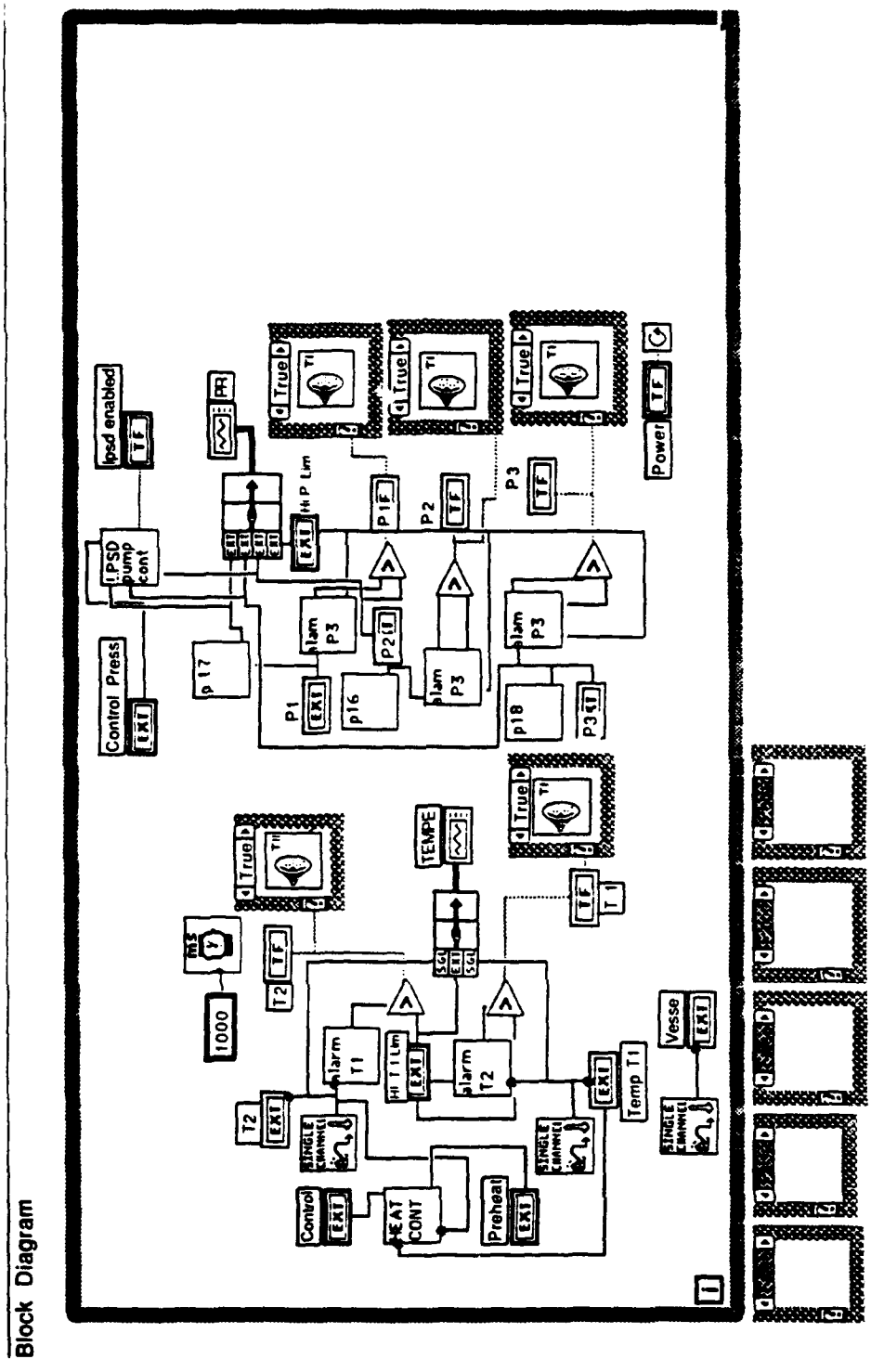

Figure E-1 Labview® Exposure System Controller (continued)

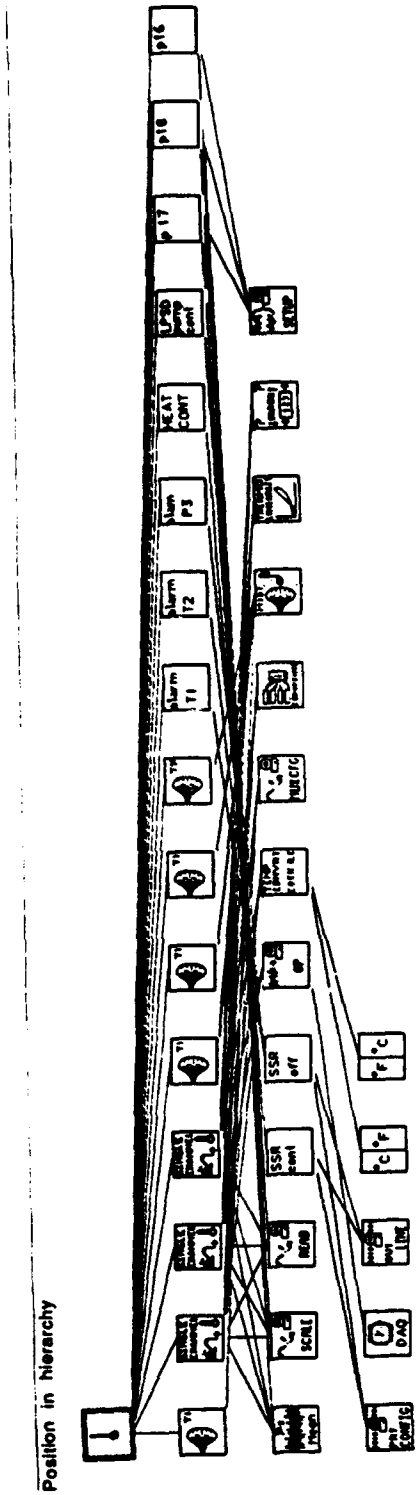

Figure E-1 Labview® Exposure System Controller (continued)

Connector Pane

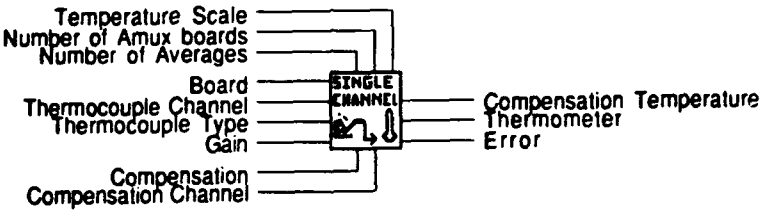

T2 Read

Reads the temperature from the selected channel.

Figure E-2 Labview® Temperature Read Instrument

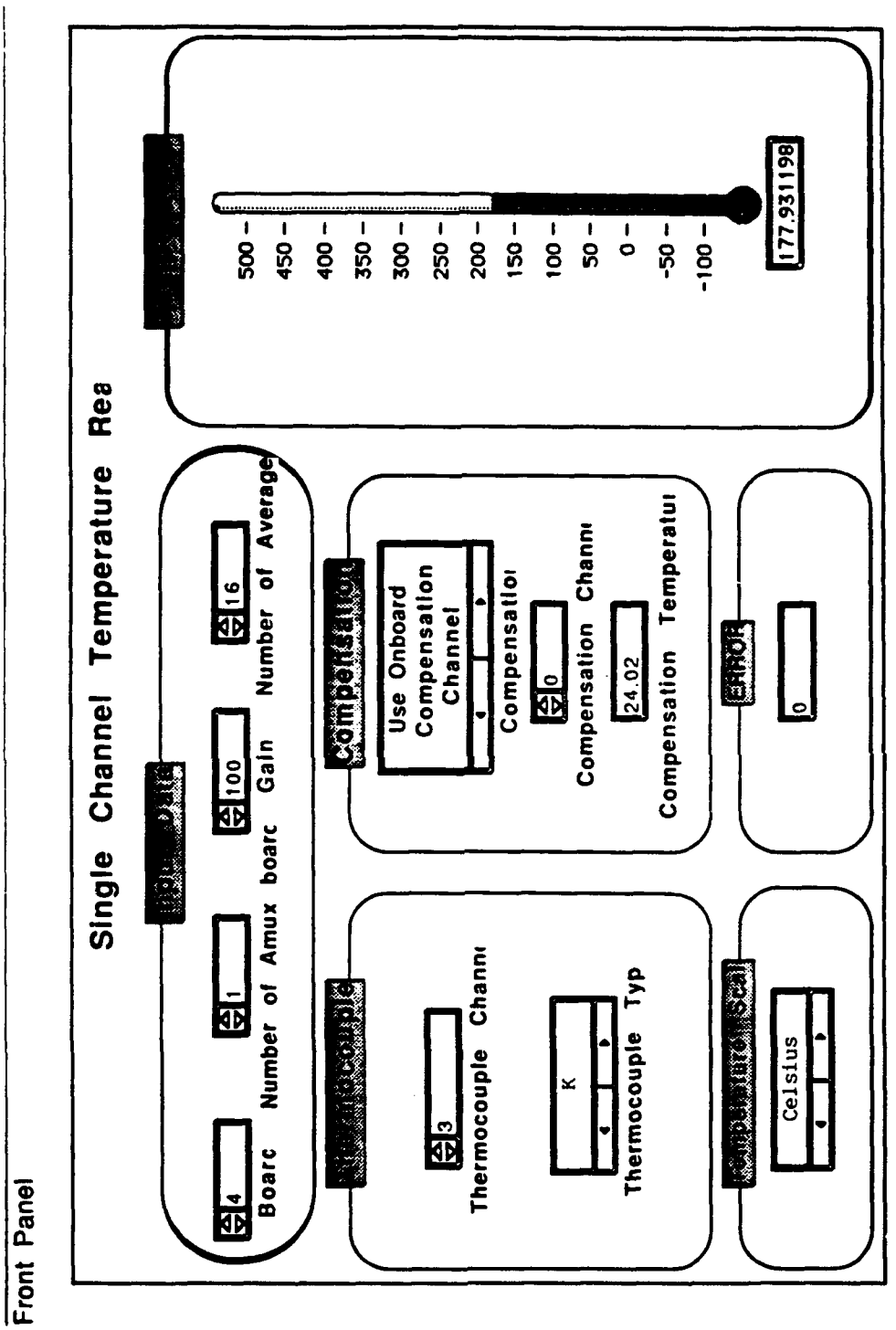

Figure E-2 Labview® Temperature Read Instrument (continued)

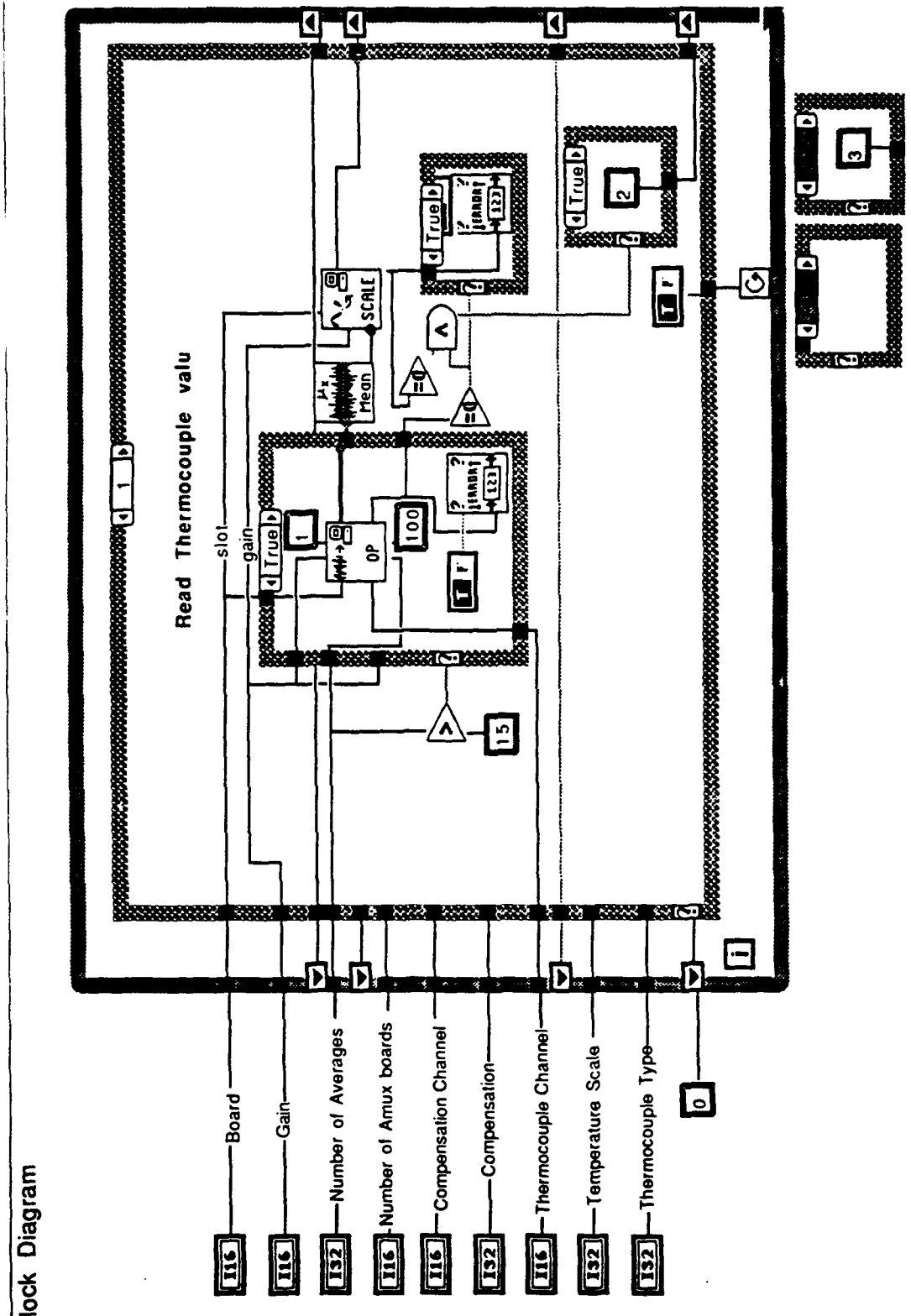

Figure E-2 Labview® Temperature Read Instrument (continued)

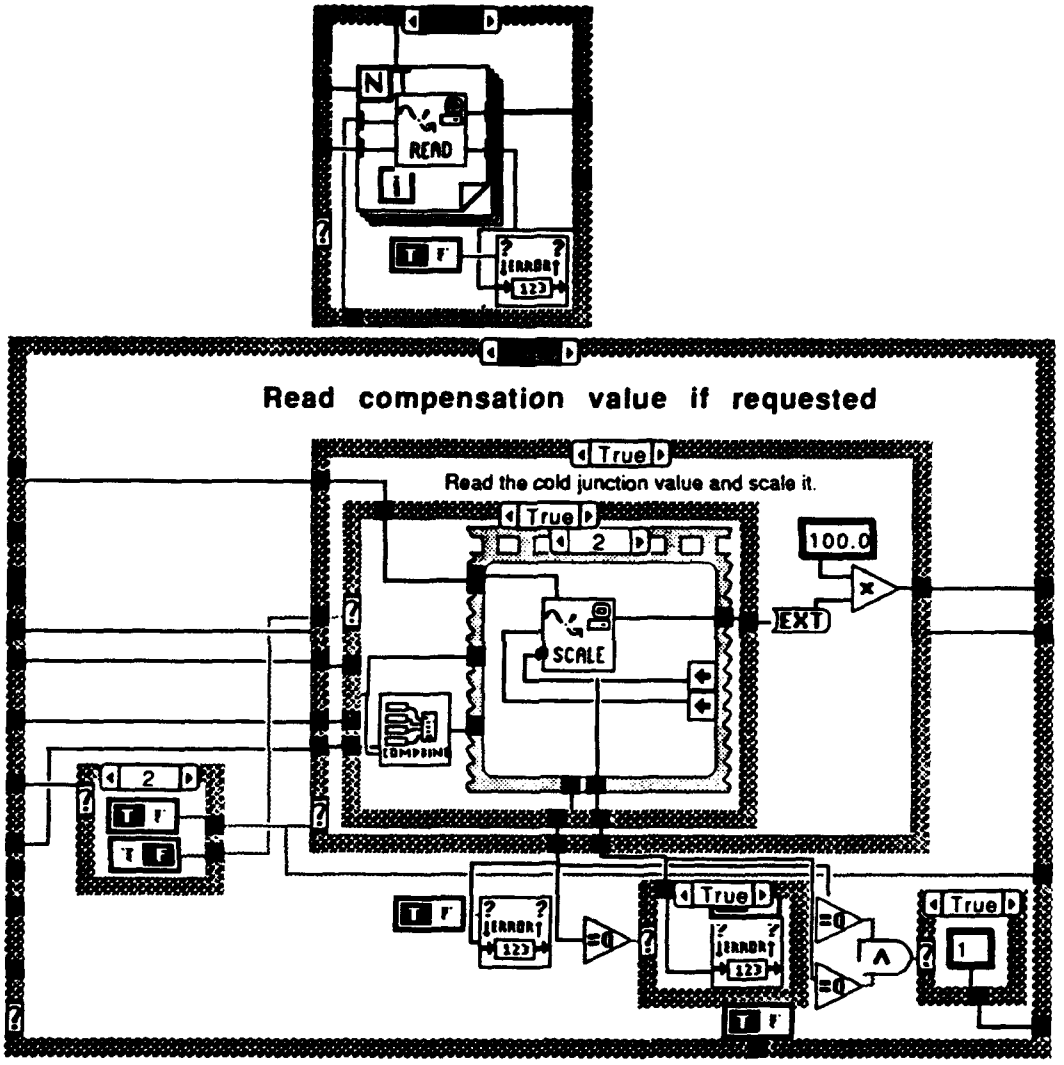

Figure E-2 Labview® Temperature Read Instrument (continued)

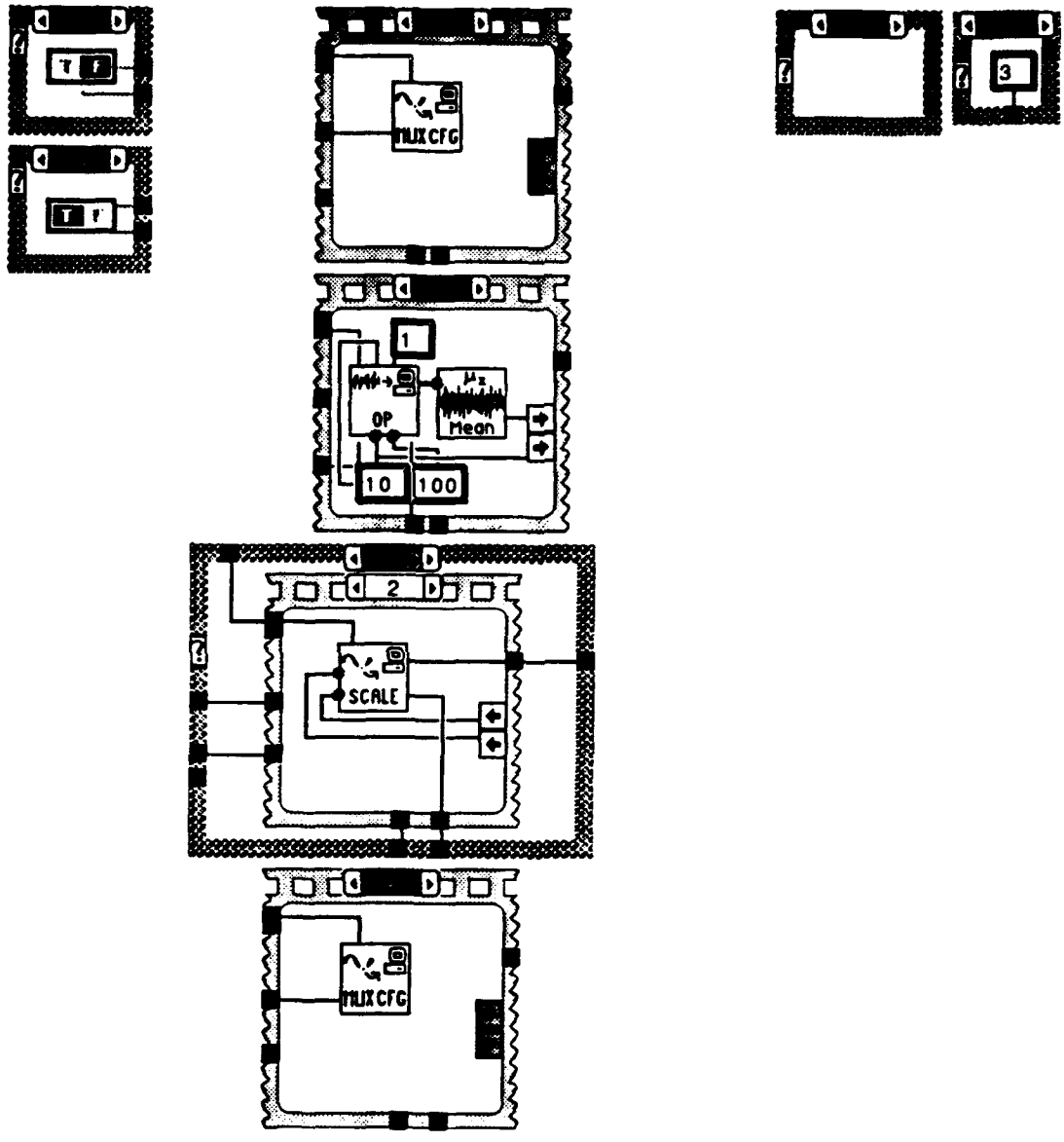

Figure E-2 Labview® Temperature Read Instrument (continued)

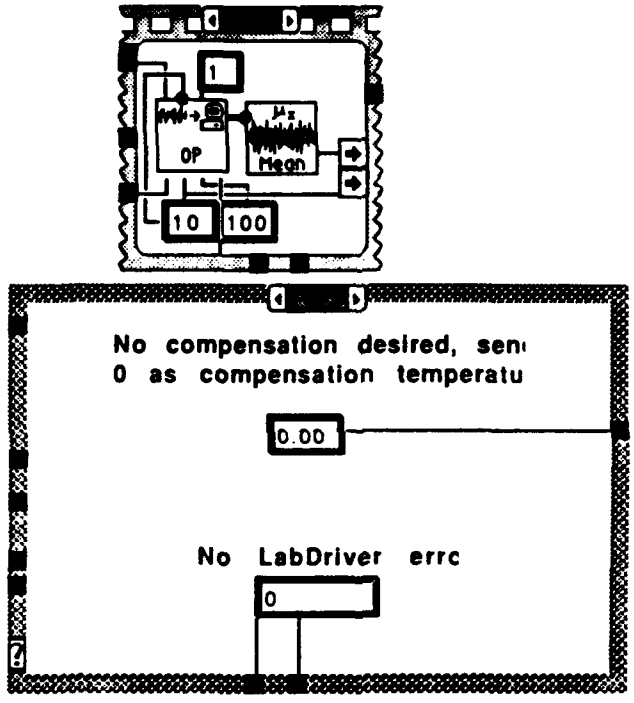

Figure E-2 Labview® Temperature Read Instrument (continued)

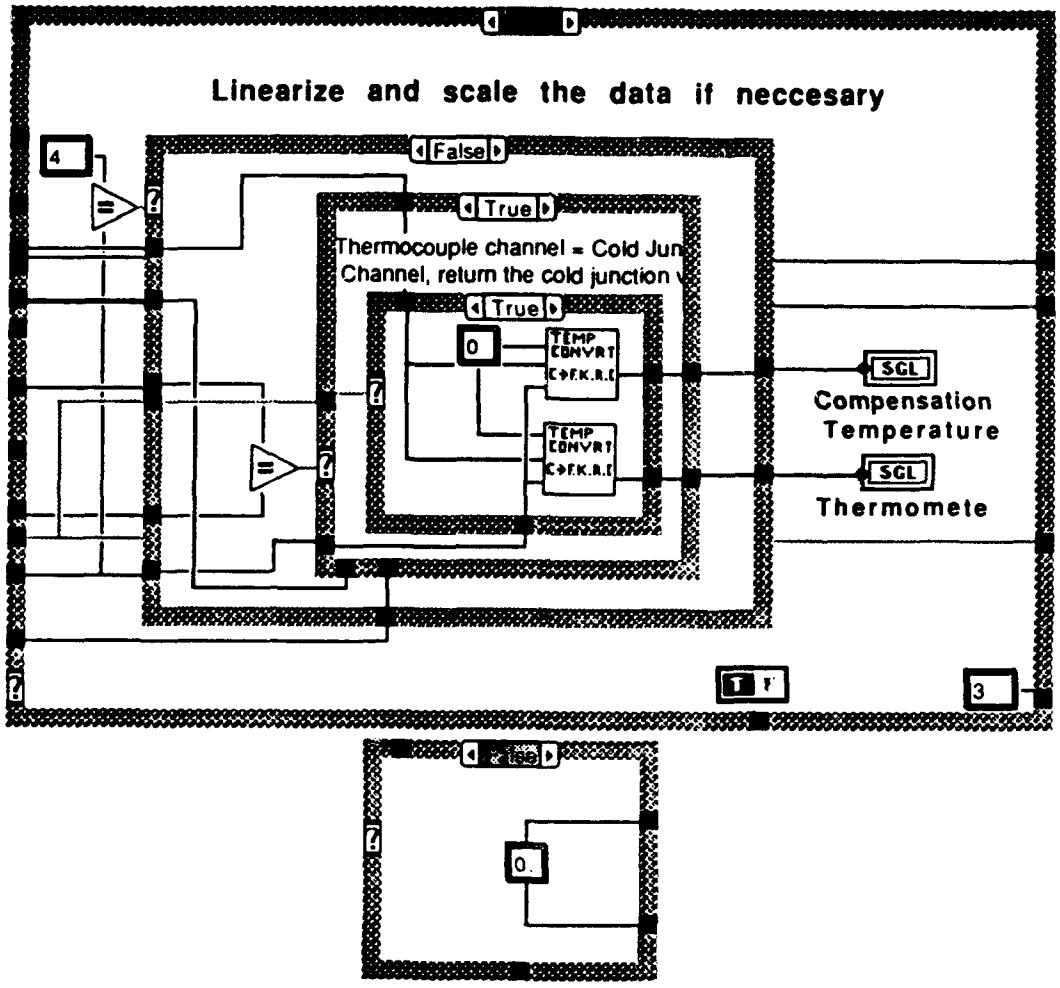

Figure E-2 Labview® Temperature Read Instrument (continued)

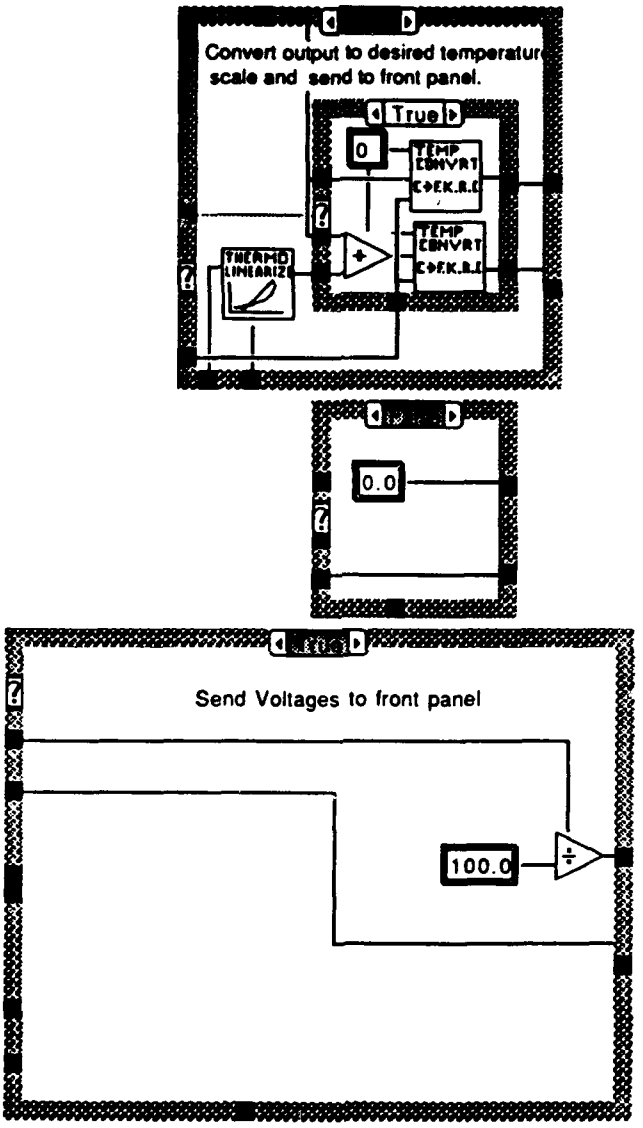

Figure E-2 Labview® Temperature Read Instrument (continued)

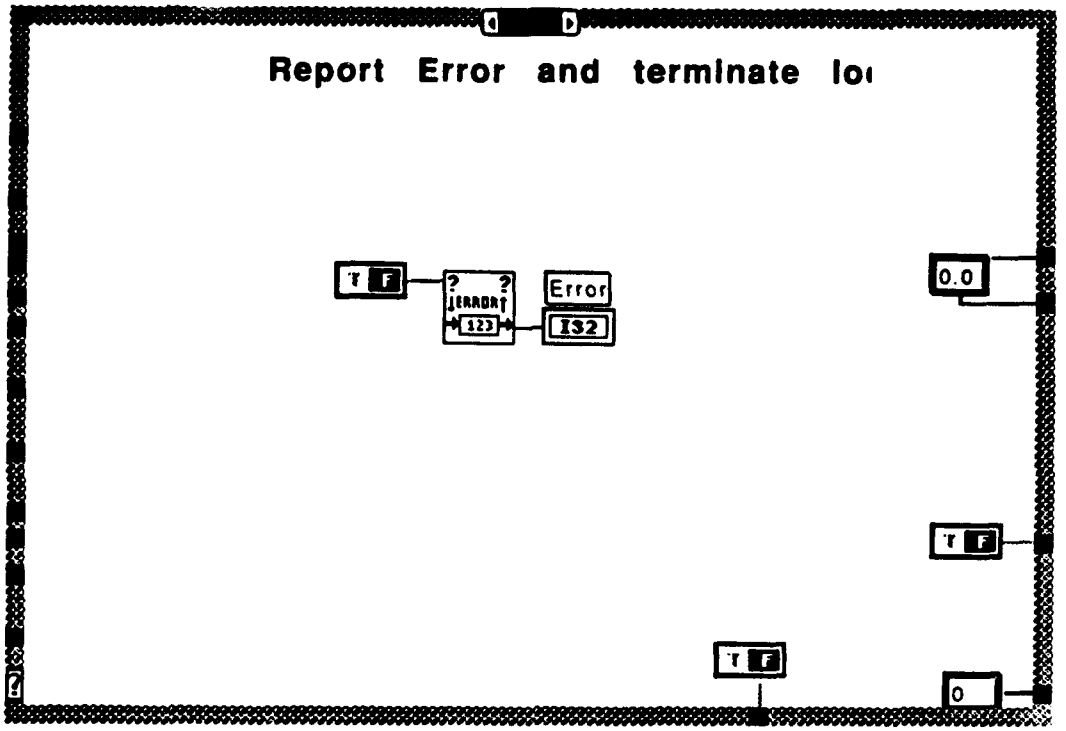

Figure E-2 Labview® Temperature Read Instrument (continued)

Connector Pane

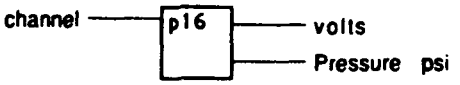

clarkeP16 average

Front Panel

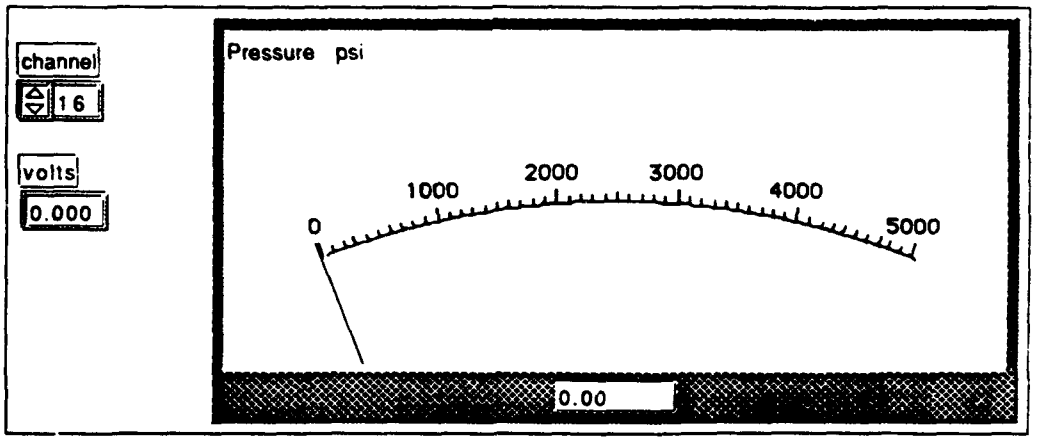

Figure E-3 Labview® Pressure Read Instument

Block Diagram

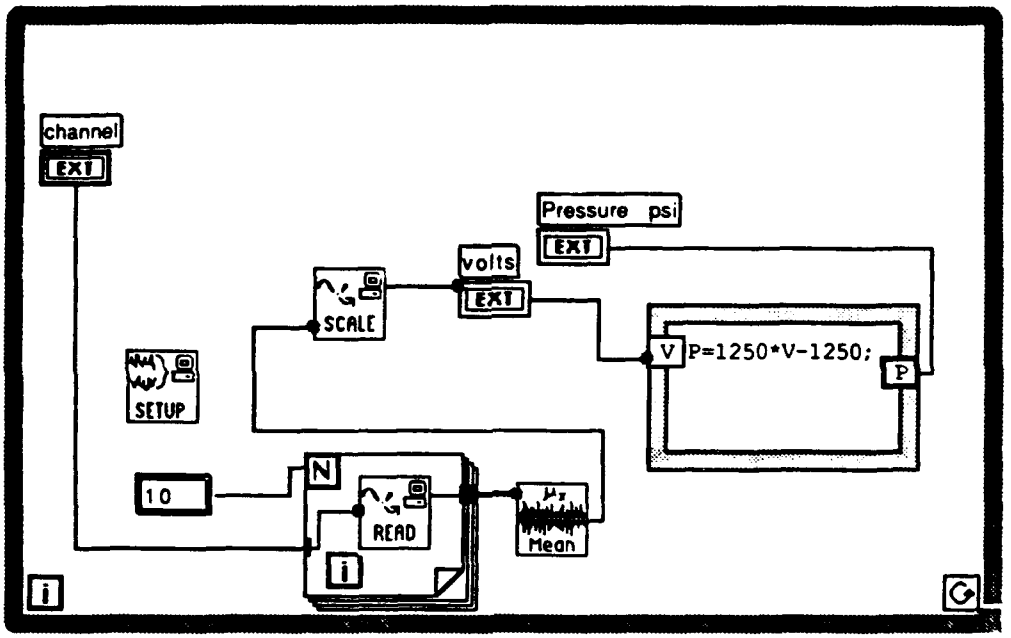

Figure E-3 Labview® Pressure Read Instument (continued)

Connector Pane

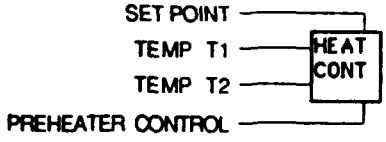

4partempcontrol

Front Panel

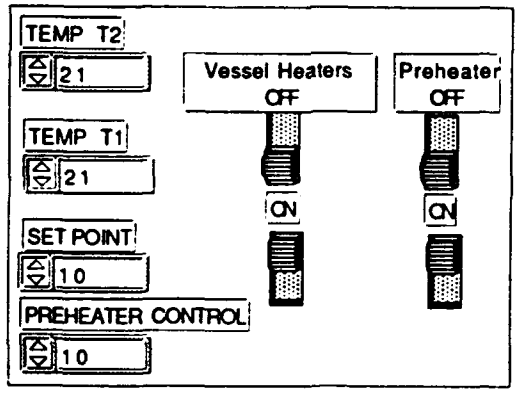

Figure E-4 Labview® Temperature Controller

Block Diagram

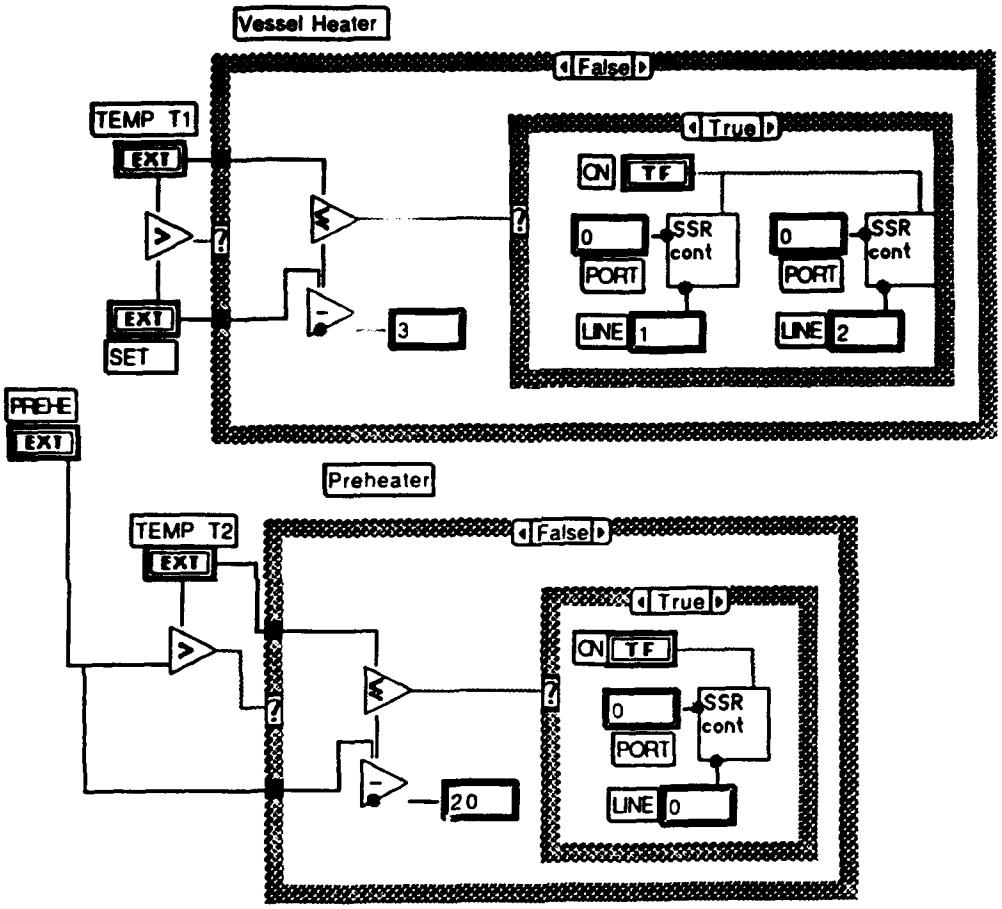

Figure E-4 Labview® Temperature Controller (continued)

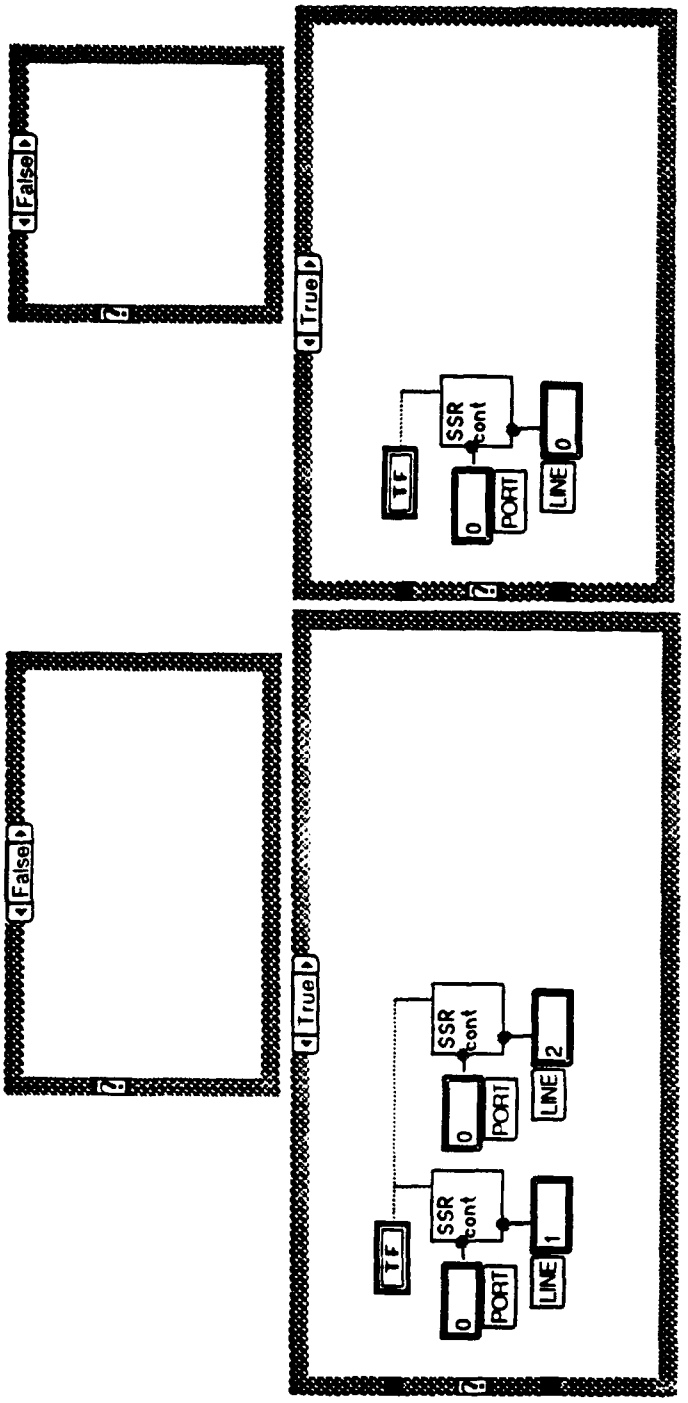

Figure E-4 Labview® Temperature Controller (continued)

Connector Pane

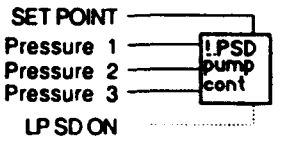

lpsdcontrol

Front Panel

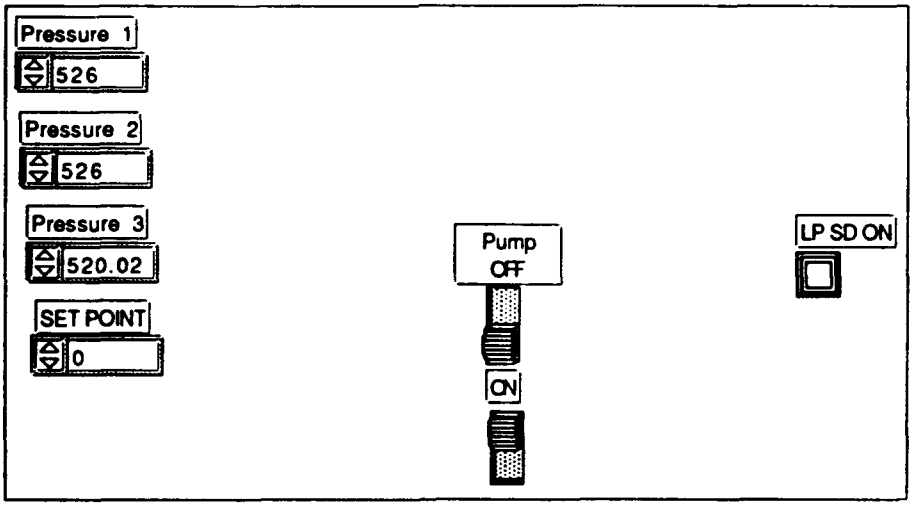

Figure E-5 Labview® Pressure Controller

Block Diagram

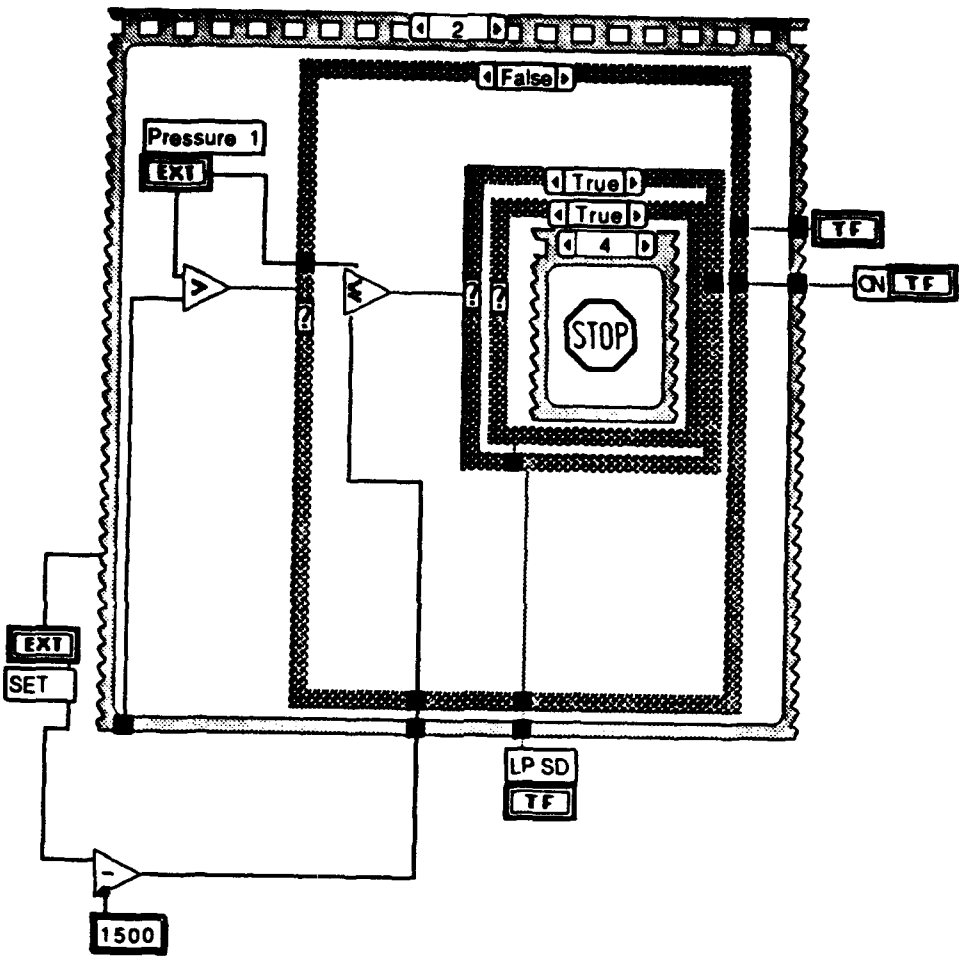

Figure E-5 Labview® Pressure Controller (continued)

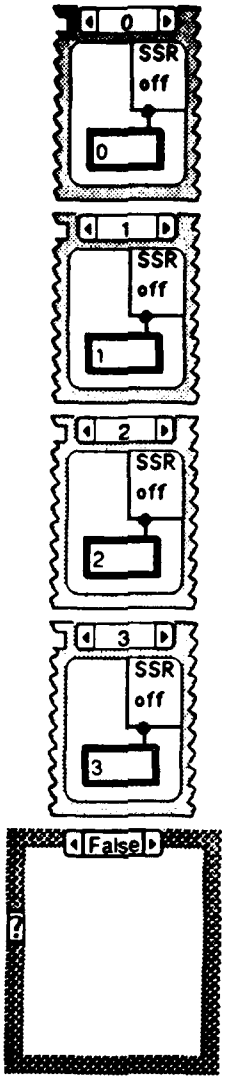

Figure E-5 Labview® Pressure Controller (continued)

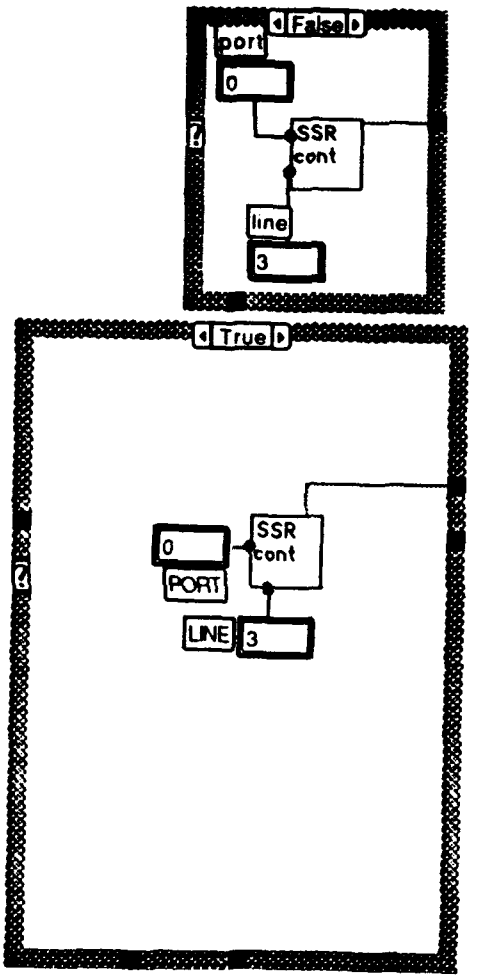

Figure E-5 Labview® Pressure Controller (continued)

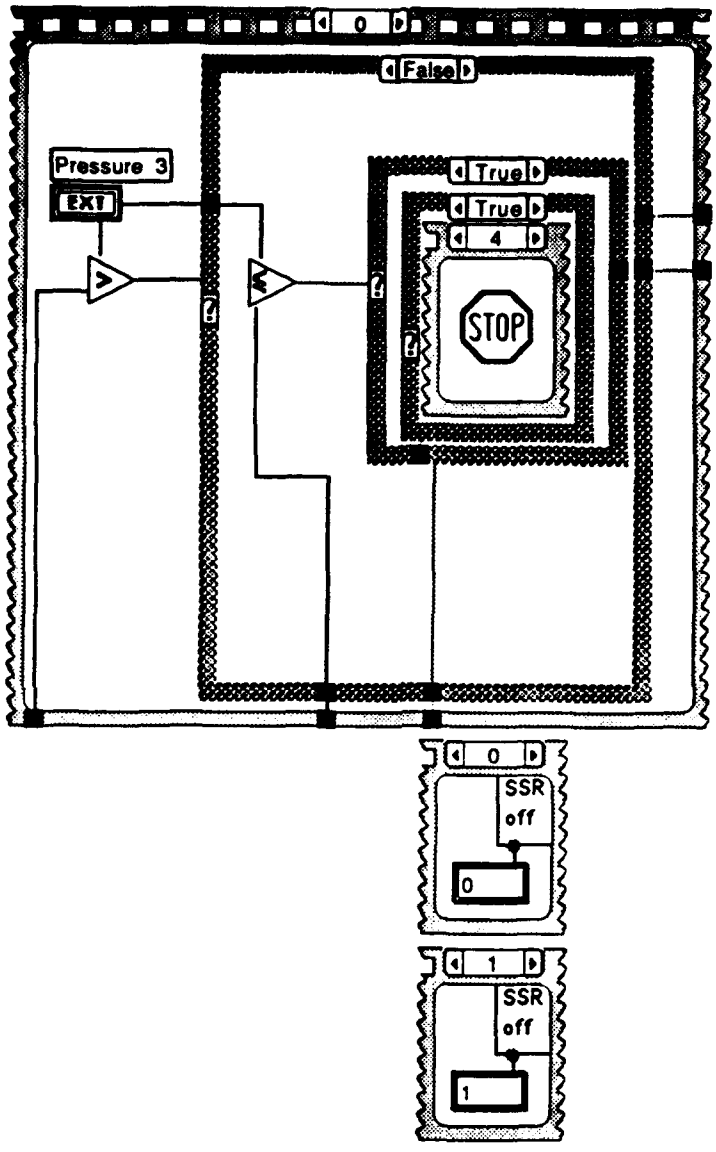

Figure E-5 Labview® Pressure Controller (continued)

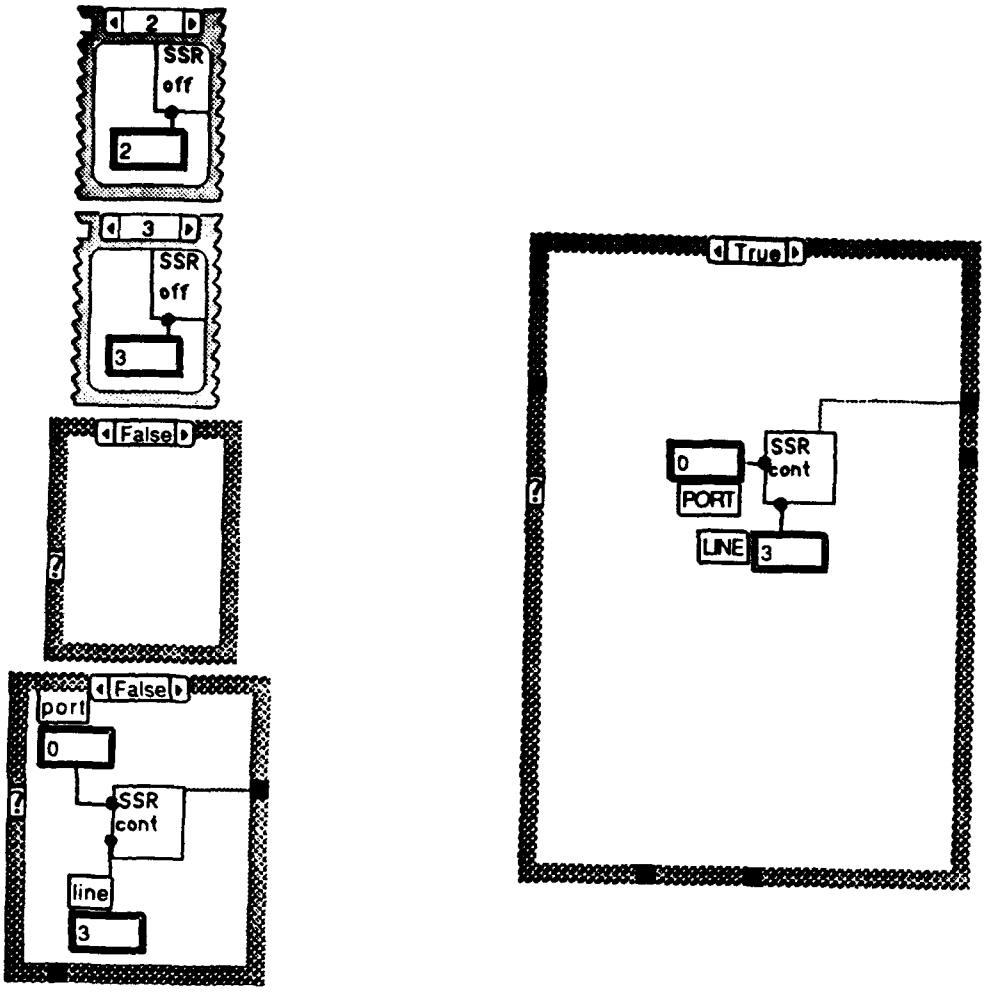

Figure E-5 Labview® Pressure Controller (continued)

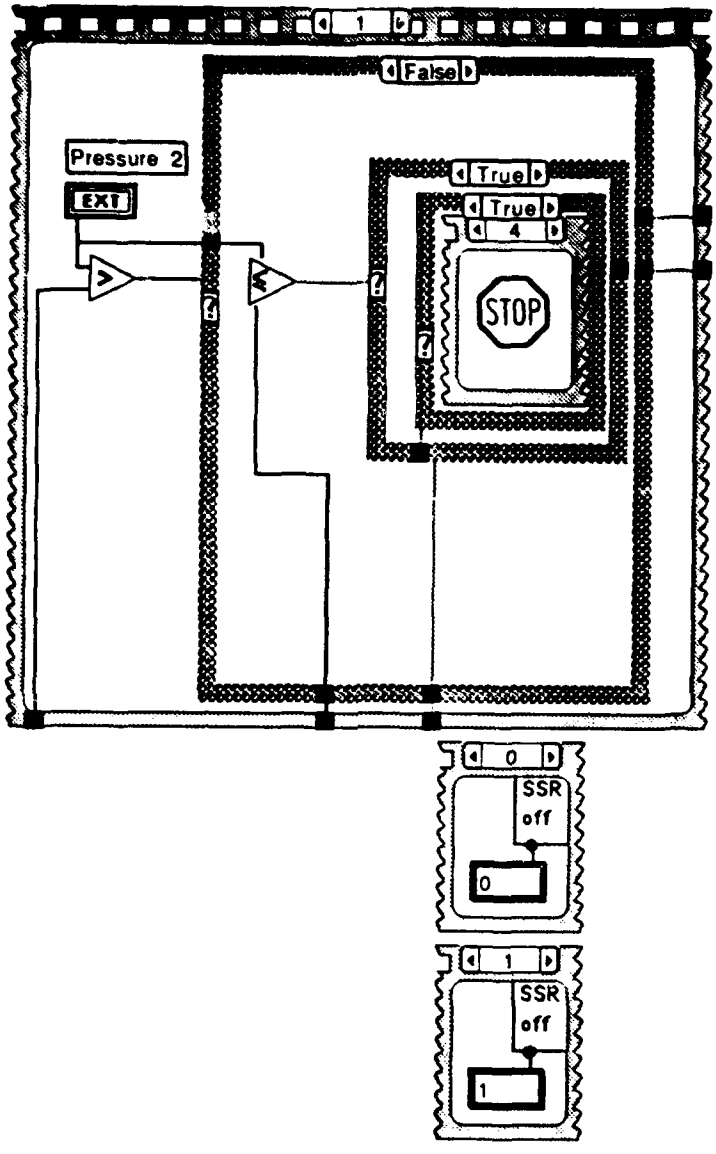

Figure E-5 Labview® Pressure Controller (continued)

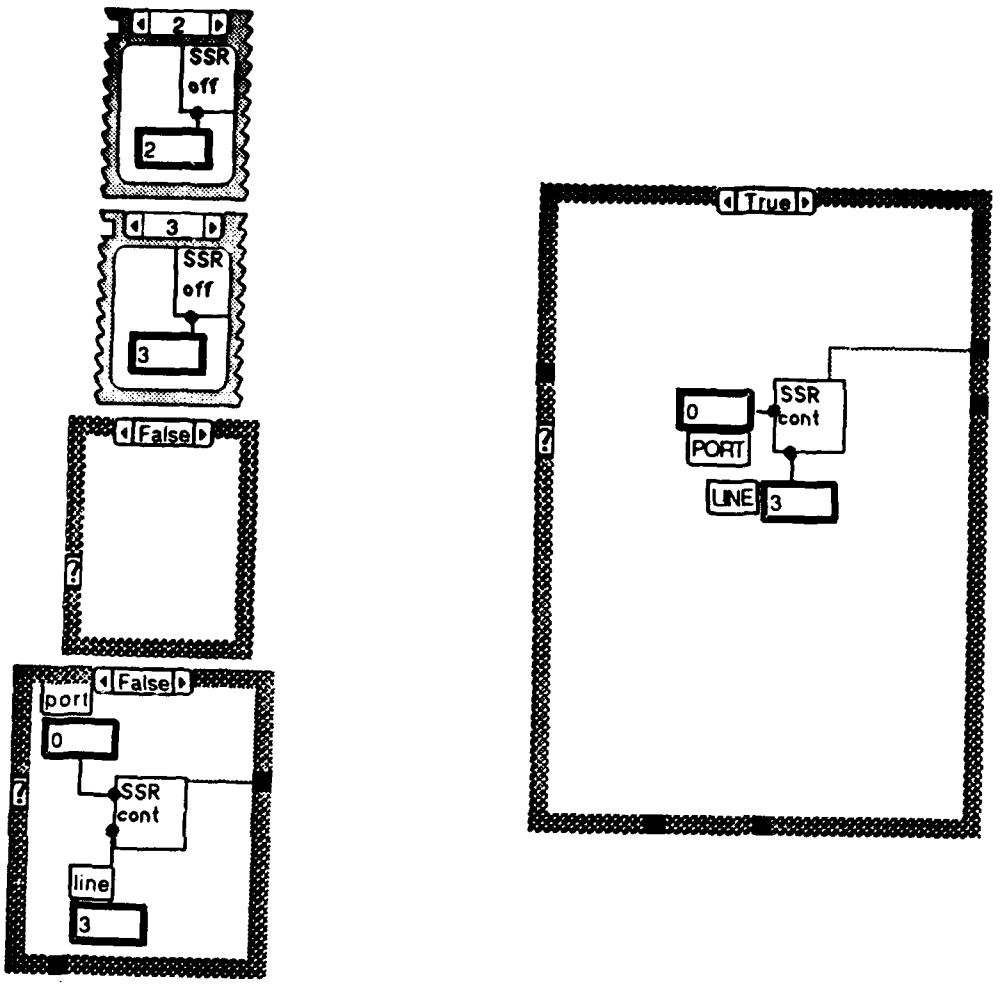

Figure E-5 Labview® Pressure Controller (continued)

Connector Pane

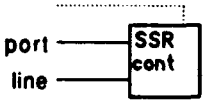

SSR control

Front Panel

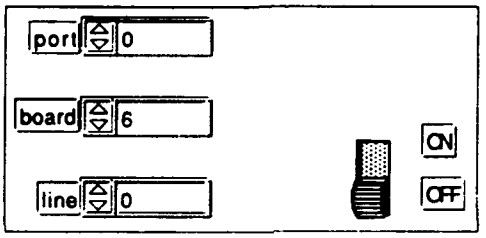

Block Diagram

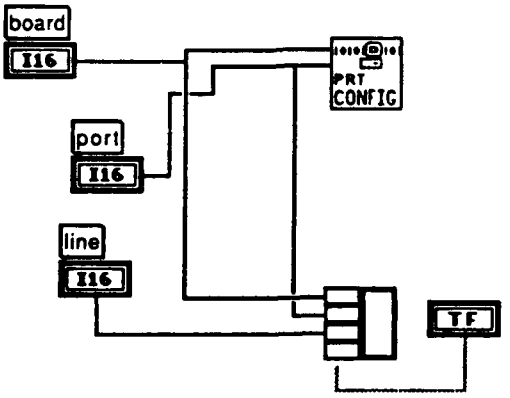

Figure E-6 Labview® Relay Controller

Connector Pane

Warning

Front Panel

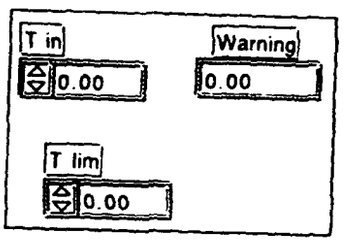

Figure E-8 Labview® Alarm Warning Circuit

Connector Pane

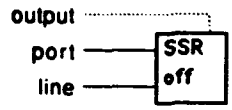

SSR off

Front Panel

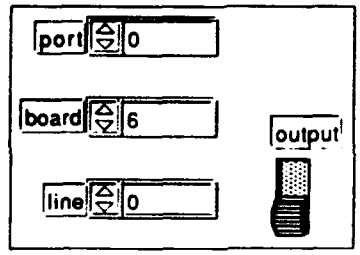

Block Diagram

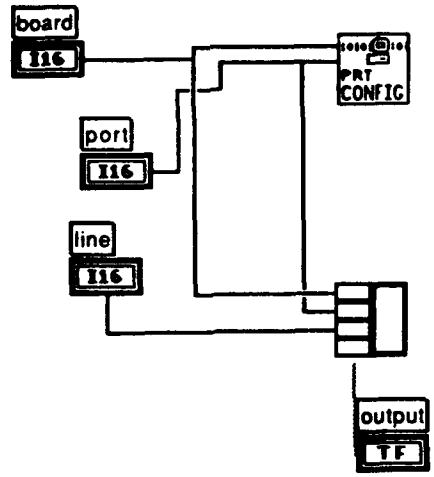

Figure E-7 Labview® Relay Shutoff Controller

Block Diagram

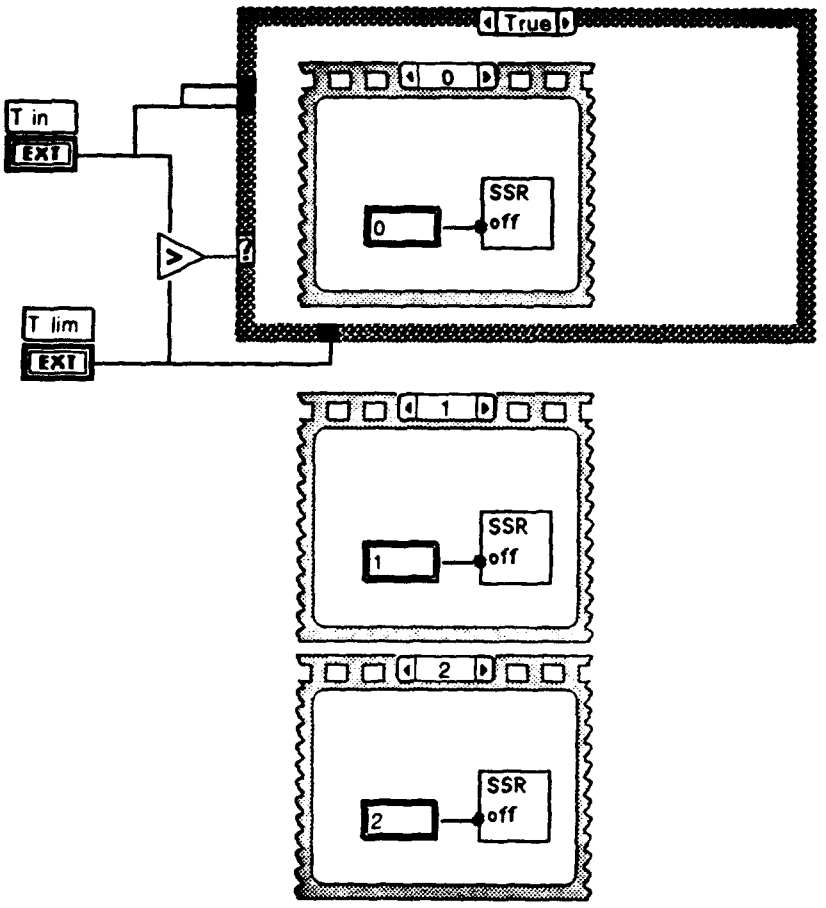

Figure E-8 Labview® Alarm Warning Circuit (continued)

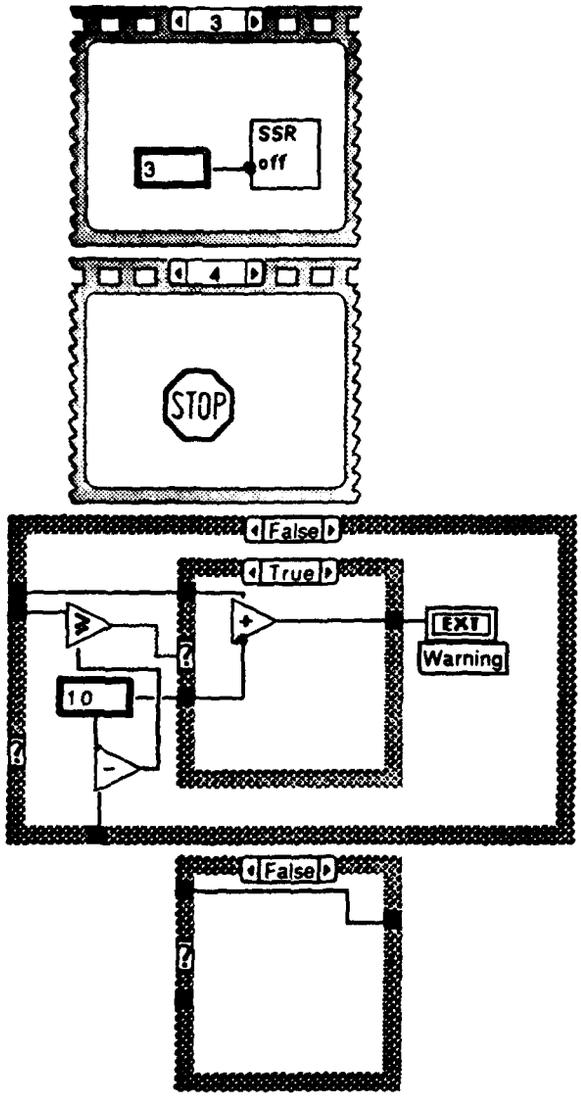

Figure E-8 Labview® Alarm Warning Circuit (continued)

Connector Pane

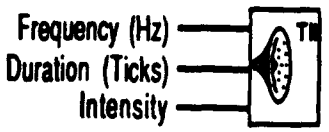

BEEP T ii

Front Panel

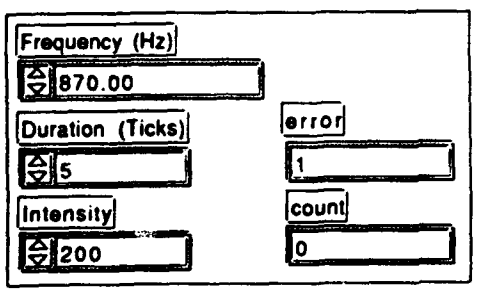

Block Diagram

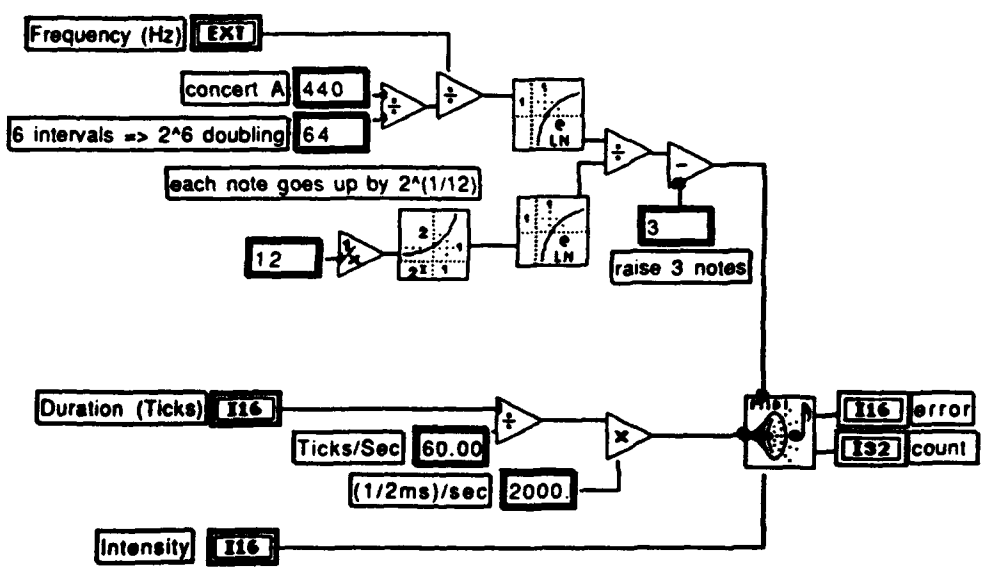

Figure E-9 Labview® Audible Alarm Circuit

Appendix F

Sample Weight Loss Data

Run 1: 96 hours at 500°C, 241.5 atm

Sample Number	Height	Width	Length
1(Inconel 625)	3.15mm	19.51mm	37.83mm
2(Inconel 625)	3.15mm	21.76mm	38.25mm
3(C-276)	3.11mm	20.14mm	38.20mm
4(C-276)	3.20mm	20.37mm	38.04mm
5(316 SS)	3.05mm	19.99mm	37.72mm
6(316 SS)	2.95mm	19.48mm	37.72mm

Surface area is reduced by drilling of a 9.525 mm diameter inch hole in the sample. There is an insulated washer covering 15.977 mm diameter circle on each flat surface.

Sample Number	Surface Area	Exposed Area	Shielded Area
1	18.45 cm^2	14.36 cm^2	4.09 cm^2
2	20.50 cm^2	16.41 cm^2	4.09 cm^2
3	19.09 cm^2	15.01 cm^2	4.09 cm^2
4	19.32 cm^2	15.23 cm^2	4.09 cm^2
5	18.68 cm^2	14.59 cm^2	4.09 cm^2
6	18.14 cm^2	14.06 cm^2	4.08 cm^2

Weight is the average of three values on a precision balance

Sample Number	Initial Weight	Final Weight	Weight Change
1	17.6255 gm	17.6265 gm	+0.0010 gm
2	17.2980 gm	17.2996 gm	+0.0016 gm
3	19.0449 gm	19.0465 gm	+0.0016 gm
4	19.0604 gm	19.0610 gm	+0.0004 gm
5	15.8525 gm	15.8529 gm	+0.0004 gm
6	14.9066 gm	14.9068 gm	+0.0003 gm

Table F-1 Dimensions and Weight Change for Run 1

Run 2: 96 hours at 300°C, 241.5 atm

Sample Number	Height	Width	Length
1(Inconel 625)	3.25mm	20.04mm	38.10mm
2(Inconel 625)	3.18mm	19.71mm	38.79mm
3(C-276)	3.18mm	20.60mm	38.15mm
4(C-276)	3.10mm	20.47mm	37.92mm
5(316 SS)	3.0mm	19.51mm	38.23mm
6(316 SS)	2.9mm	20.19mm	38.71mm

Surface area is reduced by drilling of a 9.525 mm diameter inch hole in the sample. There is an insulated washer covering 15.977 mm diameter circle on each flat surface.

Sample Number	Surface Area	Exposed Area	Shielded Area
1	19.13 cm^2	15.04 cm^2	4.09 cm^2
2	19.09 cm^2	15.00 cm^2	4.09 cm^2
3	19.54 cm^2	15.45 cm^2	4.09 cm^2
4	19.28 cm^2	15.19 cm^2	4.09 cm^2
5	18.46 cm^2	14.37 cm^2	4.09 cm^2
6	19.12 cm^2	15.04 cm^2	4.08 cm^2

Weight is the average of three values on a precision balance

Sample Number	Initial Weight	Final Weight	Weight Change
1	18.1993 gm	18.1996 gm	+0.0003 gm
2	18.5079 gm	18.5082 gm	+0.0003 gm
3	19.5607 gm	19.5606 gm	+0.0001 gm
4	19.2290 gm	19.2295 gm	+0.0005 gm
5	15.7449 gm	15.7456 gm	+0.0006 gm
6	15.9877 gm	15.9885 gm	+0.0007 gm

Table F-2 Dimensions and Weight Change for Run 2

Run 3: 24 hours at 400°C, 241.5 atm

Sample Number	Height	Width	Length
1(Inconel 625)	3.18mm	20.04mm	38.91mm
2(Inconel 625)	3.15mm	19.81mm	38.46mm
3(C-276)	3.15mm	20.47mm	38.46mm
4(C-276)	3.18mm	20.22mm	38.33mm
5(316 SS)	3.0mm	18.82mm	37.41mm
6(316 SS)	2.92mm	18.85mm	38.00mm

Surface area is reduced by drilling of a 9.525 mm diameter inch hole in the sample. There is an insulated washer covering 15.977 mm diameter circle on each flat surface.

Sample Number	Surface Area	Exposed Area	Shielded Area
1	19.43 cm^2	15.33 cm^2	4.09 cm^2
2	18.99 cm^2	14.90 cm^2	4.09 cm^2
3	19.54 cm^2	15.45 cm^2	4.09 cm^2
4	19.31 cm^2	15.21 cm^2	4.09 cm^2
5	17.53 cm^2	13.45 cm^2	4.09 cm^2
6	17.71 cm^2	13.64 cm^2	4.08 cm^2

Weight is the average of three values on a precision balance

Sample Number	Initial Weight	Final Weight	Weight Change
1	18.7242 gm	18.7245 gm	+0.0003 gm
2	18.2246 gm	18.2252 gm	+0.0006 gm
3	19.4834 gm	19.4840 gm	+0.0006 gm
4	19.5475 gm	19.5479 gm	+0.0004 gm
5	14.8848 gm	14.8852 gm	+0.0004 gm
6	14.6181 gm	14.6186 gm	+0.0005 gm

Table F-3 Dimensions and Weight Change for Run 3

Appendix G

Sample Photographs

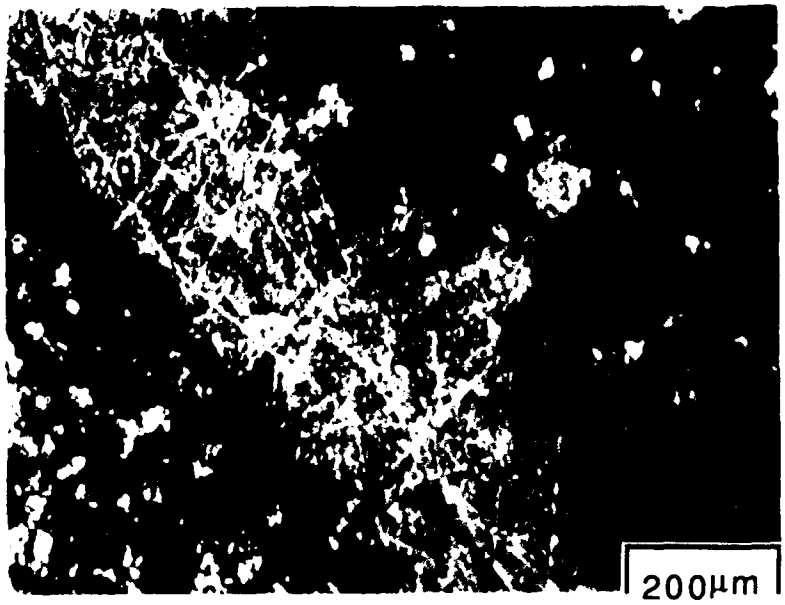

Figure G-1 Fibre-Optic microscope view of Inconel 625, exposed to deionized water for 96 hrs at 500°C, 241.5 atm, washer transition region. (100 x)

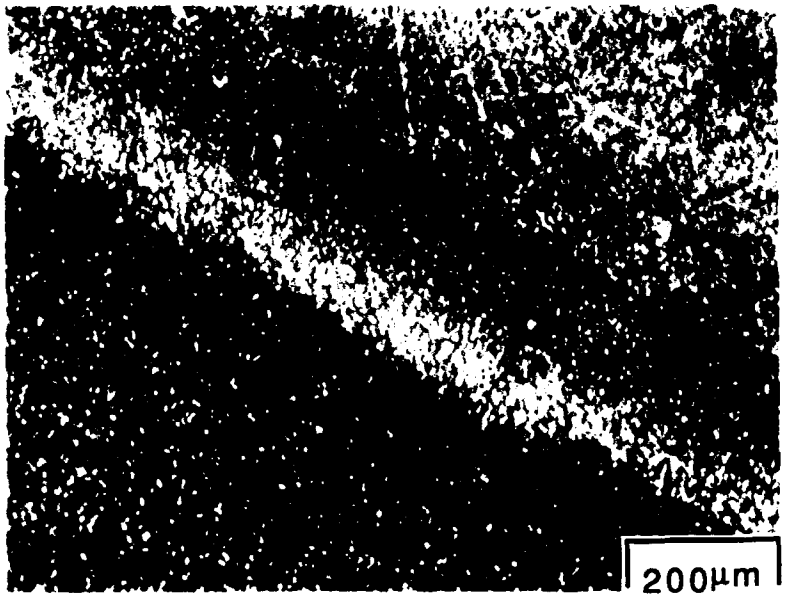

Figure G-2 Fibre-Optic microscope view of Hastelloy C-276, exposed to deionized water for 96 hrs at 500°C, 241.5 atm, washer transition region. (100 x)

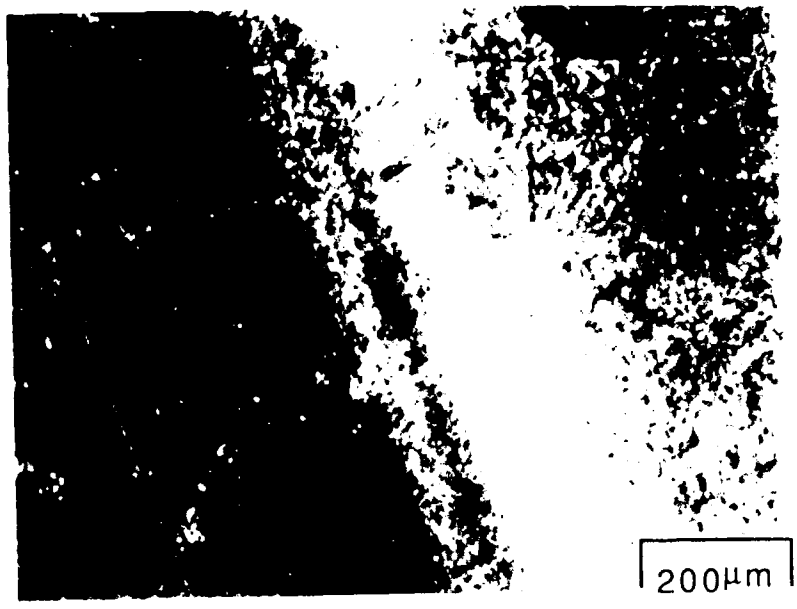

Figure G-3 Fibre-Optic microscope view of 316 SS, exposed to deionized water for 96 hrs at 300°C, 241.5 atm, washer transition region. (100 x)

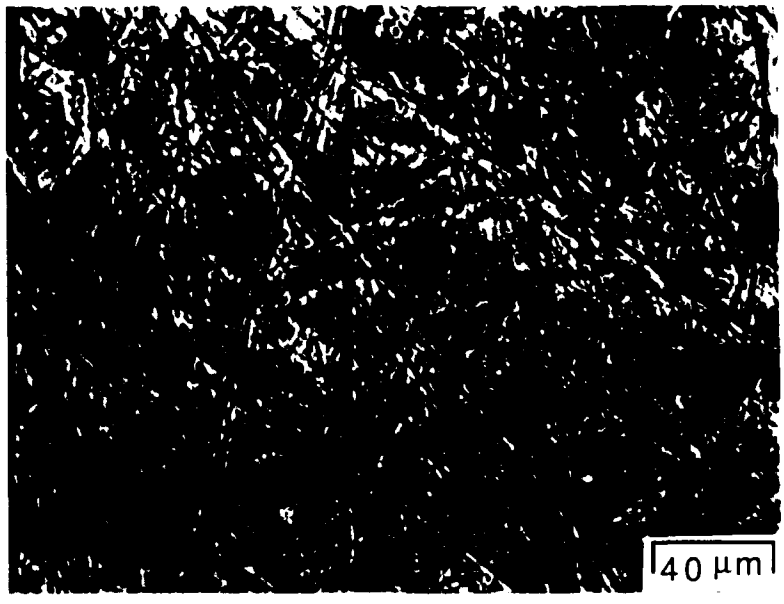

Figure G-4 Laser confocal microscope view of Inconel 625 exposed to deionized water for 96 hours at 300°C. 241 5 atm (400 x)

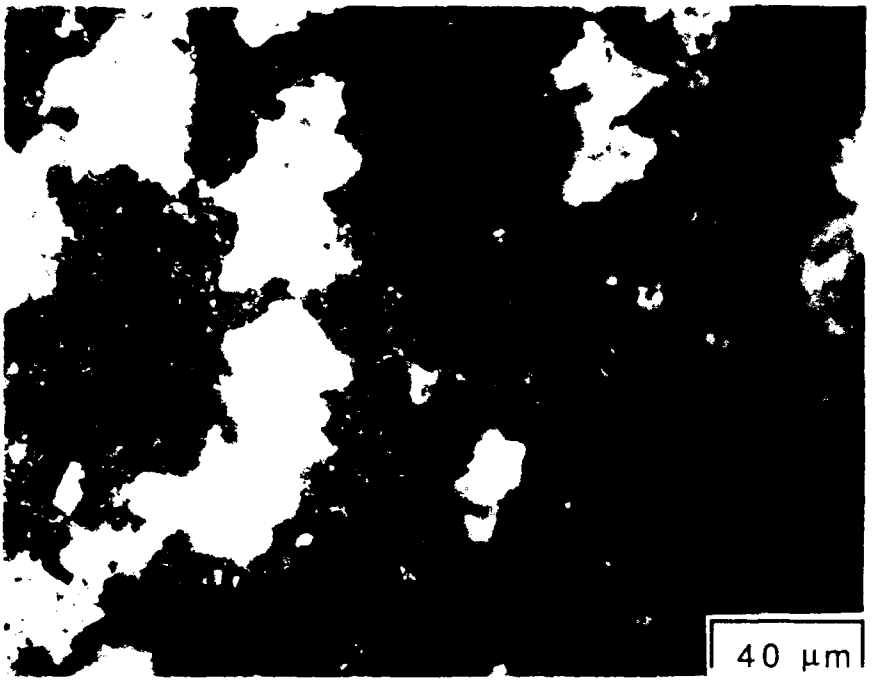

Figure G-5 Pit and shiny areas evident in light microscope view of Inconel 625 exposed to deionized water for 96 hours at 500°C, 241.5 atm. (500 x)

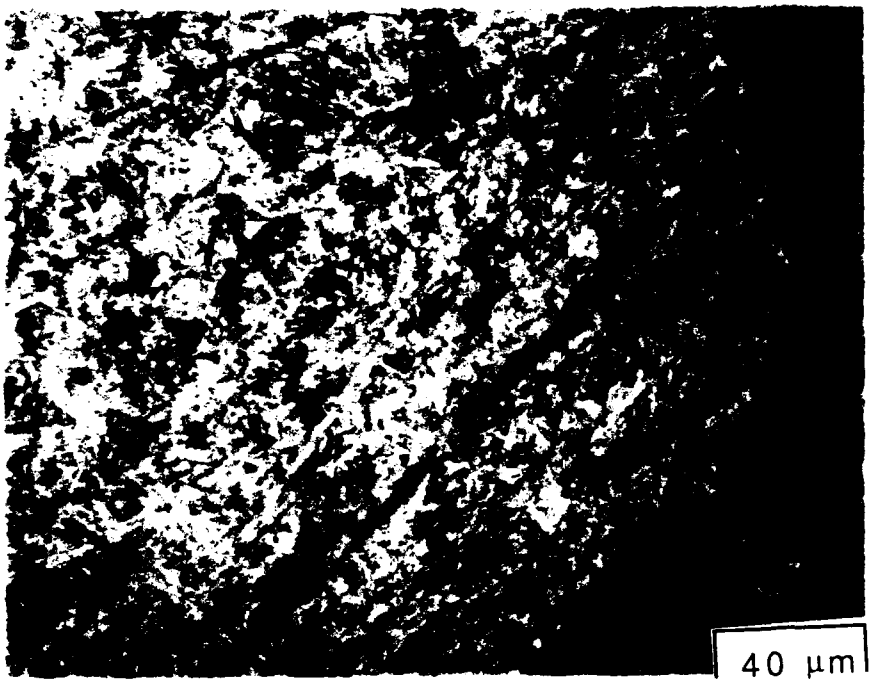

Figure G-6 Surface of Inconel 625, light microscope view, exposed to deionized water for 96 hours at 300°C, 241.5 atm (500 x)

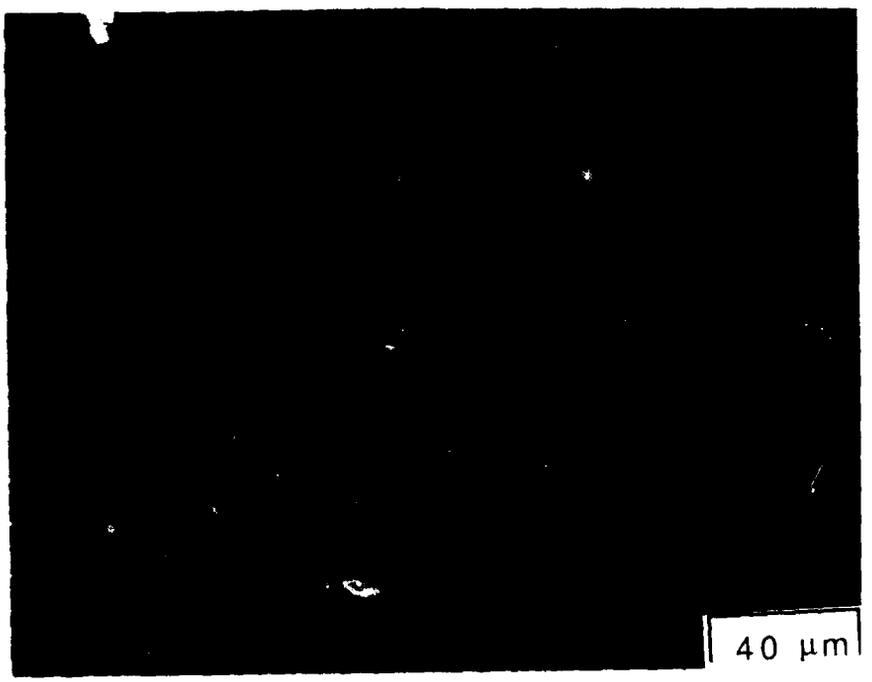

Figure G-7 Sharp features in 316 stainless steel exposed to deionized water for 96 hours at 300°C, 241.5 atm (500 x, light microscope)

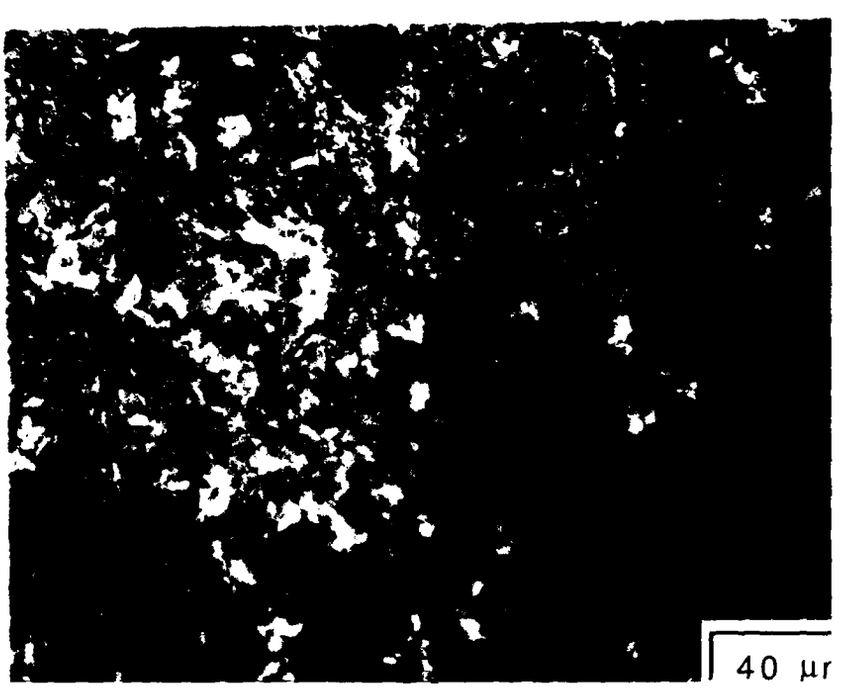

Figure G-8 Pit in Inconel 625 exposed to deionized water for 24 hours at 400°C, 241.5 atm (500 x, light microscope)

Figure G-9 Pit in Inconel 625 exposed to deionized water for 24 hours at 400°C, 241.5 atm (1000 x, light microscope)

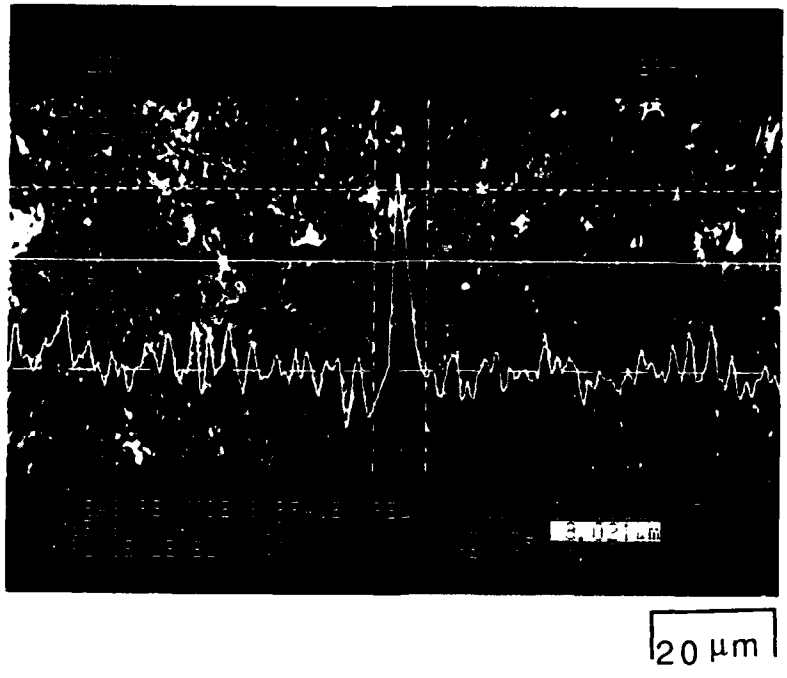

Figure G-10 Confocal laser microscope profile of raised surface on Inconel 625 exposed to deionized water for 24 hours at 400°C, 241.5 atm (800 x)

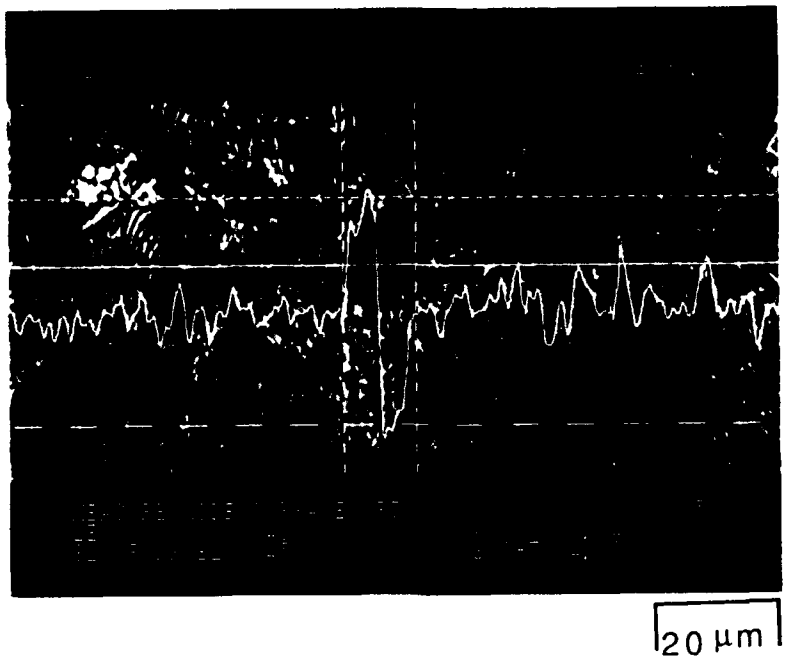

Figure G-11 Confocal laser microscope profile of irregularity on Inconel 625 exposed to deionized water for 24 hours at 400°C, 241.5 atm (800 x)

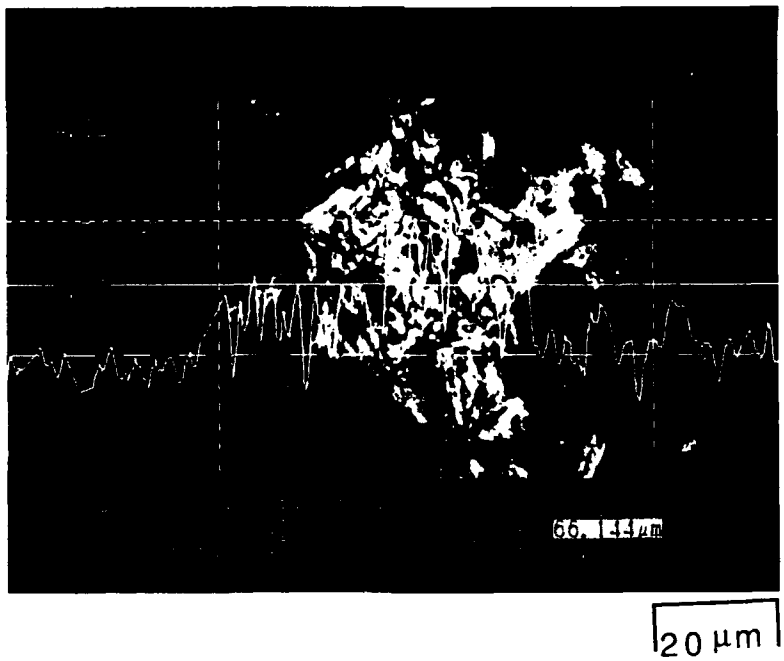

Figure G-12 Confocal laser microscope profile of shiny area on Inconel 625 exposed to deionized water for 96 hours at 500°C, 241.5 atm (800 x)

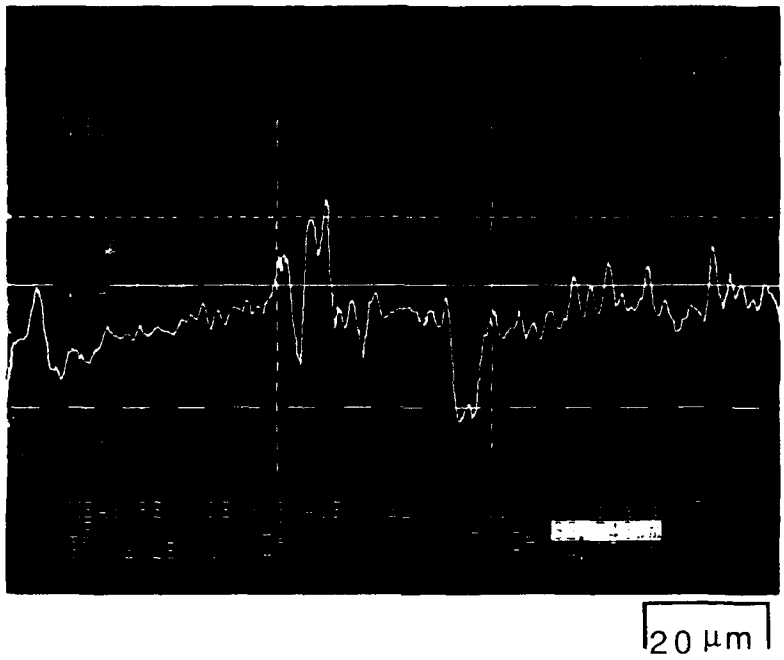

Figure G-13 Confocal laser microscope profile of irregular surface on 316 SS exposed to deionized water for 96 hours at 300 C. 241.5 atm (800 x)

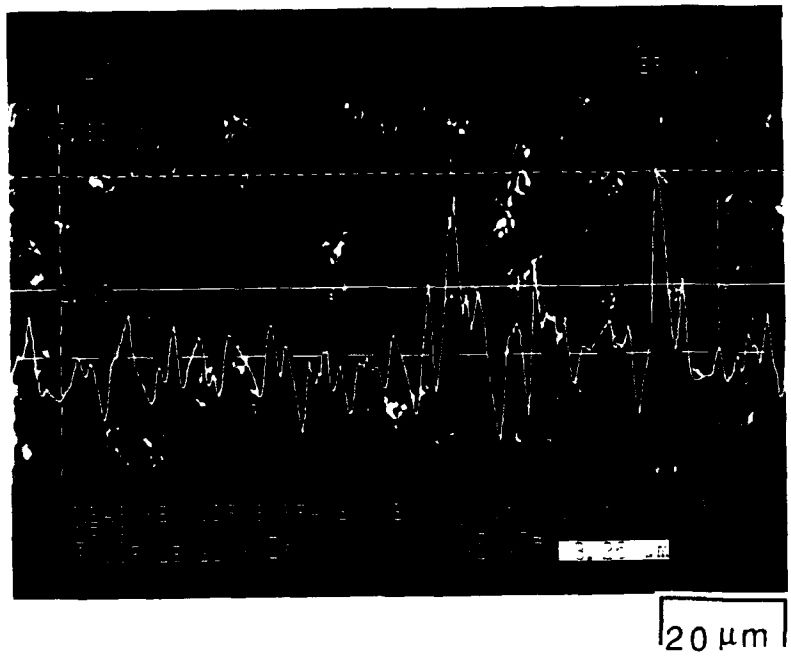

Figure G-14 Confocal laser microscope profile of rough surface on Hastelloy C-276 exposed to deionized water for 96 hours at 500°C, 241.5 atm (800 x)

BIBLIOGRAPHY

1. Kotas, Gerald, "Total Quality Management and Pollution Prevention". *Corporate Quality/Environmental Management: The First Conference*, Global Environmental Management Initiative, Washington DC, Jan 9-10 1990, page 193.

2. OPNAVINST 5090.1A Environmental and Natural Resources Program Management, Washington DC, 2 October 1990.

3. Markle, S. P, F. Colberg, M. A. Bracco, M. Smoot, G. Margelis, "Fleet Logistics Environmental Ship," Design Project for Massachusetts Institute of Technology, Department of Ocean Engineering Course 13.414, May 1994.

4. Brooks R. , "Principles of Naval Ship Design" course notes from Massachusetts Institute of Technology, Ocean Engineering Department Course 13.412, Sept 1992.

5. Martynova, O. I.: "Solubility of Inorganic Compounds in Subcritical and Supercritical Water", In *High Temperature High Pressure Electrochemistry in Aqueous Solutions*, Jones, D de G., and Staele, R. W.., Eds., National Association of Corrosion Engineers, Houston, TX 1976, pp. 131-138.

6. Modell, M. " Detoxification and Disposal of Hazardous Organic Chemicals by Processing in Supercritical Water". US Army Medical Research and Development Command, Fort Dietrick, Frederick Maryland. November 1985.

7. Jain, Vinod K. "Supercritical Fluids Tackle Hazardous Wastes", *Environmental Science Technology*, Volume 27 No. 5, 1993. pp. 806-808.

8. Takahasi, Y, T. Wydeven and C. Koo. "Subcritical and Supercritical Water Oxidation of CELSS Model Wastes", *Advanced Space Research*, Vol.9 No. 8, 1989 p. 99-110.

9. Moran, David, Office of Naval Research, Presentation to Massachusetts Institute of Technology, Joint Industry and Academic Workshop sponsored by the Ocean Engineering Department March 1992.

10. Rice, S. F., Steeper, R. R., and LaJeunesse, C. A., " Destruction of Representative Navy Wastes Using Supercritical Water Oxidation", Sandia National Laboratory paper SAND94-8203, printed October 1993.

11. Kurts, Richard, Naval Civil Engineering Laboratory, Port Hueneme CA, discussions February 1993.

12. Modell, Michael, "Supercritical Water Oxidation", *Standard Handbook of Hazardous Waste Treatment and Disposal.* McGraw-Hill, Inc., New York, NY, 1989, pp.8.153-8.167.

13. Tester, Jefferson W., H. Richard Holgate, Fred J. Armellini, Paul A. Webley, William R. Killilia, Glen T. Hong, and Herbert E. Barner. "Supercritical Water Oxidation Technology, Process Development and Fundamental Research", *Emerging Technologies in Hazardous Waste Management III*, American Chemical Society Washington D.C. 1993, pp. 35-76.

14. Armellini, F. J., J. W. Tester, "Experimental Methods for Studying Salt Nucleation and Growth from Supercritical Water", *Journal of Supercritical Fluids*, Volume 4, 1991, p. 254.

15. Armellini, F. J. and J. W. Tester, "Solubility of Sodium Chloride and Sulfate in Sub- and Supercritical Water Vapor from 450 - 550°C and 100-250 Bar", *Fluid Phase Equilibria*, Volume 84, 1993, p. 139.

16. Uhlig, Herbert H., Corrosion and Corrosion Control, 3rd Ed., John Wiley and Sons, New York, 1985.

17. Pourbaix, M. Atlas of Electrochemical Equilibria in Aqueous Solutions, Pergamon Press, New York, 1966.

18. Huang, Shaoping, Kirk Daehling, Thomas Carlson, Pat Taylor, Chien Wai and Alan Prop. "Thermodynamic Analysis of Corrosion of Iron Alloys in Supercritical Water", *Supercritical Fluid Science and Technology*, American Institute of Chemical Engineers Annual Meeting, Washington D.C., Nov 27 - Dec 2 1988, p. 276-286.

19. N. D. Greene, *Experimental Electrode Kinetics*, Renssalaer Polytechnic Institute, Troy N. Y, 1965; "Standard Reference Method for Making Potentiostatic and Potentiodynamic Anodic Polarization Measurements, G5-87, *1992 Annual Book of ASTM Standards*, Vol 03.02, American Society for Testing and Materials, Philadelphia, PA, 1992. p. 72.

20. Huang, Shaoping, Kirk Daehling, Thomas Carlson, Masud Abdel-Latif, Pat Taylor, Chien Wai and Alan Prop, "Electrochemical Measurements of Corrosion of Iron Alloys in Supercritical Water", *Supercritical Fluid Science and Technology*, American Institute of Chemical Engineers Annual Meeting, Washington D.C., Nov 27-Dec 2 1988, p. 287-300.

21. Carter J.P., B.S. Covino, Jr., J. T. Driscoll, W. D. Riley and M. Rosen. "Gaseous Corrosion of Metals in a 60% H_20, 40% HCl", *Corrosion*, Vol. 40, No. 5, May 1984, pp. 205-214.

22. Berry, Warren E.," The Corrosion Behavior of Fe-Cr-Ni Alloys in High Temperature Water", in *High Temperature High Pressure Electrochemistry in Aqueous Solutions*, University of Surrey, England, January 7-12, 1973. pp.48-66.
23. Tester, Jefferson W., Proposal for "Chemical Reactors for Supercritical Water Oxidation of Military Toxic Wastes, Fundamental and Applied Studies," Submitted to U. S. Army Research Office 1991.

24. Berkowitz, B. J. and R. D. Kane, "The Effect of Impurity Segregation of the Hydrogen Embrittlement of a High Strength Nickel Based Alloy in H_2S Environments", *Corrosion*, Vol. 36, No. 1, January 1980, pp. 25-29.

25. Kane, R. D. and B. J. Berkowitz, "Effect of Heat Treatment and Impurities on the Hydrogen Embrittlement of a Nickel Cobalt Base Alloy", *Corrosion*, Vol. 36, No. 1, January 1980, pp. 29-36.

26. Dyer, R. B., S. J. Buelow, D. M. Harradine, J. M. Robinson, B. R. Foy, J. H. Atencio, P. C. Dell'Orco, K. A. Funk, R. E. McIlroy. "Destruction of Explosives and Rocket Fuels by Supercritical Water Oxidation", Los Alamos National Laboratory paper LA-UR-92-2378, June 1992.

27. Buelow, Steven J., R. Brian Dyer, Cheryl K. Rofer, Jerry H. Atencio, and Joseph D. Wander, "The Destruction of Propellant Components in Supercritical Water", Los Alamos National Laboratory paper LA-UR-90-1338 Printed May 1990.

28. Bramlette, T. T., B. E. Mills, K. R. Hencken, M. E. Brynildson, S. C. Johnson, J. M. Hruby, H. C. Feemster, B. C. Odegard, and M. Modell. "Destruction of DOE/DP Surrogate Wastes with Supercritical Water Oxidation Technology", Sandia National Laboratory paper SAND90-8229, Printed November 1990.

29. LaJuenesse, C. A., S.F. Rice, J.J. Bartel , M. Kelley, C. A. Seibel, L. G. Hoffa, T. F. Ekelund, and B. C. Odegard, A Supercritical Water Oxidation Reactor: The Materials Evaluation Reactor (MER)", Sandia National Laboratory paper SAND91-8623, Printed February 1992.

30. Thomas, Albert Janney III, and Earnest F. Gloyna. "Corrosion Behavior of High Grade Alloys in the Supercritical Water Oxidation of Sludges", Technical Report CRWR 229, Center for Research in Water Resources. The University of Texas at Austin, February 1991.

31. Hazlebeck, D. A., K. W. Downey, D. D. Jensen, and M. H. Spritzer, "Supercritical Water Oxidation of Chemical Agents, solid Propellants, and Other DOD Hazardous Wastes", General Atomics paper released March 1993, pp. 11-13.

32. Walter, G. W., "A Review of Impedance Plot Methods Used for Corrosion Performance Analysis of Painted Metals", *Corrosion Science*, Vol 26, No. 9, 1986, pp. 681-703.

33. Barner, H. E., C. Y. Huang, T. Johnson, G. Jacobs, M. A. Martch and W. R. Killilea, "Supercritical water oxidation: An emerging technology", *Journal of Hazardous Materials*, Vol 31, 1992, pp. 1-17.

34. Crandall, S. H., N. C. Dahl, and T. J. Lardner ed, An Introduction to the Mechanics of Solids, McGraw-Hill Publishing Co, NY, 1978. p. 276.

35. McClintock, F. A. and A. S. Argon, editors, Mechanical Behavior of Materials. Addison Wesley Publishing Company, Inc. 1971, Reprinted 1993, p. 276.

36. Inco Alloys, Inconel Alloy 625 Physical Properties Data pamphlet. Fifth Edition 1985.

37. Campbell, J. E, W. E. Gerberich, and J. H. Underwood editors, Application of Fracture Mechanics for Selection of Metallic Structural Materials. American Society for Metals, Metals Park OH. p. 316.

38. Brown, Stuart, Professor of Materials Science, Massachusetts Institute of Technology discussions March 1993.

39. American Society of Mechanical Engineers Boiler and Pressure Vessel CODE VIII Division 1, section UG-101, ASME, New York, 1992. pp 79.

40. Reflange INC, Design Stress Calculations for R-CON clamp type connectors per ASME Code VIII.

41. Blass, Kathryn, "Exposure Test Vessel in 8-235", memo to file for Massachusetts Institute of Technology Safety Office, 19 Jan 1994.

42. Mitton, D. B., R. M. Latanision, J. C. Orzalli, P. A. Marrone, B. D. Phenix, J. C. Meyer, J. W. Tester. "Preliminary Failure Analysis of a Supercritical Water Oxidation Preheater Tube", presented to University Research Initiate meeting August 17, 1994, University of Delaware, Newark, Delaware.

43. Omega Engineering Incorporated Heater Manual Volume 28, 1992. p.K-11.

44. Masubuchi, K, "Laser Microscope Opens Up New Opportunities for Welding Research", *Welding Journal*, Sept 1992, p. 69-71.

45. Macdonald, D. D., Uhlig Corrosion Lab Lecture at Massachusetts Institute of Technology, Feb 1994.

46. Rofer, Cheryl K, Steven J. Buelow, Richard B. Dwyer and Joseph D. Wander. "Conversion of Hazardous Materials Using Supercritical Water Oxidation", U. S. Patent 5,133,877, July 28, 1992.

47. Massachusetts Water Resources Authority (MWRA) 320 Code of Massachusetts Regulations (CMR) 10.024.

48. Standard Recommended Practice for Conducting Plant Corrosion Tests.(G4-84) *1993 Annual Book of ASTM Standards* part 03.02. American Society of Testing Materials, Philadelphia, 1992, p. 66.

49. Jones, Denny A., Principles of Prevention of Corrosion, Macmillian, New York, 1992. Inside back cover.

BIOGRAPHICAL NOTE

John Clarke Orzalli, Commander, United States Navy.

Born: December 26, 1955, Marysville California

Institutions Attended:

United States Naval Academy: July 1974 - June 1978
B. S. in Marine Engineering
American Society of Naval Engineers Prize

Golden Gate University: Jan 1989 - August 1990
M. S. in Systems Management

Professional Training:

United States Navy Nuclear Power School:	1979
United States Navy Nuclear Power Prototype:	1979
US Naval Submarine Officer Basic Course:	1980
L. Y. Spear Award	
US Naval Submarine Officer Advance Course:	1985
L. Y. Spear Award	

Professional Experience:

USS Snook (SSN 592)	1980-1983
Completed Regular Overhaul and Deployments to South America and the Mediterranean. Reactor Controls Assistant, Main Propulsion Assistant and Weapons Officer.	
United States Naval Academy	1983-1985
29th Company Officer	
USS Helena (SSN 725)	1986-1988
Chief Engineer Officer, Completed New Construction Shakedown and Post Shakedown Availability.	
Submarine Development Group One,	1988-1991
Detachment Mare Island Officer in Charge	

Professional Awards:
Meritorious Service Medal
Navy Commendation Medal (2 Awards)
Navy Achievement Medal (4 Awards)

Other Recognition:

1988 White House Fellowship, Regional Finalist

Family:

Married to Joanne Dale (McComas) Orzalli
Three children; Sarah, Ian and Robbie.